

A CADMIUM FILTER TECHNIQUE IN  
RIABLE-ENERGY NEUTRON ACTIVATION ANALYSIS

1050 710

by

TERRY ALAN TOMBERLIN

B. S., University of Wyoming, 1970

---

A MASTER'S THESIS

submitted in partial fulfillment of the  
requirements for the degree

MASTER OF SCIENCE

Department of Nuclear Engineering

KANSAS STATE UNIVERSITY

Manhattan, Kansas

1974

Approved by:

*N. Dean Eckloff*  
Major Professor

LD  
2668  
T4  
1974  
T64  
C.2

Document

## TABLE OF CONTENTS

1.0	INTRODUCTION . . . . .	1
2.0	DESCRIPTION OF APPARATUS . . . . .	4
3.0	EXPERIMENTAL . . . . .	15
3.1	Preliminary Investigations . . . . .	15
3.1.1	Reactivity worth of a cadmium test filter . . . . .	15
3.1.2	Preliminary tests using cadmium filters . . . . .	16
3.1.3	Reactivity measurements of the final cadmium filter . . . . .	16
3.1.4	Other investigations . . . . .	17
3.2	Measurements for Record . . . . .	19
3.2.1	Reference materials and analyzed samples . . . . .	19
3.2.2	The neutron flux monitor . . . . .	22
3.2.3	Irradiation conditions . . . . .	22
3.2.4	Counting procedures . . . . .	23
4.0	THE VARIABLE-ENERGY NEUTRON ACTIVATION ANALYSIS . . . . .	26
4.1	Basic Neutron Activation Analysis . . . . .	26
4.1.1	Gamma-ray spectrometry . . . . .	27
4.1.2	Comparative analysis using a flux monitor . . . . .	30
4.2	Formulation of the Variable-Energy Analysis . . . . .	32
4.3	Initial Analysis Methods . . . . .	34
4.4	The Final Method of Analysis . . . . .	38
5.0	RESULTS AND CONCLUSIONS . . . . .	46
6.0	SUGGESTIONS FOR FURTHER STUDY . . . . .	58
7.0	ACKNOWLEDGMENTS . . . . .	59
8.0	LITERATURE CITED . . . . .	60
9.0	APPENDIXES . . . . .	63

APPENDIX A: The Approved Experiment . . . . .	64
APPENDIX B: Gamma-Ray Spectra of Reference Samples . . . . .	78
APPENDIX C: Computer Programs for Normalization of Reference Samples and for the Variable-Energy, Area-of- Interest Analysis . . . . .	88

**THIS BOOK  
CONTAINS  
NUMEROUS PAGES  
WITH THE ORIGINAL  
PRINTING BEING  
SKEWED  
DIFFERENTLY FROM  
THE TOP OF THE  
PAGE TO THE  
BOTTOM.**

**THIS IS AS RECEIVED  
FROM THE  
CUSTOMER.**



## LIST OF FIGURES

1. Kansas State University TRIGA Mark II Nuclear Reactor Core Diagram . . . . .	6
2. Vertical Section View of the TRIGA Mark II Nuclear Reactor . . . . .	9
3. Vertical Section View of the TRIGA Mark II Nuclear Reactor Tank with the Cadmium Filter . . . . .	10
4. Section View of the Modified RSR Irradiation Vial . . . . .	11
5. Effective Neutron Cutoff Energies ( $E_c$ ) for Cylindrical Cadmium Filters of Thickness $t_0$ . . . . .	13
6. Estimated Neutron Flux Profiles for the KSU TRIGA Mark II Nuclear Reactor . . . . .	20
7. A Typical Spectrum Produced by a Monoenergetic Gamma-Ray Emitter ( $E_\gamma > 1.022$ MeV) . . . . .	28
8. Nuclear Reaction Diagram Showing the Possible Modes of Production of Al-28 and Mg-27 . . . . .	35
9. Typical Gamma-Ray Spectra of Wheat . . . . .	47
10. Gamma-Ray Spectra of Horse Hair . . . . .	54
11. Gamma-Ray Spectra of Horse Hair . . . . .	55
12. Vertical Section View of the TRIGA Mark II Nuclear Reactor Tank with the Cadmium Filter . . . . .	66
13. The Aluminum Foot for the Filter Device . . . . .	73
14. Vertical Section View of the Cadmium Filter, Aluminum Tubing, and Aluminum Foot . . . . .	74
15. Gamma-Ray Spectra of Aluminum Oxide . . . . .	79
16. Gamma-Ray Spectra of Silicon Dioxide . . . . .	80
17. Gamma-Ray Spectra of Magnesium Oxide . . . . .	81
18. Gamma-Ray Spectra of Ammonium Orthophosphate . . . . .	82
19. Gamma-Ray Spectra of Ammonium Chloride . . . . .	83
20. Gamma-Ray Spectra of Manganese Dioxide . . . . .	84
21. Gamma-Ray Spectra of Sodium Carbonate . . . . .	85
22. Gamma-Ray Spectra of Potassium Carbonate . . . . .	86
23. Gamma-Ray Spectra of Calcium Sulfate . . . . .	87

## LIST OF TABLES

I.	Neutron Flux Values for a TRIGA Reactor Operating at 250 kW . .	5
II.	Radionuclides and Their Respective Gamma-Ray Energies and Half-Lives Considered for the AOI Analyses . . . . .	44
III.	Concentrations of Al, Si, Mg, and P in Wheat Grain as Determined by the Cadmium Filter Technique . . . . .	50
IV.	Concentrations of Al, Si, Mg, and P in Wheat Grain According to Schrenk (30), Peterson (31), and Morrison (32) . .	51

# NOMENCLATURE

$\dot{N}$	time rate of change of the number of product nuclei
$\sigma$	microscopic neutron absorption cross section ( $\text{cm}^2/\text{nucleus}$ )
$\Phi$	neutron flux ( $\text{neutrons}/\text{cm}^2 \cdot \text{sec}$ )
$\lambda$	decay constant ( $\text{min}^{-1}$ )
$N$	number of product nuclei
$N_0$	number of parent nuclei
$t_i$	time of irradiation (min)
$A_0$	activity at the end of an irradiation (d/min)
$A$	activity (d/min)
$A_s$	saturation activity (d/min)
$A_{st}$	activity normalized to standard irradiation (d/min)
$t_w$	decay time (min)
$f$	fraction or concentration of an element in a given sample
$y_i$	total counts in the $i$ -th channel for the unknown sample
$a_{ij}$	total counts in the $i$ -th channel of the $j$ -th reference sample
$e_i$	error or residual term for the $i$ -th channel
$\underline{Y}$	$(n \times 1)$ vector of data from unknown sample
$\underline{A}$	$(n \times m)$ matrix of data from reference samples
$\underline{f}$	$(m \times 1)$ vector of estimated concentrations
$\underline{e}$	$(n \times 1)$ error vector
$\underline{e}^T$	transpose of $\underline{e}$
$\underline{W}$	$(n \times n)$ weighting matrix
$t_c$	counting time (min)
$t_s$	standard irradiation time (min)
$C$	total number of counts accumulated during a counting interval
$A_1$	activity at the beginning of a count (d/min)

## 1.0 INTRODUCTION

Many analytical methods for the qualitative and quantitative analysis of material constituents are quite time consuming and often require the destruction of the samples. Many methods are also unsuitable for trace element analysis. One increasingly important analytical tool for rapid, nondestructive, trace element analysis is neutron activation analysis (NAA). NAA was first reported by Hevesy and Levi in 1936, and since that time its value has increased rapidly (1). A recent study (an extensive bibliography of activation analysis) has shown that there are currently about 4000 literature items concerning activation analysis and that several hundred items are being added annually (2). NAA composes the major part of general activation analysis work, and thus its importance is partially obvious by this tremendous publication rate. So, NAA has received considerable attention, but most of these studies have centered around activation produced by thermal neutrons, i.e., neutrons in thermal equilibrium with their environment (0.025 eV neutrons, at 20° C). As in any analytical method, there are limitations involved with thermal-neutron activations. For example, some thermal-neutron activation products are not suitable for normal gamma-ray spectrometry.  $^{32}\text{P}$  is a typical product which emits only beta radiation and thus often involves a measurement of the resulting Bremsstrahlung radiation. Such a measurement involves many assumptions and can lead to ambiguous results for complex matrices. By using fast neutrons (neutrons with high kinetic energies, typically in the MeV range) products other than  $^{32}\text{P}$  can be formed from the stable parent,  $^{31}\text{P}$ . In this work it was desired to detect and measure  $^{28}\text{Al}$  produced by an (n, $\alpha$ ) reaction with the  $^{31}\text{P}$ . Such a reaction requires a fast neutron (energy greater than

1.9 MeV), but the product,  $^{28}\text{Al}$ , emits a 1.78 MeV gamma-ray which is suitable for normal gamma-ray spectrometry. So, an analyst utilizing NAA can expand its versatility and usefulness by using both thermal and fast neutrons.

The process of utilizing both thermal- and fast-neutron activations is essentially employing variable-energy activation analysis. According to Kruger (3):

"Variable-energy activation analysis is the technique for activation of samples with irradiating particles of selected energies so that variations in reaction threshold energy, coulomb barriers, and excitation functions can be used to increase the selectivity of activation."

Several sources, such as nuclear reactors, cyclotrons, and accelerators are available to produce variable neutron energies. Cyclotrons and accelerators are not as dependable as nuclear reactors and they also pose other problems which can be avoided by using nuclear reactors. Thus, the Kansas State University TRIGA Mark II nuclear reactor was used in this work as a source of a wide spectrum of neutron energies. A cadmium filter was used to produce a distinctly different neutron energy spectrum than the normal (predominantly thermal neutron) spectrum available. Thus, by using both a normal sample irradiation and a cadmium-filtered irradiation it was possible to achieve a type of variable-energy activation analysis.

The purpose of this work was to design and construct a suitable cadmium filter for in-core operation and to develop a NAA technique for the variable-energy activations. The objective concerning this technique was to combine two sets of data from a given sample into a single analysis, one data set being obtained from a normal irradiation and the other from a cadmium-filtered irradiation. This technique was mainly oriented toward the solution of the problem of phosphorus analysis by NAA. Several authors have reported

techniques of phosphorus analysis by NAA (4, 5, 6, 7, 8), but none of these have incorporated variable-energy NAA utilizing a reactor source of neutrons. The method developed in this work could be expanded for other nuclides which present problems for normal gamma-ray spectrometry.

## 2.0 DESCRIPTION OF APPARATUS

The Kansas State University 250-kW TRIGA Mark II Pulsing Nuclear Reactor was used as a source of neutrons for this work. The TRIGA nuclear reactor is a common research reactor and it supplies sufficient neutron flux for common activation analyses. Neutron flux levels for several energy groups have been reported for the TRIGA nuclear reactor. See Table I. Although the values for Table I were obtained for a TRIGA Mark I nuclear reactor, they will also apply to a TRIGA Mark II since there is almost no difference in the cores of the two reactors. In fact, the manufacturer of the TRIGA reactor has published identical values for the thermal and  $>10$  keV flux groups for the KSU TRIGA Mark II nuclear reactor (9). Slight variations in these flux values would be possible, but order of magnitude differences would be unlikely. In regard to Table I, the rotary specimen rack (RSR) of the TRIGA is a watertight container which fits in a slot in the graphite reflector surrounding the core. The actual rack of the RSR is a ring of sample holders which can be rotated around the core. Access to the RSR is provided by an aluminum tube which extends from the top of the reactor to the RSR. Samples are inserted and removed from the RSR through this tube. See Figure 1 for a description of the TRIGA fuel-element D and F rings. It also shows the location used for the cadmium filter.

Part of the objective of this work was to use a cadmium filter to change the energy spectrum of neutrons being used to activate samples. Cadmium is commonly used as a filter in small foil activation analysis, but the amount of cadmium necessary to construct a filter for normal-sized samples would present a radiation hazard after normal irradiations in a TRIGA reactor at full power operation. Preliminary experiments with relatively

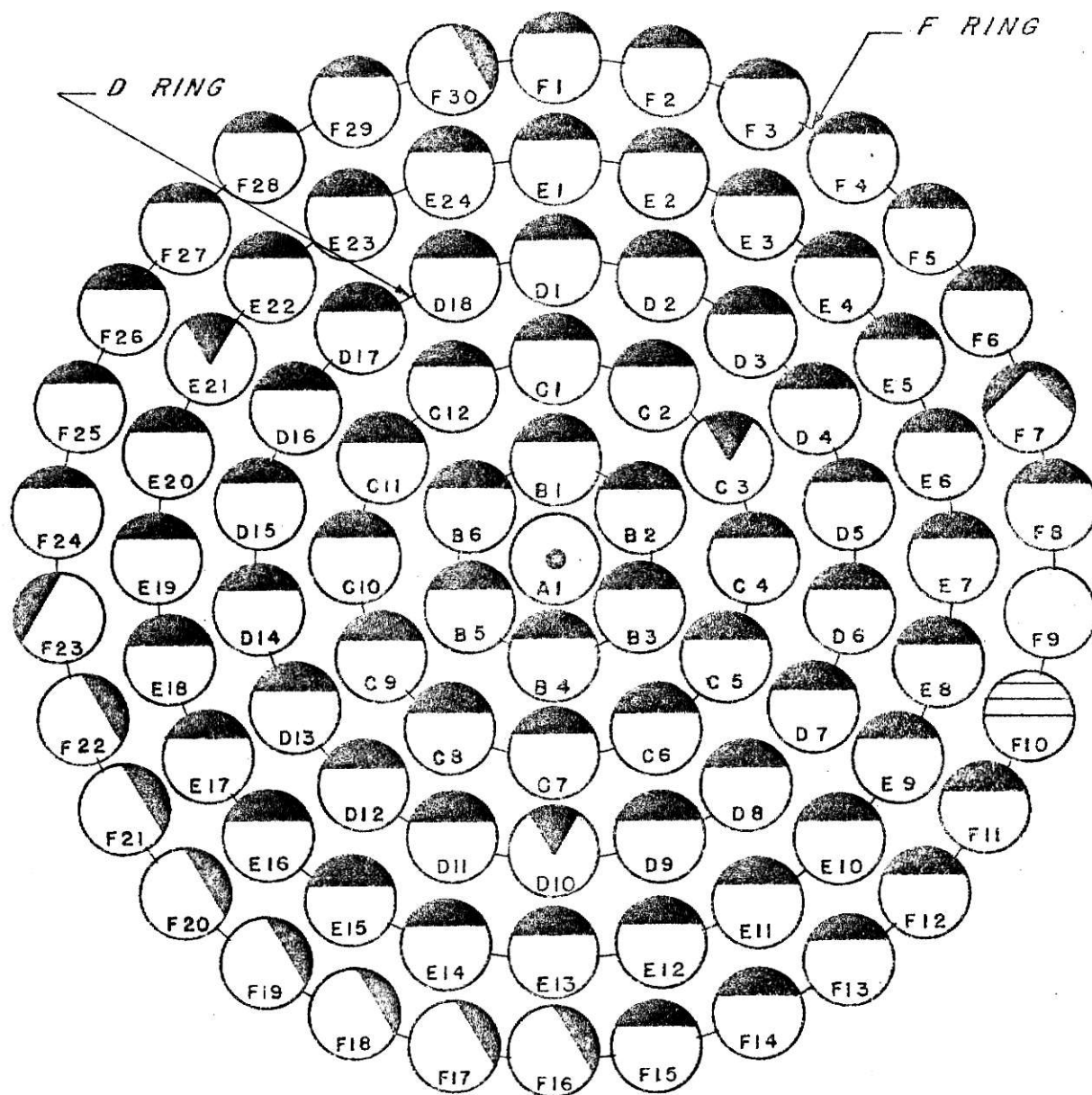
Table I  
Neutron Flux Values for a TRIGA Reactor Operating at 250 kW (10).

Irradiation Position	Neutron Flux (n/cm <sup>2</sup> ·sec)				
	Thermal	>10 keV	>1.35 MeV	>3.68 MeV	>6.1 MeV
Rotary Specimen Rack	$1.8 \times 10^{12}$	$1.5 \times 10^{12}$	$1.8 \times 10^{11}$	$2.5 \times 10^{10}$	$4.0 \times 10^9$
Fuel-element ring D	$4.9 \times 10^{12}$	$9.0 \times 10^{12}$	$2.3 \times 10^{12}$	$4.1 \times 10^{11}$	$6.2 \times 10^{10}$
Fuel-element ring F	$4.3 \times 10^{12}$	$3.5 \times 10^{12}$	$7.5 \times 10^{11}$	$1.25 \times 10^{11}$	$1.9 \times 10^{10}$
Reactor pool outside reflector	$6.8 \times 10^{11}$	$6.8 \times 10^{10}$	$5.1 \times 10^9$	$6.3 \times 10^8$	$1.1 \times 10^8$



**THIS BOOK  
CONTAINS  
NUMEROUS PAGES  
WITH DIAGRAMS  
THAT ARE CROOKED  
COMPARED TO THE  
REST OF THE  
INFORMATION ON  
THE PAGE.**

**THIS IS AS  
RECEIVED FROM  
CUSTOMER.**










CODE:  - CENTRAL THIMBLE  - CONTROL ROD  
 - PNEUMATIC RABBIT  - SOURCE ELEMENT  
 - FUEL ELEMENT  - CADMIUM FILTER  
 - GRAPHITE ELEMENT

Figure 1. Kansas State University TRIGA Mark II Nuclear Reactor Core Diagram.

small cadmium filters irradiated in the RSR of the Kansas State University TRIGA Mark II nuclear reactor have shown that radiation levels of several hundred mr/hr are not uncommon for short irradiations. Therefore, for a cadmium filter of any useful size for activation analysis, it was obvious that some type of shielding was desirable. Effective shielding is provided by distance, shielding materials, or a combination of both. The RSR was not a suitable location for the filter since the filter would have to be removed along with the irradiated sample. Thus, no significant distance or shielding materials could conveniently be used by the person removing the samples from the filter. For shielding reasons and for increased fast-neutron flux levels it was decided to design a cadmium filter which could be used in a vacant fuel-element position in the core of the TRIGA nuclear reactor. It was also desired to design the filter such that it could remain in the reactor tank at a suitable distance underwater to provide adequate shielding. Another necessary design feature was the requirement that the sample be removed from the filter and from the reactor as quickly as possible since a short-lived nuclide, 2.3 minute  $^{28}\text{Al}$ , was to be studied.

To satisfy all of the requirements, a cadmium filter in the shape of a cylinder was designed and tightly fitted into the end of a special aluminum tube. An aluminum foot was then inert-gas welded to the end of the tube. This foot sealed the end of the tube and also served to position the filter in a vacant fuel-element position in the core. The tube was designed to extend from the core to the top of the reactor tank so that samples could be inserted and removed from the cadmium filter in a manner similar to that which is used for the RSR. The tube was carefully bent to an S-shape with a 24 inch offset to prevent radiation-streaming from the core. See Figures

2 and 3. The tube and filter were designed so that materials could be irradiated in a dry environment at the approximate horizontal midplane of the core and also so that the RSR recovery tool could be used to remove samples from the filter. The tube extended through the top grid plate of the core with the filter at the end. Standard polyethylene sample vials used in the RSR were slightly modified to pass through the tube and into the filter. The top of the cadmium filter had to be incorporated in the top portion of a modified vial as shown in Figure 4. When a sample was removed from the reactor, the top of the vial, including the small cadmium top, could be removed quickly from the samples. The samples could then be treated according to normal procedures. The actual samples were contained in small polyethylene vials approximately 1 inch long and 7/16 inch in diameter. These small sample vials were placed inside a modified RSR irradiation vial for a cadmium-filtered irradiation and inside a standard RSR irradiation vial for a nonfiltered irradiation.

The thickness of the cadmium filter was approximately 40 mils. The height was 4.5 inches and the outside diameter was 1.33 inches. For further details see Appendix A. Cadmium filters have been commonly used in reactor flux measurements to separate thermal from epithermal neutron flux. Therefore, several authors have studied the effects caused by different filter geometries and thicknesses (12, 13, 14). Some of their results are applicable to this work, even though they were primarily concerned with effective cutoff energies. Stoughton and Halperin (12) concluded that, "Cadmium---with a thickness of 30 or preferably 40 mils---is perhaps the most useful all-around filter." It was also found that, for a sample displaced a significant distance from the center of a cylindrical filter, the effective filter thickness was changed very little, e.g., about 0.2%

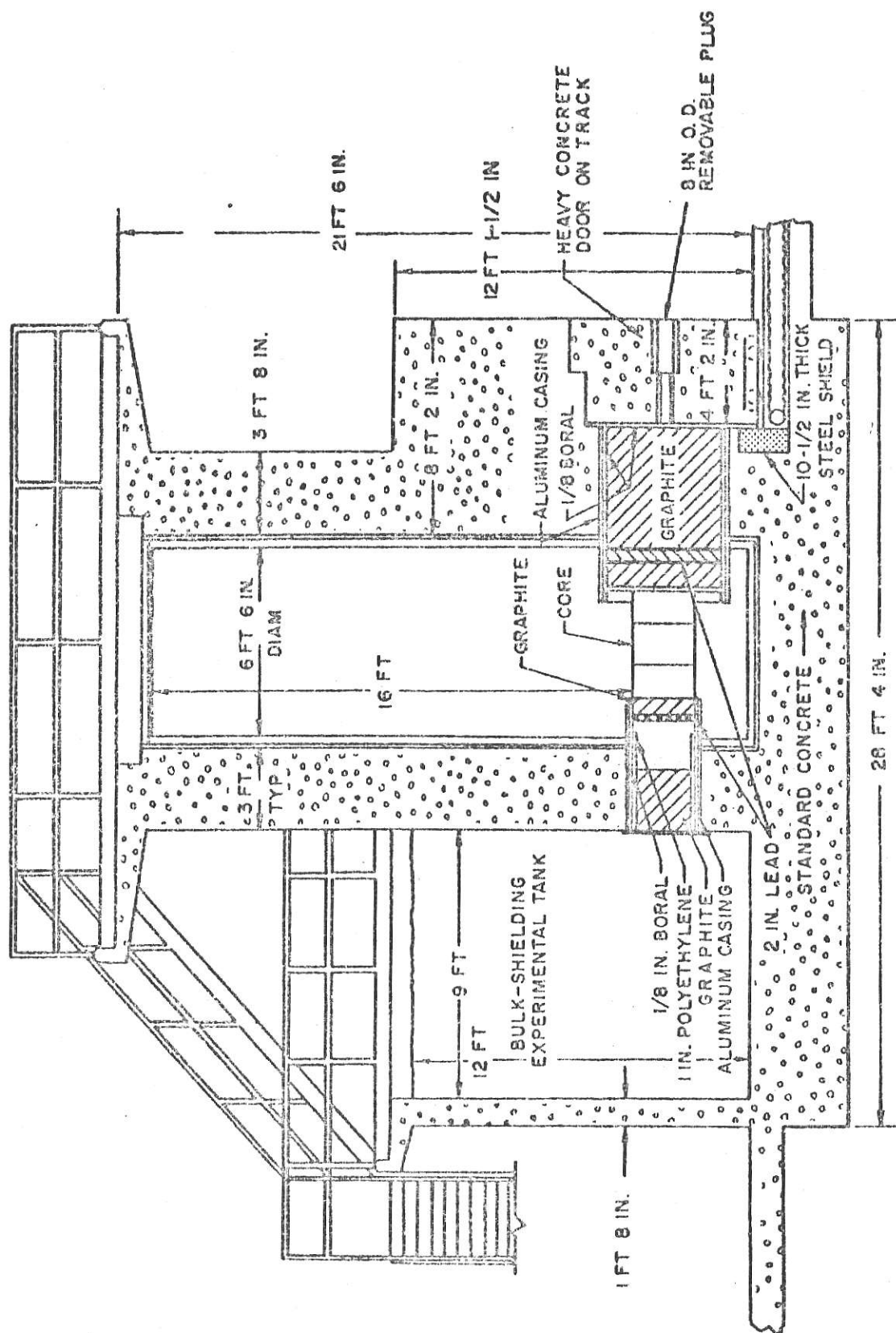


Figure 2. Vertical Section View of the TRIGA Mark II Nuclear Reactor (11).

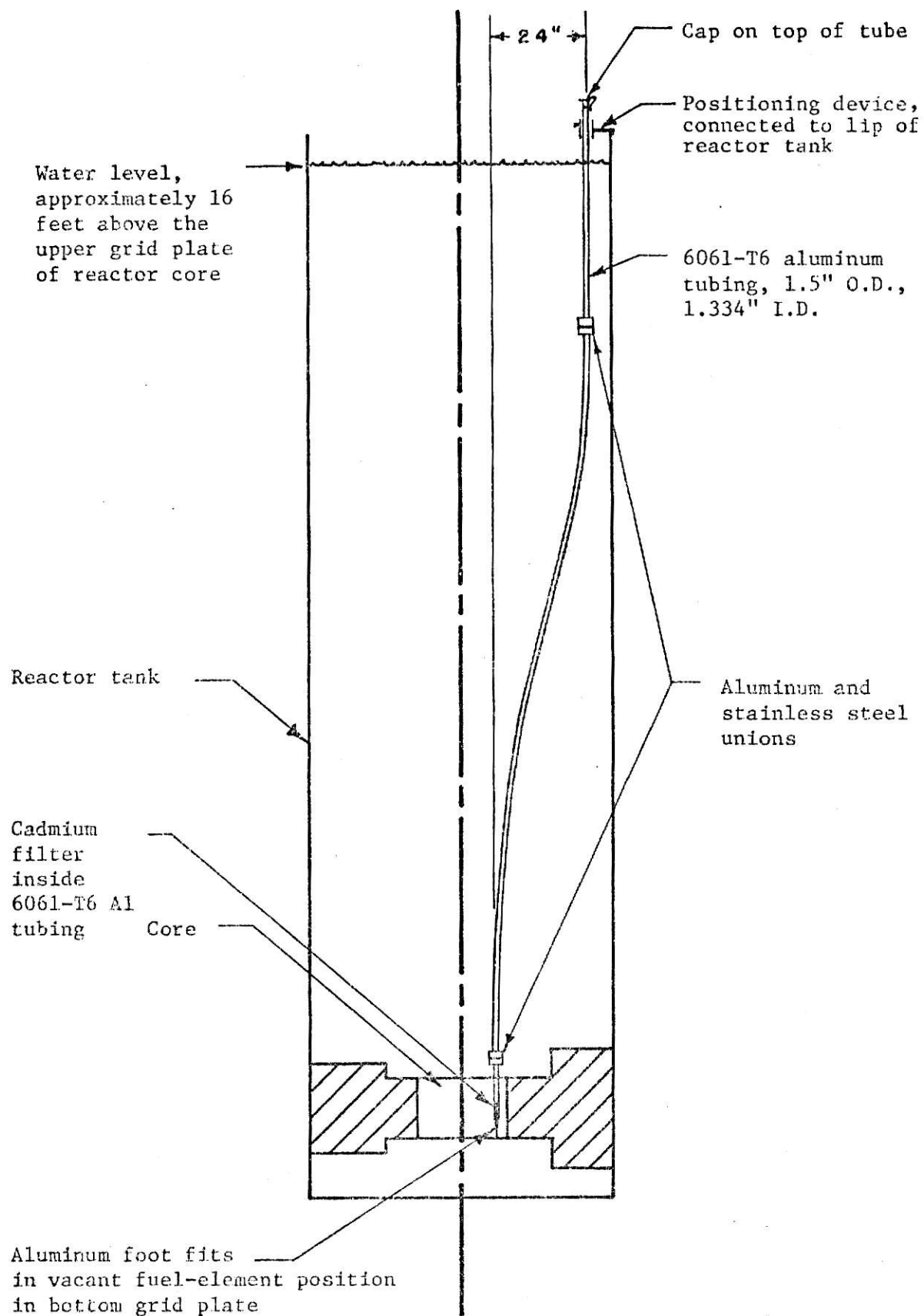


Figure 3. Vertical Section View of the TRIGA Mark II Nuclear Reactor Tank with the Cadmium Filter.

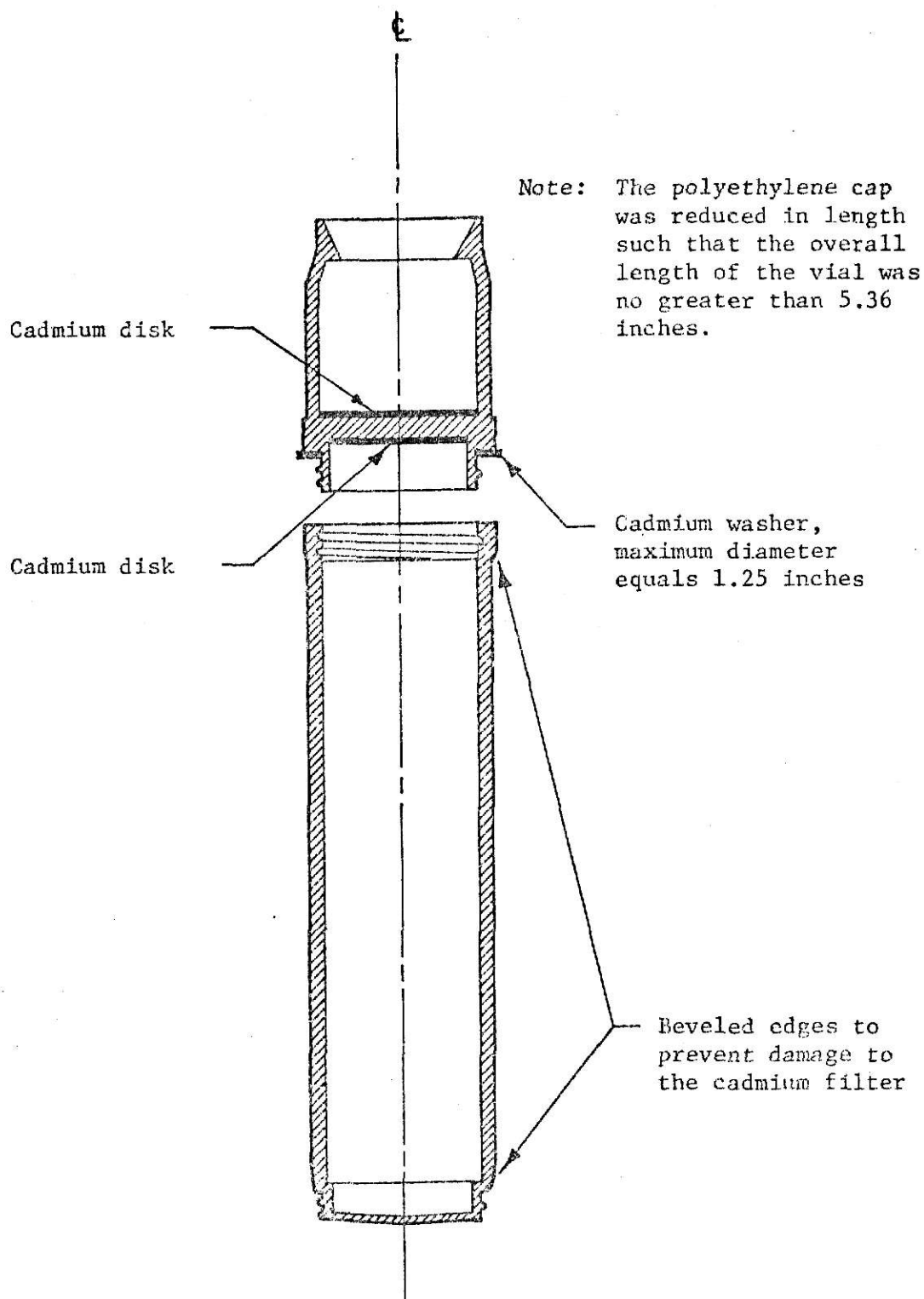


Figure 4. Section View of the Modified RSR Irradiation Vial.

for a sample at half the distance between the center and the end of the cylinder (13). This is important to this work since the comparative method of activation analysis was used and reference materials were irradiated at different positions in the filter than the unknown samples. It is known that the effective cutoff energy for a neutron filter varies with the filter thickness. The effective cutoff energy has been defined (12) as, "the cutoff of a perfect (infinitely sharp) filter that allows the same total number of absorptions by the filtered sample as does the given filter." See Figure 5. In the case of a cylindrical filter it also varies with the ratio of cylinder height to cylinder diameter. Therefore, if the effective filter thickness for a given sample in the filter was strongly dependent on the sample position, then the effective cutoff energy would also be position dependent. This would destroy the validity of the comparative analysis method. The comparative analysis method assumes that the unknown sample and the reference sample experience identical neutron flux during irradiation.

A cadmium cylinder with walls 40 mils thick and 4.5 inches in height with a diameter of 1.33 inches constitutes a significant negative reactivity worth when placed in the core of a small research reactor. Therefore, safety and general compatibility with the reactor core were very important in considering the use of this filter. To comply with existing regulations a written experiment was submitted to the Kansas State University Reactor Safeguards Committee for consideration. The approved experiment is included in this thesis as Appendix A. For further details concerning the safety and construction of the filter consult Appendix A.

A Canberra Model 7227 (37.5 mm dia., 22.5 mm length, drifted coaxially) germanium lithium-drifted [Ge(Li)] detector was used in the gamma-ray



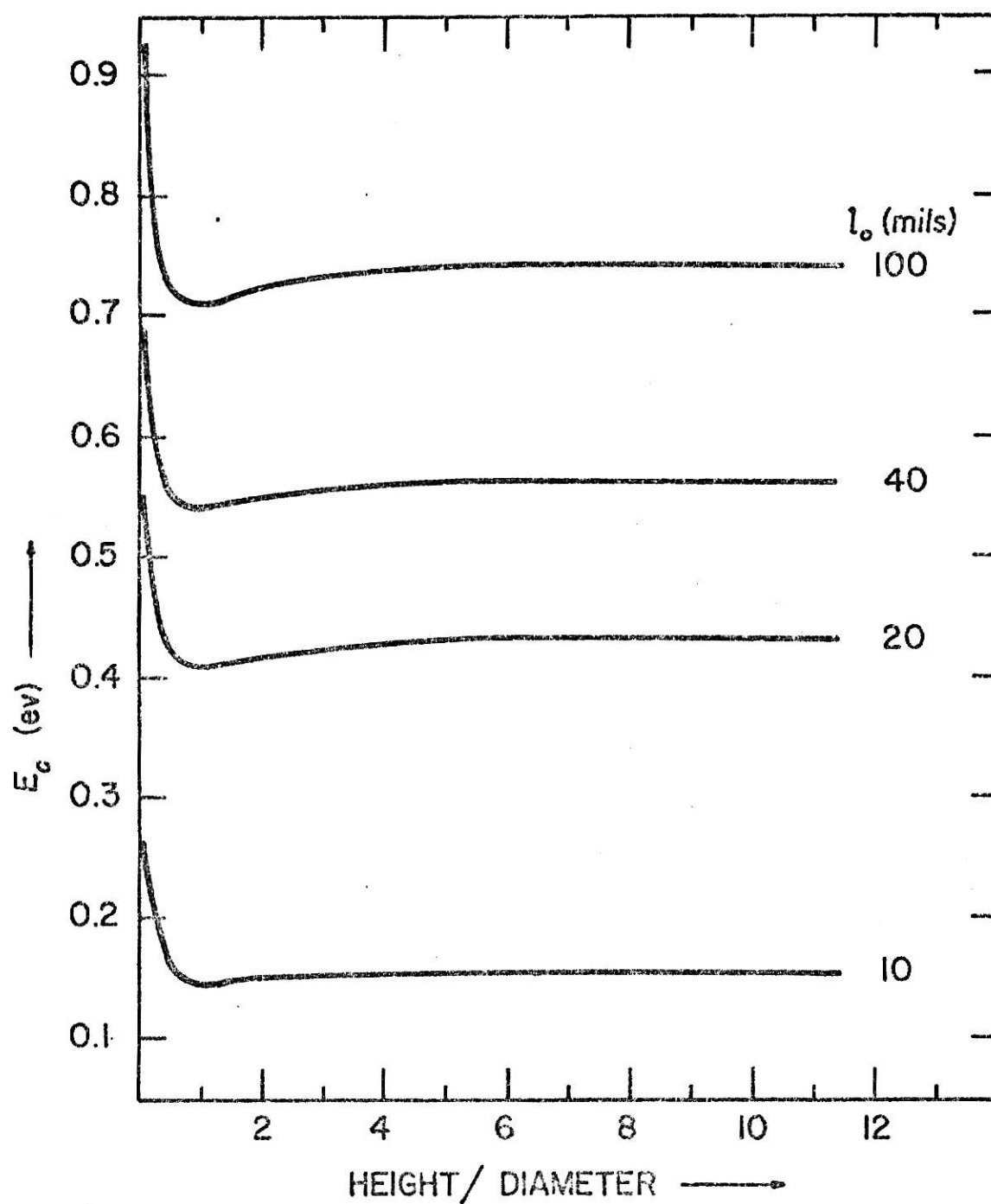


Figure 5. Effective Neutron Cutoff Energies ( $E_c$ ) for Cylindrical Cadmium Filters of Thickness  $l_0$  (12).

spectrometry for this work. A Canberra Model 970 preamplifier was coupled directly to the Ge(Li) detector. The power for the detector was supplied by a Fluke, Model 415 B, high voltage power supply. The main amplifier was an Ortec, Model 451, spectroscopy amplifier, and it was coupled to a Northern Scientific, Model NS-623, analog-to-digital converter (ADC). Data in digital form were transferred from the ADC to a Northern Scientific, Model NS-636 Series Memory Unit, which served as a multichannel analyzer with 4096 channels. Data were then recorded on magnetic tape and a mechanical printer was also available for quick printouts of the data.

The detector was contained in a lead shield to reduce background interference. The inside walls of the container were no less than 4 inches from the source. The walls were lined with copper to reduce X-rays, produced in the lead from source gamma-rays, from interacting with the detector. A plexiglass absorber approximately 0.6 inches thick was used between the detector and the samples to attenuate beta radiation and at the same time reduce the resulting Bremsstrahlung interference. This plexiglass beta-ray absorber was also constructed to provide accurate positioning of the unknown samples so that consistent geometry could be maintained throughout the experiment.

Two digital computers were used in processing the data for this work, an IBM 360/50 and an IBM 370/158.

### 3.0 EXPERIMENTAL

#### 3.1 Preliminary Investigations

Several preliminary experiments were performed in relation to this work before the actual data for record were taken. The purpose of these investigations was to gain information that could be used in the final analysis and also to develop a functional experimental procedure.

##### 3.1.1 Reactivity worth of a cadmium test filter

A small cylindrical filter made of cadmium was constructed and used to obtain information which could be used to predict the performance of a larger filter made of the same material. This test filter was constructed from the same stock material that was to be used for the final filter. Sheet cadmium with a thickness of 20 mils was formed into a cylinder with an approximate height of 3.25 inches and diameter 0.75 inch. It was desired that the final filter be larger than this test filter, thus causing some concern about reactivity effects. Therefore the reactivity worth of the test filter was determined in the central thimble of the TRIGA nuclear reactor. This value was then used to make an estimate of the reactivity worth of a larger filter to be placed in the F-ring of the reactor core. For further information on this estimate see Appendix A. After measuring the reactivity worth of the test filter, two large strips of the stock cadmium were placed inside the test filter and the reactivity worth was redetermined. The new reactivity worth was less than 5% greater than that for the empty test filter, thus indicating that the filter was at least 95% opaque to thermal neutrons. The results of these two reactivity measurements were used in the design of the final filter. They justified the decision that a larger filter was feasible and that a filter thickness greater than 20 mils would be desirable.

### 3.1.2 Preliminary tests using cadmium filters

Several tests were performed with cadmium filters to obtain initial data for use in development of a sound procedure and analysis. These tests were used to determine necessary sample sizes, necessary reference materials, necessary irradiation times, etc. In the case of wheat, these tests helped to show what reactor power levels would be needed and how large the reference samples would need to be for suitable counting statistics. The tests also led to the decision to heat some of the reference compounds to a temperature greater than the boiling point of water to drive the water off before weighing the samples. It was found that this heating procedure especially affected the silicon dioxide. Driving the water from the silicon dioxide caused its weight to drop by several percent. These tests also involved the irradiation of samples without using cadmium filters to make it possible to complete preliminary analyses.

### 3.1.3 Reactivity measurements of the final cadmium filter

The reactivity worth of the cadmium filter used in this work was determined for three different core locations, F7, F8, and F9. The reactivity worth varied from  $\$-0.23$  to  $\$-0.33$  over the three positions. Two different core loadings were involved in these reactivity measurements. The first core (aluminum fuel cladding) yielded a reactivity worth of  $\$-0.33$  for the F7 position, but the second core (stainless steel fuel cladding) yielded a value of  $\$-0.25$  for the F7 position. The second core was used in obtaining the data for record and the majority of the filtered irradiations were performed in the F7 position. The average excess reactivity for this second core was approximately  $\$1.78$  (15).

### 3.1.4 Other investigations

One of the disadvantages of the cadmium filter design was the fact that the polyethylene irradiation container was inside the filter but outside of the samples. Therefore, it was known that some neutron thermalization would take place in this polyethylene, thus tending to reduce the effect of the filter. To obtain an indication of how much thermalization was produced by the polyethylene, two gold foils were irradiated in the container in the filter. One foil was bare and the other was covered with cadmium. If any significant thermalization was taking place then the specific activities of the two foils should have been quite different. It was found that the specific activities differed by only 5.9%. This was not a large enough difference to warrant any changes in the irradiation container.

The linearity and drift of the Northern Scientific multichannel pulse-height analyzer was checked by using several gamma-ray reference sources, such as  $^{60}\text{Co}$ ,  $^{22}\text{Na}$ ,  $^{54}\text{Mn}$ , and  $^{137}\text{Cs}$ . The linearity (less than  $\pm 1\%$  deviation) was satisfactory for the work to be performed. The drift was negligible for count times similar to those to be used. It was possible to reproduce photopeak channel numbers within three channels of the same photopeak energies measured almost two months previously.

Since wheat was the main material to be analyzed in this work, it was desired to determine approximately how much self-shielding would occur during the measurement of the induced radioactivity. All samples were contained in small polyethylene vials approximately one inch high and 7/16 inch diameter. The vials were in an upright position during measurements, with the detector below the vials. A  $^{60}\text{Co}$  source was used to obtain an estimate of the maximum possible error that self-shielding in the wheat

could produce. A measurement of the  $^{60}\text{Co}$  activity was made with the source sitting on top of an empty sample vial, and then a measurement was made with the same source on top of a wheat-filled vial. The 1.33 MeV photopeak was used for this measurement. The difference between the two measurements was approximately 8.6%, and so the maximum error produced by self-shielding had to be less than this on the average, especially for gamma-ray energies greater than 1.33 MeV.

Another investigation was made to determine the uniformity of the fast-neutron flux in the cadmium filter. Iron wire was used for this measurement and only neutron energies great enough to produce the (n,p) reaction with  $^{56}\text{Fe}$  were considered. According to the results from the iron wire there was approximately a 3-4% flux depression in the area of wheat samples relative to reference samples above and below the wheat.

Unrealistic results were encountered in the first attempts to analyze data from the preliminary tests. It was suspected that such results were partially due to interference from radiation being emitted from the polyethylene vials being used to contain the samples. Therefore, an empty vial was irradiated, and the induced radioactivity was observed on the analyzer. It was found that the vial was contributing significant interference with the  $^{28}\text{Al}$  photopeak. Aluminum in the vial was the apparent cause. Buchanan (10) has reported polyethylene vials to contain a few parts per million of aluminum. Therefore, it was necessary to transfer all irradiated samples, including reference samples, to new, clean, weighed vials before making gamma-ray spectrometry measurements. This procedure also eliminated the possibilities of interferences from any materials remaining on the handled vials which were irradiated after being handled.

### 3.2 Measurements for Record

All cadmium filtered irradiations (for data for record) were performed in the F-ring of the KSU TRIGA Mark II nuclear reactor core. The corresponding nonfiltered irradiations were performed in the RSR of the reactor. A greater (fast-neutron flux)/(thermal-neutron flux) ratio was available by using the F-ring of the reactor core instead of the RSR for the filtered irradiations. In fact, such a position for the filter was somewhat optimal. This can be seen by considering Figure 6. In considering an optimal position for a filter it must be realized that the negative reactivity worth of a large filter could severely limit the maximum power level of the TRIGA reactor if it were to be placed in the center of the core. It was found that even using the filter in the F-ring of the TRIGA core reduced the maximum possible reactor power level by approximately 11%. On the other hand, placing a filter in the RSR (in the reflector) would be the least desirable position due to the fast-to-thermal flux ratio. Maximum power levels were desired in this work so that irradiation times could be as small as possible. Short irradiations were necessary since  $^{28}\text{Al}$  with a 2.31 minute half-life was the primary radionuclide of interest. Longer irradiations would present increasing interference from longer lived radionuclides in the sample. The use of the F-ring position for the filter is further supported by fast-neutron activation studies performed by H. P. Yule, et al. Yule (16) used a pneumatic-transfer system with the irradiation position in the F-ring of a TRIGA reactor core and he also incorporated various filter materials for his irradiations.

#### 3.2.1 Reference materials and analyzed samples

The analyzed samples consisted of several varieties of wheat and hair clipped from several horses. One wheat sample was from the 1973 Colorado

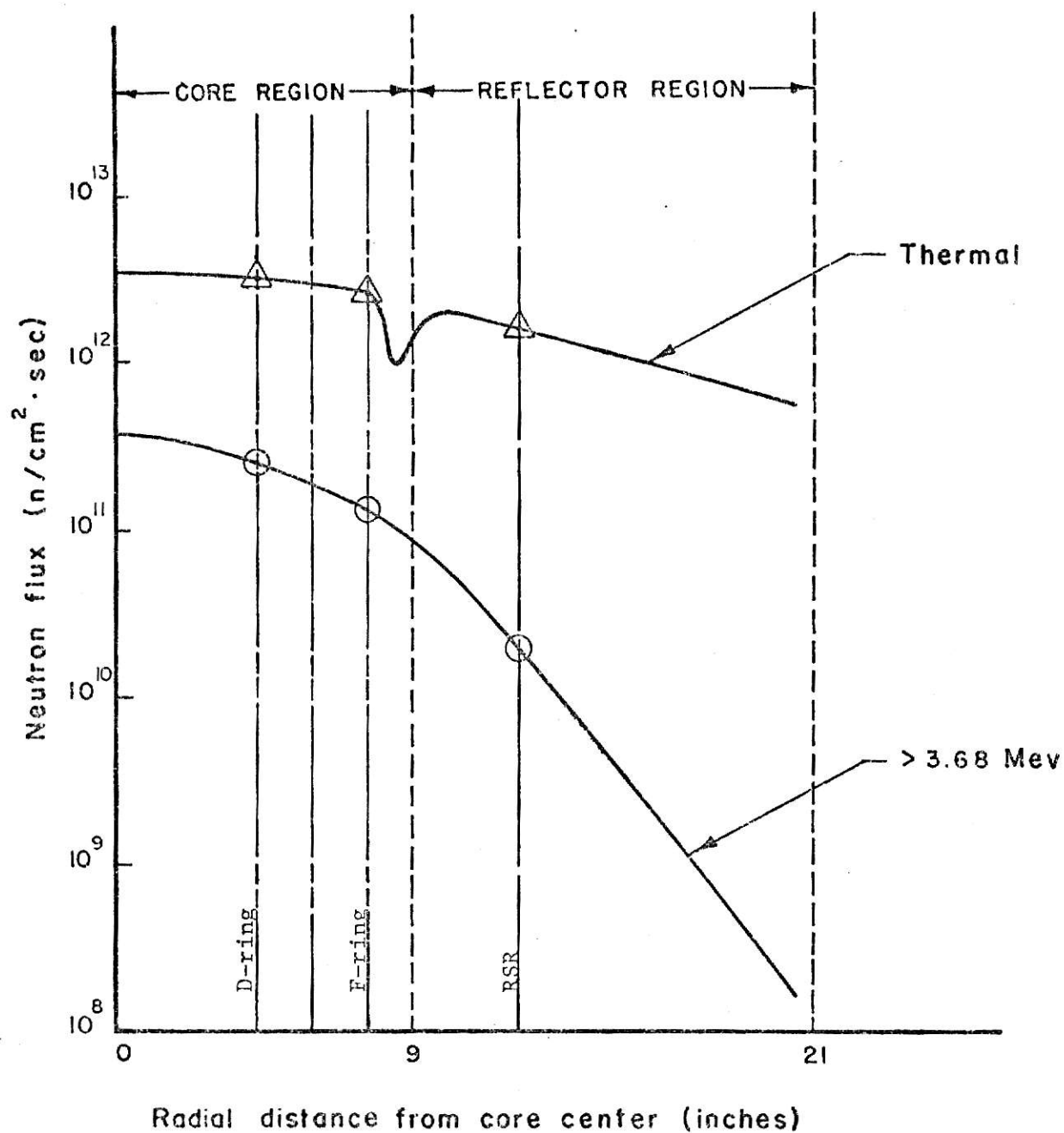


Figure 6. Estimated Neutron Flux Profiles for the KSU TRIGA Mark II Nuclear Reactor.\*

\* The shape of the two neutron flux profiles was based on values from Table I and a general profile of fast and thermal neutron flux in a reflected reactor (23). These profiles do not apply to regions within the fuel.



wheat crop, but the majority of the wheat samples were from the 1973 Kansas crop. The Kansas wheat samples were donated by Mr. Tom Roberts of the Kansas Wheat Improvement Association, Manhattan, Kansas. The Kansas wheat varieties consisted of Eagle, Centurk, and Santanta. The wheat samples were not treated in any way, nor were they handled. Each wheat sample weighed approximately one gram and was contained in a small polyethylene vial approximately one inch in height and 7/16 inch in diameter. The horse hair samples were contained in the same type of vials. Like the wheat samples, they were not treated except for the drying of two of the samples before they were weighed. Each hair sample weighed approximately 0.2 gram.

All weighing of samples and vials was performed on a Mettler balance which had been checked with a standard weight and several precisely weighed foils. The accuracy of the balance was approximately  $\pm 0.0001$  gram. Since irradiated samples had to be transferred to new vials before counting, it was necessary to weigh empty vials before irradiations and then weigh the same vials with the samples in them after the counting was completed.

All compounds used for reference samples were of reagent or better chemical grade. The compounds used were  $\text{NH}_4\text{H}_2\text{PO}_4$  for a phosphorus reference,  $\text{MgO}$  for a magnesium reference,  $\text{CaSO}_4 \cdot 2\text{H}_2\text{O}$  for Ca,  $\text{NH}_4\text{Cl}$  for Cl,  $\text{Al}_2\text{O}_3$  for Al,  $\text{SiO}_2$  for Si,  $\text{MnO}_2$  for Mn,  $\text{Na}_2\text{CO}_3$  for Na, and  $\text{K}_2\text{CO}_3$  for K. The  $\text{MgO}$ ,  $\text{Al}_2\text{O}_3$ ,  $\text{SiO}_2$ ,  $\text{MnO}_2$ ,  $\text{Na}_2\text{CO}_3$ , and  $\text{K}_2\text{CO}_3$  were heated to drive off any water they may have contained before they were weighed. The  $\text{NH}_4\text{H}_2\text{PO}_4$  samples were the largest of any of the reference samples, and they were approximately 0.5 grams in weight. All reference samples were as small as reasonable to minimize flux perturbations.

### 3.2.2 The neutron flux monitor

Iron wire was chosen as a flux monitor for this work. Each wire monitor was approximately 3 inches long and 1/64 inch in diameter. For each irradiation a weighed iron wire was carefully wrapped around the center of the vial containing the sample to be analyzed. The iron wire was in the shape of a helix surrounding the center portion of an unknown sample during irradiation. The iron wire was analytical reagent grade, and each monitor weighed approximately 0.06 gram.

Iron wire was chosen as the flux monitor for several reasons. First, it was easy to manipulate and it did not require a container. Also, it had been used successfully in normal NAA. The iron in each wire formed sufficient quantities of  $^{56}\text{Mn}$  such that the 0.84 MeV photopeak was observed with good counting statistics. The formation of the  $^{56}\text{Mn}$  was due to the (n,p) reaction with  $^{56}\text{Fe}$ ; the Q value for this reaction was -2.9 MeV. This Q value was in the range of Q values of interest, such as -1.9 MeV for  $^{31}\text{P}(\text{n},\alpha)^{28}\text{Al}$ . Therefore, iron was a reasonable flux monitor.

### 3.2.3 Irradiation conditions

Five or six samples were irradiated at one time for the wheat analysis portion of this work. Only one wheat sample was irradiated during a given irradiation, the remaining samples being some of the reference samples. Reference samples were irradiated with each unknown sample to maintain consistent geometry and irradiation conditions throughout the experiment. It was especially important to use reference samples with each irradiation in the cadmium filter to maintain consistent thermalization due to the polyethylene sample containers. Since the primary radionuclide of interest was  $^{28}\text{Al}$  (half-life equals 2.31 minutes) it was only feasible to irradiate one or two unknown samples at one time. There was almost a two minute decay

between the end of an irradiation and the beginning of the first gamma-ray measurement. There was not sufficient time to count more than one or two unknown samples before the  $^{28}\text{Al}$  was essentially reduced to insignificant levels. Samples to be analyzed were placed between reference samples during the irradiations. Care was taken to insure that one sample was not positioned in front of another sample in relation to the center of the core.

A minimum of approximately two days was allowed to elapse between the filtered irradiation of a sample and the nonfiltered irradiation of the same sample. The filtered irradiation was always performed first. A typical filtered irradiation of wheat was for 10 minutes at a reactor power level of 160 kW. This 160 kW was essentially the maximum power level attainable with the filter in the F7 core location. Nonfiltered wheat irradiations were typically for 5 minutes at 150 kW. Typical horse hair irradiations were for 5 minutes at 150 kW. For each irradiation the reactor was brought to the desired power level before the large irradiation vial containing the samples was dropped into the filter or the RSR. At the end of the irradiation the reactor was scrammed and the capsule was retrieved by the RSR specimen-recovery tool as quickly as possible. A stop watch was started when the reactor was scrammed and was then used to measure the elapsed time between the end of the irradiation and the counting of a given sample. Filtered irradiations were performed in the F-ring of the core and nonfiltered irradiations were performed in the RSR.

#### 3.2.4 Counting procedures

All samples were transferred to nonirradiated polyethylene vials before they were counted. A Ge(Li) detector was used for the counting of all samples. Additional details on the equipment can be found in the "Description of

Apparatus" section of this text. Data for a particular sample spectrum were accumulated in 1024 channels of the multichannel analyzer. Most samples were counted for 128 "live" seconds. The analyzer dead time was not greater than approximately 10% for any of the measurements. The lower level control and the zero level control of the ADC were maintained at 0.20 and 0.09 respectively, which made it easier to calculate gamma-ray energies for given channel numbers, i.e., these settings yielded a gamma-ray energy versus channel number plot which essentially crossed the origin at zero energy and zero channel number. Wheat data were measured using amplifier gains of 8.5 and 20. Horse hair data were accumulated using gains of 12.9 and 10. These gains yielded spectra with approximately 2.47 keV/channel for the wheat and 3.26 keV/channel for the horse hair. Typical decay times between the end of irradiations and beginning of counts varied from 90 to 2890 seconds for samples to be analyzed. Spectrum data were transferred from the memory system of the analyzer to magnetic tape which was then used to store the data and also for data processing.

Counting geometry is important in comparative gamma-ray spectrometry. It was given careful consideration in this work. A beta-ray attenuator made of plexiglass was used to position the samples during counting measurements. This attenuator was approximately 0.6 inch thick with a fixture on top of it to hold the cylindrical sample vials in the same position for each measurement. The attenuator was placed directly on the top of the detector. Therefore the samples were counted at an average distance of about 1 inch from the detector. The axis of the sample containers coincided with the axis of the detector. It was not feasible for this particular type of work to make the reference samples in solution form as is often done to maintain

consistent geometry between unknown samples and reference samples. The reference samples essentially represented disc sources of radiation, but the unknown samples (wheat and hair) were approximate cylindrical volume sources of radiation. To provide a correction for this difference the reference samples were positioned at the approximate center of a cylindrical sample vial for their counting. This provided an averaging effect to correct for the differences in the sample sizes. All flux monitors were counted in the same manner. Each iron wire was counted while in the shape of a helix almost identical to the shape it was in during the irradiation.

## 4.0 THE VARIABLE-ENERGY NEUTRON ACTIVATION ANALYSIS

### 4.1 Basic Neutron Activation Analysis

The four nuclear reactions of primary interest in neutron activation analysis (NAA) are the  $(n,\gamma)$ ,  $(n,p)$ ,  $(n,\alpha)$ , and  $(n,2n)$  reactions. The  $(n,\gamma)$  reaction is predominantly produced by thermal neutrons, whereas the  $(n,p)$ ,  $(n,\alpha)$ , and  $(n,2n)$  reactions usually require fast neutrons. For each nuclear reaction the activity of the product nuclide is directly proportional to the number of atoms of the parent nuclide. Therefore, the activity of the product can be used to calculate the amount of the parent which was originally in the sample being studied. The well known differential equation used to describe the rate of change of the product nuclei is

$$\dot{N} = N_0 \sigma \phi - \lambda N, \quad (1)$$

where  $\dot{N}$  represents the rate of change of the number of product nuclei  $N$ .  $N_0$  is the number of parent nuclei,  $\sigma$  is the microscopic cross section for the reaction under consideration,  $\phi$  is the neutron flux, and  $\lambda$  is the decay constant of the product. The parameters  $\phi$  and  $N_0$  are usually considered to be constant. These assumptions are reasonable for most nuclear reactor irradiations since most reactor irradiations are performed during relatively steady-state operations and for relatively short times. Obviously  $N_0$  cannot be a constant if any product nuclei are formed, but nevertheless it can be shown that the assumption of  $N_0$  being a constant produces an insignificant error in the final results (17). With  $N_0$  and  $\phi$  as constants, the solution to equation 1 is simply

$$A_0 = \lambda N = N_0 \sigma \phi (1 - e^{-\lambda t_1}), \quad (2)$$

where  $t_1$  is the time of irradiation in the flux  $\phi$  and  $A_0$  is the activity

of the product at the end of the irradiation. The activity of the product after an elapsed time  $t_w$  from the end of the irradiation would then be  $A$ , where

$$A = A_0 e^{-\lambda t_w} = N_0 \sigma \phi (1 - e^{-\lambda t_i}) e^{-\lambda t_w}. \quad (3)$$

The most common procedure in NAA is to measure the gamma radiation associated with the activity  $A$ . Since most samples contain several types of parent nuclei, such a measurement requires a detector which is sensitive to gamma radiation such that it can differentiate between different gamma-ray energies. Making such measurements thus involves gamma-ray spectrometry.

#### 4.1.1 Gamma-ray spectrometry

There are three basic modes of gamma-ray interaction with matter. These modes are designated as the photoelectric process, the Compton process, and the pair production process. These processes are discussed by many authors (3, 18, 19, 20, 21) and will not be covered in any detail in this text. The photoelectric process, wherein a gamma-ray deposits all of its energy in a material in a single event, is the most useful of the three processes in gamma-ray spectrometry. A suitable detector and amplification system in connection with a multichannel analyzer makes it possible to distinguish a given gamma-ray energy by a characteristic, Gaussian-shaped peak (photopeak) in the analyzer pulse-height spectrum (see Figure 7). As shown in Figure 7, the Compton process also contributes to the gamma-ray spectrum as does the pair production process when the gamma-ray energy is large enough. Even though the pair production process has a 1.022 MeV threshold energy, it is not evident in practice when the gamma-ray energy is below about 1.5 MeV (22). The Compton process produces no significant

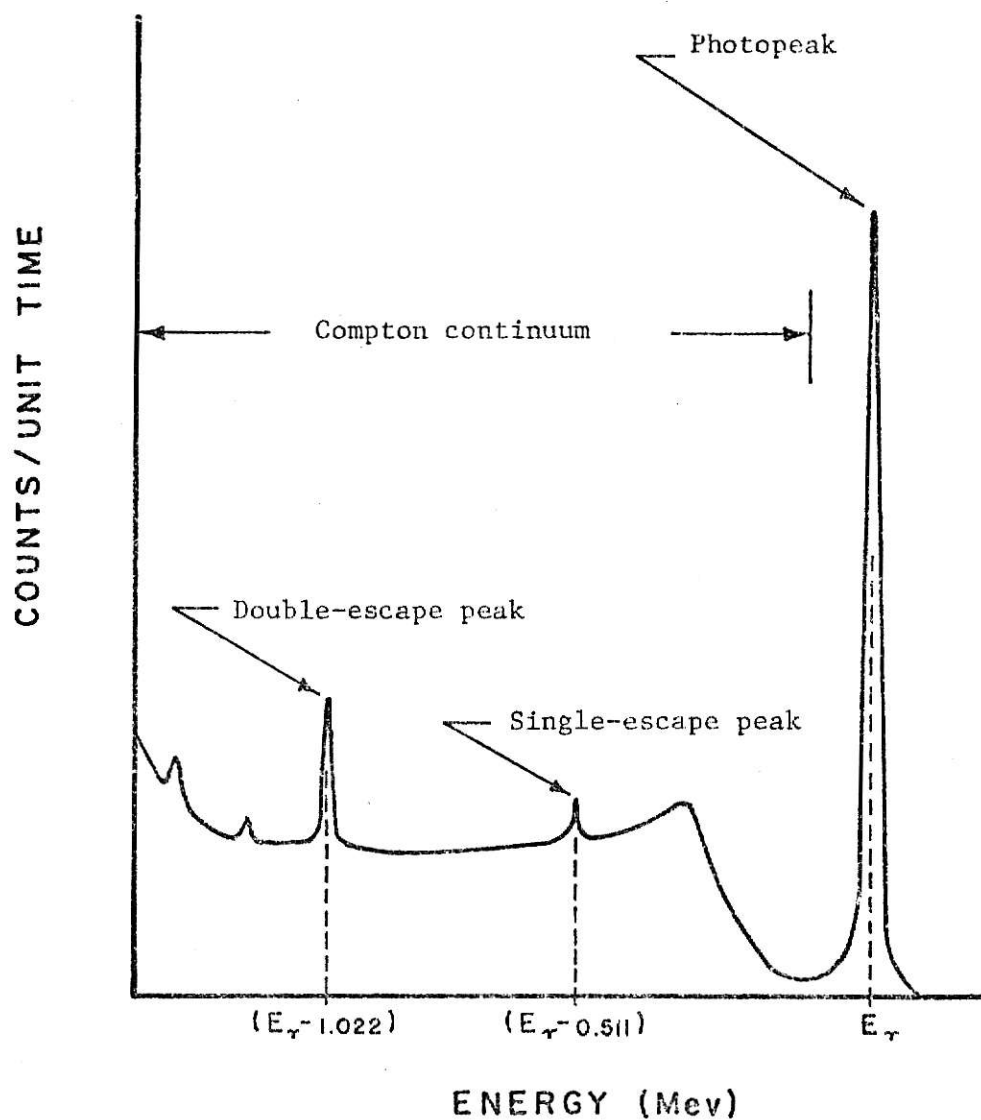


Figure 7. A Typical Spectrum Produced by a Monoenergetic Gamma-Ray Emitter ( $E_\gamma > 1.022$  Mev).



peaks in a gamma-ray spectrum, but the photoelectric and pair production processes do. Photoelectric events produce the photopeak as previously described and pair production events produce peaks known as single-escape peaks and double-escape peaks (see Fig. 7). A pair production event produces an electron-positron pair in the detector material, whereupon the positron is quickly annihilated, yielding two 0.511 MeV gamma-rays. Events where only one of these 0.511 MeV gamma-rays escape the detector undetected leads to the formation of the single-escape peak, but if both 0.511 MeV gamma-rays escape undetected the double-escape peak is formed. So, for a nuclide emitting a single gamma-ray energy greater than about 1.5 MeV, a unique gamma-ray spectrum will be formed with three identifying peaks evident, one photopeak and two escape peaks. An activated sample with several nuclides in it could then yield a spectrum which would be the superimpositions of many photopeaks, escape peaks, etc.

Theoretically the photopeak should be a spike in a gamma-ray spectrum, but due to the statistical nature of the detection process in a Ge(Li) detector, the spike is spread out to form an approximate Gaussian-shaped peak. Basically, a determination of the area under a photopeak can be used to calculate the number of nuclei in the sample which produces the photopeak. This area is directly proportional to the activity  $A$  in equation 3. Knowing other factors to relate the area to  $A$  it is ultimately possible to obtain  $N_0$ , the number of parent nuclei in the sample. The escape peaks are superimposed on the Compton continuum, and therefore this continuum must be taken into account in calculating their areas. A sample containing many nuclides usually yields a rather complex gamma-ray spectrum and resolving all the necessary components of the spectrum is the desired result of gamma-ray spectrometry in NAA.

#### 4.1.2 Comparative analysis using a flux monitor

There are two major types of neutron activation analysis. They are designated as (1) comparative and (2) absolute. Absolute NAA assumes that the cross sections and neutron energy distributions are well known, thus making it possible, by the previous discussion, to determine the  $N_0$  of equation 3. A reactor neutron spectrum covers a wide range of energies. Since cross sections are neutron-energy dependent, it becomes a very complex process to perform an analysis of even the simplest material by the absolute method when using a reactor as a source of neutrons. Consequently, this method is used very little. The comparative method of NAA is used extensively, because it tends to cancel out ambiguities in cross sections and neutron energy distributions. It also tends to cancel out uncertainties in branching ratios and isotopic abundances.

Comparative NAA simply involves the comparison of an unknown sample to a known sample, or to a group of known samples. At least one known sample is required for each element that is to be considered in the analysis of the unknown. This method requires that the known samples and unknown samples experience identical irradiation conditions and identical counting geometries. To achieve identical irradiation conditions the known and unknown samples are often irradiated together. If many known samples are necessary, however, it often becomes necessary to irradiate the known samples and unknown samples at different times. Also, it is not feasible, in many cases, to measure all the known samples for each unknown sample measurement. As previously mentioned, in this work only one or two unknown samples were irradiated at one time. So, it was not feasible in this work, as in many comparative neutron activation analyses, to irradiate and measure all the known samples

for each unknown irradiation. In a situation such as this it is necessary to use a suitable flux monitor to make it possible to relate irradiations which are performed separately. Each known sample and each unknown sample must be irradiated with a flux monitor which acts as a factor to essentially normalize all the samples to identical irradiation conditions. The valid use of the flux monitor requires that the neutron-energy spectrum remain constant from irradiation to irradiation. When each sample is irradiated in the same position in a reactor, such as the TRIGA reactor, it is reasonable to assume that the neutron-energy spectrum is constant and therefore that use of a flux monitor is valid.

Comparative analysis using a flux monitor can be demonstrated in the following manner. Of course not all samples are measured (counted) at the same time after the end of an irradiation. For this reason it is necessary to correct the activity of all samples to the activity at a certain time, usually the time at the end of the irradiation. The activity of a sample at the end of its irradiation has been expressed as  $A_o$  in equations 2 and 3. This activity is obtained by solving equation 3 for  $A_o$ , that is,

$$A_o = Ae^{\lambda t_w} \quad (4)$$

where  $A$  is the measured activity after the elapsed time  $t_w$ . Therefore, using equation 3, it is possible to relate the samples and flux monitors for a single unknown sample and a single known sample as follows:

$$f = \frac{\frac{A_{ou}}{A_{oFu}}}{\frac{A_{ok}}{A_{oFk}}} = \frac{\frac{A_u e^{\lambda_u t_{wu}}}{A_{Fu} e^{\lambda_F t_{wFu}}}}{\frac{A_k e^{\lambda_k t_{wk}}}{A_{Fk} e^{\lambda_F t_{wFk}}}} \quad (5)$$

where  $f$  is the fraction of the given element in the unknown sample, and where all the activities have been normalized to a unit mass. For example,  $A_u$  is the activity of the unknown sample per unit mass of the unknown sample and  $A_{Fu}$  is the activity of the flux monitor, used with the unknown sample, per unit mass of flux monitor material. The subscripts  $u$ ,  $F$ , and  $k$  denote values for the unknown sample, the flux monitors, and the known sample, respectively. The known sample is assumed to contain a known amount of the given element being measured in the unknown sample. It has been assumed in this simple example that the measured activity of the unknown sample has been produced entirely by the "given element." In many situations a given radionuclide is produced from several different elements in the sample; in such situations all modes of production of that radionuclide should be considered.

Flux monitor materials are usually chosen such that they emit gamma radiation at a suitable energy with reasonable counting statistics. Elemental iron and copper are common flux monitors. In this particular work the primary nuclear reaction in the flux monitor was important. Iron was chosen as the flux monitor because of its ease of handling and because it undergoes the  $(n,p)$  reaction to the extent that sufficient  $^{56}\text{Mn}$  is formed for suitable counting statistics.

#### 4.2 Formulation of the Variable-Energy Analysis

Basic neutron activation analysis assumes that each radionuclide, in an irradiated sample, has been produced by only one parent nuclide. When both fast and thermal neutrons are used for the irradiation this assumption is often not valid. Most nuclear reactor irradiations (performed near the core of the reactor) will involve significant fast and thermal-neutron fluxes. The fast-neutron reactions usually have such small cross sections that they

can be neglected, but particularly when a thermal-neutron filter is used the fast-neutron activation reactions should be considered. In this work the primary element of interest was phosphorus. It was detected in a sample by observing the gamma radiation from  $^{28}\text{Al}$  produced by the fast-neutron,  $(n,\alpha)$  reaction with  $^{31}\text{P}$ . The problem was, however, that other neutron reactions could also produce  $^{28}\text{Al}$ , these reactions being  $^{27}\text{Al}(n,\gamma)^{28}\text{Al}$ ,  $^{28}\text{Si}(n,p)^{28}\text{Al}$ , and the second-order reaction  $^{26}\text{Mg}(n,\gamma)^{27}\text{Mg} \rightarrow ^{27}\text{Al}(n,\gamma)^{28}\text{Al}$ , this second-order reaction resulting from the beta decay of the  $^{27}\text{Mg}$  during the irradiation. Koch (1) reports that this second-order reaction can present significant problems in the analysis of  $^{28}\text{Al}$  when Mg is present in the sample. The total  $^{28}\text{Al}$  activity of an unknown sample would then be due to the sum of the activities from these various reactions. Assuming the comparative method of NAA and a known sample for each possible reaction irradiated with the unknown, the following equation can be written.

$$A_{\text{P} \rightarrow \text{Al}} f_{\text{P}} + A_{\text{Al} \rightarrow \text{Al}} f_{\text{Al}} + A_{\text{Si} \rightarrow \text{Al}} f_{\text{Si}} + A_{\text{Mg} \rightarrow \text{Al}} f_{\text{Mg}} = A_{\text{Al}} \quad (6)$$

The right-hand side of this equation represents the  $^{28}\text{Al}$  activity of the unknown sample corrected to the time at the end of the irradiation. The "f" values represent the fraction of their subscripted elements which exist in the unknown. The "A" values on the left-hand side of the equation represent the  $^{28}\text{Al}$  activities of the known samples for each of the possible reactions. The subscripts on the left-hand side of the equation denote the particular reactions for each A value, i.e.,  $A_{\text{P} \rightarrow \text{Al}}$  implies the activity from the  $^{31}\text{P}(n,\alpha)^{28}\text{Al}$  reaction. Three more equations are necessary to determine the four "f" values. It is possible to generate three additional equations by using variable-energy activation analysis, which in this work meant two separate irradiations, one cadmium-filtered irradiation and one nonfiltered

irradiation. Figure 8 indicates how two equations can be formed by considering the production of  $^{27}\text{Mg}$ . A general equation for the  $^{27}\text{Mg}$  activity produced simultaneously with the  $^{28}\text{Al}$  is,

$$A_{\text{Mg} \rightarrow \text{Mg}}^f f_{\text{Mg}} + A_{\text{Al} \rightarrow \text{Mg}}^f f_{\text{Al}} + A_{\text{Si} \rightarrow \text{Mg}}^f f_{\text{Si}} = A_{\text{Mg}}^f \quad (7)$$

The symbols in equation 7 are similar in meaning to those in equation 6.

If equations 6 and 7 are applied to two separate irradiations, then the following set of linear equations can be written, where the superscript "Cd" represents a filtered irradiation and "B" represents a nonfiltered irradiation.

$$\begin{aligned} A_{\text{P} \rightarrow \text{Al}}^{\text{Cd}} f_{\text{P}} + A_{\text{Al} \rightarrow \text{Al}}^{\text{Cd}} f_{\text{Al}} + A_{\text{Si} \rightarrow \text{Al}}^{\text{Cd}} f_{\text{Si}} + A_{\text{Mg} \rightarrow \text{Al}}^{\text{Cd}} f_{\text{Mg}} &= A_{\text{Al}}^{\text{Cd}} \\ A_{\text{Al} \rightarrow \text{Mg}}^{\text{Cd}} f_{\text{Al}} + A_{\text{Si} \rightarrow \text{Mg}}^{\text{Cd}} f_{\text{Si}} + A_{\text{Mg} \rightarrow \text{Mg}}^{\text{Cd}} f_{\text{Mg}} &= A_{\text{Mg}}^{\text{Cd}} \\ A_{\text{P} \rightarrow \text{Al}}^{\text{B}} f_{\text{P}} + A_{\text{Al} \rightarrow \text{Al}}^{\text{B}} f_{\text{Al}} + A_{\text{Si} \rightarrow \text{Al}}^{\text{B}} f_{\text{Si}} + A_{\text{Mg} \rightarrow \text{Al}}^{\text{B}} f_{\text{Mg}} &= A_{\text{Al}}^{\text{B}} \\ A_{\text{Al} \rightarrow \text{Mg}}^{\text{B}} f_{\text{Al}} + A_{\text{Si} \rightarrow \text{Mg}}^{\text{B}} f_{\text{Si}} + A_{\text{Mg} \rightarrow \text{Mg}}^{\text{B}} f_{\text{Mg}} &= A_{\text{Mg}}^{\text{B}} \end{aligned} \quad (8)$$

Thus, using these four equations it is theoretically possible to solve for the four desired "f" elemental concentration values. All activities in equation 8 would of course be corrected to the end of irradiation; the known or reference activities would be per unit mass of the given element in the reference sample. The use of a flux monitor is also assumed. Although these equations have been written for a specific case, similar sets of equations are possible for other nuclides.

#### 4.3 Initial Analysis Methods

There are various methods used in gamma-ray spectrometry to determine the activity of measured samples. In comparative gamma-ray spectrometry it is not necessary to know the absolute activity of a given nuclide in a sample,

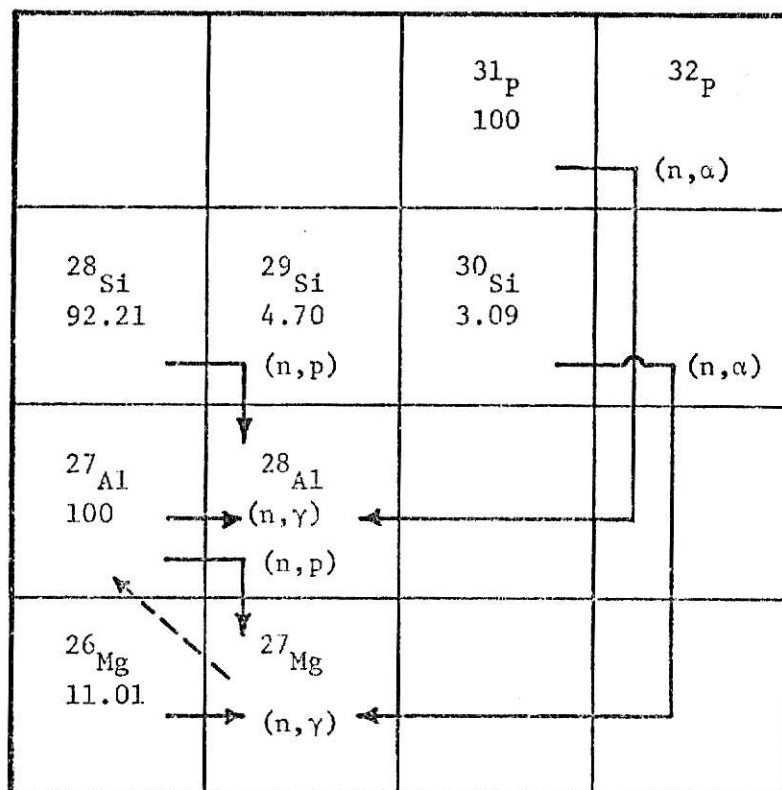


Figure 8. Nuclear Reaction Diagram Showing the Possible Modes of Production of Al-28 and Mg-27.\*

\* Isotopic abundances (in percent) are shown below the nuclide identifications (24). Reactions are identified in parentheses. The dashed line represents the beta decay of Mg-27 to Al-27.

but the nuclide in the unknown sample must be measured in the same manner as the same nuclide in the known sample. This means that a consistent method must be used in determining the area under the photopeaks used for the analysis. Many different approaches have been taken in the determination of photopeak areas and the first method used in this work is probably the most common approach for first approximations in NAA.

As shown in Figure 7, a photopeak is not a pure Gaussian even for a monoenergetic gamma-ray. Furthermore, when a complex unknown is observed, it is usually found that most photopeaks are superimposed on Compton continua of other nuclides. Therefore, it becomes necessary to determine how much of a given photopeak is actually due to photoelectric events of gamma-rays at that energy. This usually involves the subtraction of some portion of the area under the peak from the total area.

The first method used in this work was performed manually. It involved finding the minimum (in the valley) on each side of the photopeak under consideration and then calculating the average number of counts per channel over each minimum channel count and several channels adjacent to the minima. This average value per channel was then subtracted from the total number of counts in each channel within the photopeak. The effective area under the photopeak was then calculated as the summation of these corrected counts over all the channels within the photopeak. Only one photopeak was used for each nuclide considered. This method proved to be unsuccessful when the computed activities were placed in the system of equations, i.e., equations 8. Several assumptions were made which eliminated some of the terms in the equations, but it was still not possible to obtain reasonable solutions to the equations. For this reason, and also because this method involved a subjective decision for each photopeak, it was decided to try another approach. Also, this method did



not account for the statistical nature of the detection process. Gamma-ray spectral analysis usually involves fitting data to some function by the method of least squares. Therefore the next approach to the analysis involved the use of the method of least squares.

The second approach to the analysis involved two least-squares fits per photopeak. This approach, like the first, used only one photopeak per nuclide as an indication of the activity due to that nuclide. The first step in this approach was to find the minimum in the valley on each side of a chosen photopeak. Next, four channels adjacent to each minimum channel were chosen. The total counts in each channel were used in a least-squares fit of the two minima channels and the eight adjacent channels to a straight line function. This linear function then served as the effective equation for the Compton continuum in the region of the photopeak. The next step involved the choice of which channels were to be used in the least-squares fit of the photopeak to a Gaussian function. Since the right-hand side of a photopeak usually more closely approximates a Gaussian shape, those channels near the top of the photopeak and those on the right-hand side of the peak were used in the fitting routine. Due to the excellent resolution of the Ge(Li) detector, the photopeaks required very few channels and therefore the greatest number of points used in a given Gaussian fit was 6.

After the channels to be used in a given photopeak least-squares fit were chosen, it was possible to make use of the Compton continuum function previously determined by a least-squares method. The Compton continuum function made it possible to estimate the contribution to a particular channel count which was due to Compton events. Therefore, a channel number to be used in the photopeak fit was substituted into the Compton continuum function to determine what portion of its total count was due to Compton

events. This portion was then subtracted from the total counts in that channel to give the real value due to photoelectric events. The Compton continuum was subtracted from each photopeak channel count before the photopeak data were fitted to a Gaussian function.

A computer program was used to perform both least-squares fits for the second approach. The same program also incorporated the statistical analysis of the Gaussian fits. After the fits were determined, the computer program was used to calculate the areas under the Gaussian curves. These areas were then used to calculate the activities to be used in equations 8. Substitution of these activities into equations 8 yielded unrealistic solutions. Simplifying assumptions were made, as in the first approach, but the results were still not feasible. Therefore, it was decided to try the approach which follows.

The two preceeding initial analysis attempts are included in this thesis for sake of completeness. Both depict methods which might be satisfactory in some cases. The outstanding weakness of each approach was that a least squares method was not used to solve Eqs. 8. The final method of analysis did use a least squares solution of Eqs. 8.

#### 4.4 The Final Method of Analysis

The normal gamma-ray spectrum acquired from an unknown sample can be represented by

$$y_i = \sum_{j=1}^m f_j a_{ij} \quad (i = 1, 2, 3, \dots, n), \quad (9)$$

where  $y_i$  is the total number of counts in the  $i$ -th channel per unit time per unit mass of the unknown;  $f_j$  is the fraction of the  $j$ -th element in the unknown, and  $a_{ij}$  is the total number of counts in the  $i$ -th channel per unit time per unit mass of the  $j$ -th element in the reference sample used for the

comparative analysis for the  $j$ -th element; the number of elements to be considered is  $m$ , and  $i$  varies from 1 to the total number of channels,  $n$ , in the spectrum. Thus, a system of equations, similar to Eqs. 8, can be used to perform the analysis of an unknown on a channel-by-channel basis. Such an analysis using modern Ge(Li) detector spectrometer systems is not always economical, however, because the spectra normally involve 1024 to 4096 channels. Therefore, a method has been developed which uses only certain selected channels in connection with equation 9. These channels are chosen to coincide with photopeaks and escape peaks associated with the elements being analyzed. By using a method such as this, the amount of data processing and computer time can be substantially reduced. Furthermore, it has been reported that this method, referred to as "area-of-interest unfolding" (AOI), improved analytical results in some instances (25).

The  $y_i$  and  $a_{ij}$  values of Eq. 9 are measured quantities and the objective of NAA is to estimate the required  $f_j$  values to satisfy the group of equations that are generated. Due to the statistical nature of radioactive decay and the detection processes, it is not possible to obtain  $f_j$  values which will exactly satisfy all the equations. Therefore, a least-squares analysis is appropriate. To accomplish a least-squares analysis, an error term must be added to Eq. 9, i.e.,

$$y_i = \sum_{j=1}^m f_j a_{ij} + e_i \quad (i = 1, 2, 3, \dots, n). \quad (10)$$

The error term,  $e_i$ , is then the difference between the measured  $y_i$  and the estimate for  $y_i$  generated by the summation.

It is physically impossible to have negative fractions of any elements in a sample and therefore Eq. 10 must be constrained in the analysis, i.e.,

$$f_j \geq 0 \quad (j = 1, 2, 3, \dots, m). \quad (11)$$

Several assumptions are usually made when a least-squares NAA is performed. The residuals are assumed to be normally distributed, and the channel data of the pulse height spectra are assumed to be statistically independent of each other. Other assumptions are given in this thesis and in the literature (3, 26, 27, 28). It is convenient to express Eq. 10 in matrix form, i.e.,

$$\underline{Y} = \underline{A} \underline{f} + \underline{e}, \quad (12)$$

where  $\underline{Y}$  is an  $(n \times 1)$  vector of normalized data from the areas-of-interest in the unknown sample ( $n$  equals the number of areas-of-interest);  $\underline{A}$  is an  $(n \times m)$  matrix generated by the  $m$  reference samples for the  $n$  areas-of-interest;  $\underline{f}$  is an  $(m \times 1)$  vector of the estimated fractions of the  $m$  elements in the unknown sample;  $\underline{e}$  is an  $(n \times 1)$  vector of the errors associated with the estimates made for  $\underline{f}$ . It is necessary that the number of areas-of-interest,  $n$ , be chosen such that  $n$  is greater than  $m$ . The sum of the squares of the error values (residuals) can now be expressed in matrix form as

$$\underline{e}^T \underline{e} = (\underline{Y} - \underline{A} \underline{f})^T (\underline{Y} - \underline{A} \underline{f}). \quad (13)$$

The superscript  $T$  represents the transpose of the matrix to which it is applied. Thus, the method of least squares calls for estimates for the elements of the  $\underline{f}$  vector such that  $\underline{e}^T \underline{e}$  is a minimum. If it is assumed that the  $\underline{f}$  parameters are known then  $\underline{e}^T \underline{e}$  can be minimized by differentiating each of its elements with respect to the appropriate  $\underline{f}$  values and equating the results to zero. In matrix form these results can be expressed as

$$\underline{A}^T \underline{A} \underline{f} = \underline{A}^T \underline{Y} \quad (17) \quad (14)$$

The variances associated with the measurements of the reference samples can be made to be negligible in comparison to those for the unknown samples. Therefore, the elements of the  $\underline{A}$  matrix in Eq. 14 are often considered to

have zero variance. The validity of the method of least squares requires that the variances associated with all the elements of  $\underline{Y}$  be identical, but since this does not occur experimentally, it is necessary to introduce a weighting matrix in Eq. 14 (28). This weighting matrix,  $\underline{W}$ , is assumed to be a diagonal matrix, the diagonal elements of which are the reciprocals of the  $\underline{Y}$  variances. Therefore, Eq. 14 can be changed to,

$$(\underline{A}^T \underline{W} \underline{A}) \underline{f} = \underline{A}^T \underline{W} \underline{Y} \quad (15)$$

The estimated solution vector  $\underline{f}$  can now be represented as

$$\underline{f} = (\underline{A}^T \underline{W} \underline{A})^{-1} (\underline{A}^T \underline{W} \underline{Y}) \quad (16)$$

where the  $-1$  designates the inverse of the  $(\underline{A}^T \underline{W} \underline{A})$  matrix. The variance of the  $j$ -th element of  $\underline{f}$  is equal to the  $(j,j)$  element of the  $(\underline{A}^T \underline{W} \underline{A})^{-1}$  matrix (28).

Three computer codes were used in the final analysis for this work. The first code, TRAPL, was routinely used throughout the work to transfer data from magnetic tapes to printed data, punched computer cards, and plots of the gamma-ray spectra. A second code, NORM, was used to normalize the data from the reference samples. This code was also used to extract the normalized data for the chosen areas-of-interest. The extracted data were then used in the final analysis code, referred to as the AOI (area-of-interest) code.

The AOI code was developed from an area-of-interest code used to perform routine NAA (25). The original code was modified to perform the variable-energy NAA for this work. The AOI code was based on the least-squares matrix formulation of the NAA problem as previously developed in this section.

Equations 8 can easily be applied to the matrix formulation in Eq. 16. In this work the cadmium-filtered data were used to form the upper half of

the A matrix and the upper half of the Y vector of Eq. 16. The nonfiltered data were used to form the lower halves of the A matrix and Y vector. All data were normalized to a certain irradiation time and to a certain neutron flux. The  $\underline{A}^T \underline{W} \underline{A}$  matrix was formed first. This symmetrical matrix was then inverted using "successive congruent transformations" (see Appendix C). Each peak in the analysis formed three areas-of-interest; data from the two channels below the peak channel formed one area; the peak channel data formed the second area; data from the two channels above the peak channel formed the third area. The  $\underline{A}^T \underline{W} \underline{Y}$  matrix was then formed, thus making it possible to form the f vector, the elements of which were the estimates for the concentrations of the chemical elements under consideration. The code also computed the standard deviation for each of the estimated concentrations. See Appendix C for a listing of the extraction routine and the modified AOI code.

It was indicated previously that the Compton continuum contribution to a photopeak should be removed from the total area of the photopeak to obtain a true indication of the number of photoelectric events. This correction was applied during initial analysis attempts, but it was not necessary in the AOI method of analysis. The AOI method accounted for the Compton contribution by assuming that each significant element in the sample would be included in the summation as represented in Eq. 10. Thus, it was necessary to qualitatively determine the major elements contributing to the total spectrum of a typical unknown. After these major elements were determined it was possible to generate their reference spectra to be used in the quantitative analysis. All other radionuclides which were not prominent in the gamma-ray spectra were assumed to produce minor errors when not included in the analyses. The elements and respective gamma-ray energies considered

for this work are given in Table II. Some escape peaks, determined by the gamma-ray energies, were also considered. Typical raw-data gamma-ray spectra of these reference elements, for both cadmium-filtered and non-filtered neutron irradiations, are shown in Appendix B.

Due to the relatively short half-life of  $^{28}\text{Al}$  it was necessary to modify the normal expression for the measured activity of the  $^{28}\text{Al}$ . This was necessary since all samples were counted for periods of time which were comparable to the  $^{28}\text{Al}$  half-life. The theoretical expression for the activity at the end of an irradiation is given by Eq. 4. The activities,  $A_0$  and  $A$ , in Eq. 4 represent activities of the considered nuclide at certain points in time. Since it takes time to actually measure the activity of a radionuclide the equation must be modified to suit this experimental limitation. If the length of time used to measure the activity is short compared to the half-life of the nuclide under consideration then Eq. 4 can be expressed as

$$A_0 = \frac{C e^{\lambda(t_w + 0.5t_c)}}{t_c}, \quad (17)$$

where  $C$  is the total number of counts accumulated during the count time  $t_c$ , and  $t_w$  is the elapsed time (decay time) between the end of the irradiation and the beginning of the count. This expression assumes that there is negligible decay during the count, but if the count time becomes comparable to the half-life this assumption is not valid. If the later case should occur then the following procedure should be used.

The activity at the beginning of the count is assumed to be  $A_1$ . Therefore,

$$A_1 = A_0 e^{-\lambda t_w}. \quad (18)$$

TABLE II

Radionuclides and Their Respective Gamma-Ray  
Energies and Half-Lives Considered for the AOI Analyses. \*

<u>Nuclide</u>	<u>Half-Life (min.)</u>	<u>Gamma-Ray Energies (MeV)</u>
$^{28}\text{Al}$	2.31	1.7789
$^{27}\text{Mg}$	9.5	1.0144
		0.8438
		0.1708
$^{38}\text{Cl}$	37.3	2.1676
		1.6427
$^{56}\text{Mn}$	154.8	2.1126
		1.8112
		0.8466
$^{49}\text{Ca}$	8.8	3.0844
$^{24}\text{Na}$	900	2.7539
		1.3685
$^{42}\text{K}$	744	1.5247

\* Energies and half-lives were taken from M. A. Wakat's "Catalogue of  $\gamma$ -Rays Emitted by Radionuclides" --- (29).



The total number of counts accumulated during the count time,  $t_c$ , would then be

$$C = \int_0^{t_c} A_1 e^{-\lambda t} dt = \frac{A_1 (1 - e^{-\lambda t_c})}{\lambda} = \frac{A_o e^{-\lambda t_w} (1 - e^{-\lambda t_c})}{\lambda} \quad (19)$$

So, the expression for  $A_o$  would then be,

$$A_o = \frac{\lambda C e^{\lambda t_w}}{(1 - e^{-\lambda t_c})} \quad (20)$$

It was necessary to use  $A_o$  as given in Eq. 20 for the  $^{28}\text{Al}$  measurements in this work. This expression was also used for the other nuclides which were considered. This was possible since it is actually more exact than the normal expression even for normal, short count time, measurements.

All activities in the final method of analysis were normalized, not only with respect to neutron flux and mass, but also to a standard irradiation time,  $t_s$ . To achieve this it was necessary to correct the activities to their saturation values and then to the standard irradiation time. The saturation activity,  $A_s$ , can be expressed as

$$A_s = \frac{A_o}{(1 - e^{-\lambda t_i})} \quad (21)$$

where  $t_i$  is the irradiation time. The activity normalized to a standard irradiation time is  $A_{st}$ ,

$$A_{st} = A_s (1 - e^{-\lambda t_s}) = \frac{A_o (1 - e^{-\lambda t_s})}{(1 - e^{-\lambda t_i})} \quad (22)$$

## 5.0 RESULTS AND CONCLUSIONS

The cadmium filter technique described in this work was used to successfully analyze wheat for phosphorous content. This method exhibited three distinct advantages over the Bremsstrahlung method of determining phosphorus content; the later method involves the measurement of the Bremsstrahlung radiation resulting from the decay of  $^{32}\text{P}$ . First, the cadmium filter technique used gamma-ray spectrometry which made it possible to identify a given nuclide by its characteristic gamma-ray energies. The continuous spectrum of beta particles (and thus Bremsstrahlung radiation) from  $^{32}\text{P}$  makes it almost impossible to differentiate between the Bremsstrahlung from  $^{32}\text{P}$  and that which may result from other radionuclides in a sample. Thus, for a complex sample the Bremsstrahlung method would yield ambiguous results. Second, the Bremsstrahlung method includes the production of  $^{32}\text{P}$  by reactions other than the  $(n,\gamma)$  reaction. This could lead to significant errors, especially in analyses of biological samples, since sulfur and chlorine can also produce  $^{32}\text{P}$  by the  $(n,p)$  and  $(n,\alpha)$  reactions respectively. The cadmium filter technique differentiates between the  $(n,\gamma)$ ,  $(n,p)$ , and  $(n,\alpha)$  reactions and uses these reactions to achieve the analysis for the phosphorus content. The third advantage of the filter technique was the time required for an analysis. A typical decay time of 14 days is required in the Bremsstrahlung method. This decay time hopefully allows other interfering nuclides to decay to insignificant levels before the measurement is made. Only a few days were necessary for a cadmium filter analysis, and refinements of the technique could probably reduce this time significantly.

Typical raw-data gamma-ray spectra of wheat are shown in Figure 9. If the two spectra are compared it is possible to see that the cadmium

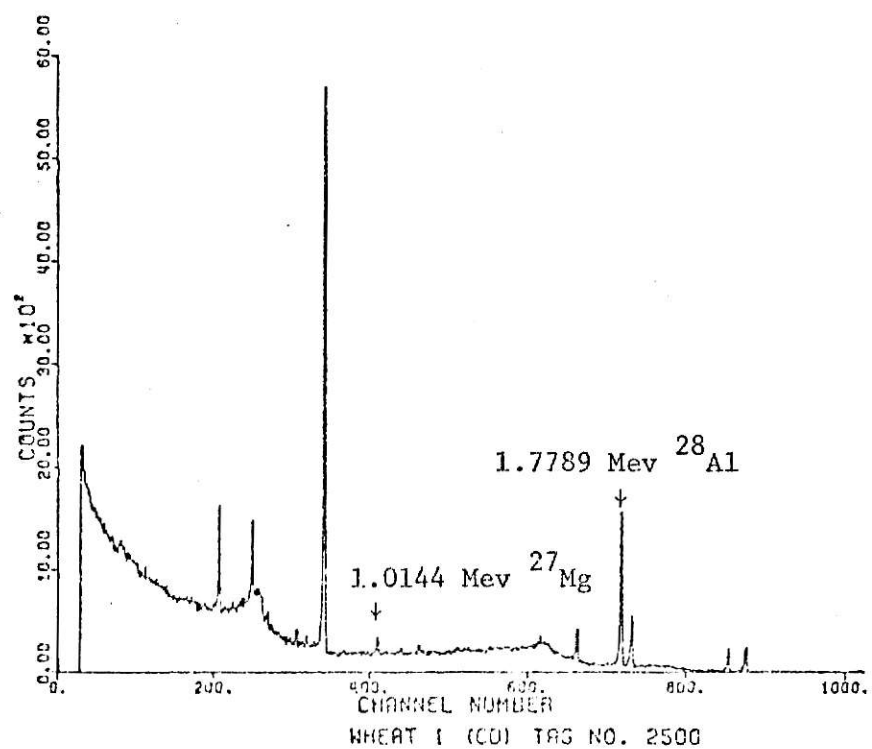
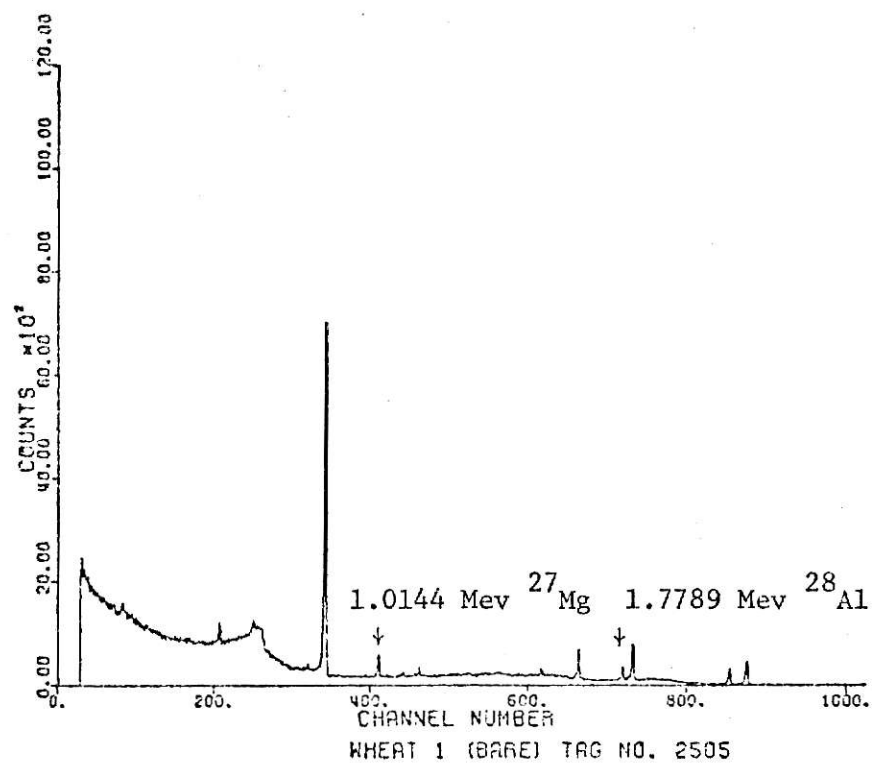


Figure 9. Typical Gamma-Ray Spectra of Wheat. Cadmium-Filtered Irradiation--(CD), Nonfiltered Irradiation--(BARE).

filter does indeed change the relationships among the various products, especially those relationships involving  $^{28}\text{Al}$ . The production of distinctly different coefficients for the system of equations can be seen by comparing the spectra in Appendix B. The largest peak in each spectrum of Fig. 9 points out one of the interferences that was experienced in this work. This peak is composed of counts from both  $^{27}\text{Mg}$  (0.8438 MeV) gamma-rays and  $^{56}\text{Mn}$  (0.8466 MeV) gamma-rays. Due to the nature of the method of analysis, it was therefore necessary to use the 1.0144 MeV photopeak for the analysis for  $^{27}\text{Mg}$ . Single- and double-escape peaks, from 1.7789 MeV  $^{28}\text{Al}$  for instance, are not visible in Fig. 9. Such peaks were observed, however, in numerical listings of the spectra. It was not possible to use the  $^{28}\text{Al}$  escape peaks due to interferences from  $^{31}\text{Si}$ .  $^{31}\text{Si}$  emits a 1.2662 MeV gamma-ray which essentially coincides with the single-escape peak from  $^{28}\text{Al}$  at 1.2679 MeV (29). The difference between these two energies is only 1.7 keV which is less than the resolution of the detector. Also, there would be interference in the double-escape peak from  $^{28}\text{Al}$  since it would coincide with the single-escape peak from  $^{31}\text{Si}$ . Even if no Si were present in the sample this interference would still occur since  $^{31}\text{P}$  can produce  $^{31}\text{Si}$  by the (n,p) reaction. Because of these interferences it was concluded that only the 1.7789 MeV photopeak should be used for an indication of the activity of the sample due to  $^{28}\text{Al}$ .

The four photopeaks near the  $^{28}\text{Al}$  photopeak in Fig. 9 were produced by 1.6427 MeV ( $^{38}\text{Cl}$ ), 1.8112 MeV ( $^{56}\text{Mn}$ ), 2.1126 MeV ( $^{56}\text{Mn}$ ), and 2.1676 MeV ( $^{38}\text{Cl}$ ) gamma-rays. Therefore, it seemed that Mn and Cl had to be considered in the wheat analyses. Other elements such as sodium, calcium, and potassium were also initially considered even though they were not really apparent in the gamma-ray spectra. It was known that these three elements are common

in wheat, but it was finally concluded that they did not activate to a significant extent to merit their inclusion in the analysis. Since two distinct photopeaks were generated for both the  $^{38}\text{Cl}$  and  $^{56}\text{Mn}$ , it was decided that the use of their escape peaks in the analysis was not necessary. So, incorporating the Cl and Mn yielded an analysis for Cl, Mn, Al, P, Si, and Mg by observing 12 photopeaks, 6 in the filtered spectrum and 6 in the nonfiltered spectrum. It was found, however, that such an analysis yielded unreasonable results. It was concluded that the reason for the invalid results was mainly due to the effective reduction of the influence of the Al, Si, P, and Mg coefficients in the system of equations by the inclusion of the two additional terms in each equation for the Cl and Mn. Therefore, the Cl and Mn were removed from the analysis. This simplified the analysis to that in accord with the theory of the method (see section 4.2). Meaningful results were then achieved for the wheat analyses. These results are presented in Table III.

Table IV shows the values of concentrations of Al, Si, Mg, and P in wheat grain according to several authors. A comparison of the values of Table IV with those of Table III shows that there is reasonable agreement. The Mg values show excellent agreement. All Mg values were within the range of Mg values reported by Schrenk, and the maximum deviation from an average of Peterson's and Morrison's values was only 19%. The Al and Si values determined by the cadmium filter technique are higher than those of Table IV, but the difference is not unreasonable. Different growing conditions could account for part of the difference, but dust on the grain was the more probable reason for the difference. The wheat was not treated, washed, or handled, and therefore the dust was included in the analysis. Different growing and harvesting conditions could easily alter the amount of dust on

Table III

Concentrations of Al, Si, Mg, and P in Wheat Grain as  
Determined by the Cadmium Filter Technique.

Wheat Sample	Variety	Al (ppm)	Si (ppm)	Mg (ppm)	P (ppm)
1 <sup>a</sup>	Eagle	11.1 (0.5) <sup>b</sup>	304 (14)	1620 (58)	2272 (114)
2	"	12.8 (0.6)	341 (17)	1640 (61)	1989 (131)
3	Centurk	10.4 (0.5)	484 (19)	1655 (55)	2695 (145)
4	"	10.0 (0.5)	453 (18)	1784 (58)	2976 (139)
5	Eagle	11.9 (0.5)	398 (15)	1416 (51)	2662 (119)
6	"	11.3 (0.5)	371 (17)	1550 (54)	2871 (132)
7	Santanta	12.3 (0.5)	419 (17)	1647 (58)	2831 (134)
8	"	15.9 (0.6)	382 (16)	1489 (54)	2624 (129)
9	Centurk	13.8 (0.5)	397 (17)	1435 (52)	2249 (128)
10	"	13.3 (0.5)	459 (18)	1344 (51)	2084 (131)
11	Eagle	11.8 (0.5)	357 (15)	1428 (52)	2084 (119)
12	"	10.7 (0.5)	355 (16)	1447 (53)	2624 (125)
13	Santanta	12.4 (0.7)	436 (15)	1453 (72)	1498 (106)
14	"	11.7 (0.5)	424 (15)	1490 (51)	1628 (108)
15	Centurk	12.8 (0.5)	417 (15)	1415 (52)	1328 (106)
16	"	12.5 (0.5)	393 (14)	1527 (54)	1514 (104)
17	unknown	12.8 (0.5)	365 (14)	1701 (55)	1508 (102)
18	"	14.0 (0.5)	359 (13)	1416 (53)	1320 (096)

<sup>a</sup>Two portions of a given large sample were analyzed. Samples 1 and 2 were from one large sample, 3 and 4 from another large sample, etc.

<sup>b</sup>The values in parentheses are standard deviations. Samples 17 and 18 were Colorado wheat samples; all other samples were from the 1973 Kansas wheat crop.

Table IV  
Concentrations of Al, Si, Mg, and P in Wheat Grain According to  
Schrenk (30), Peterson (31), and Morrison (32).

Element	Concentrations		
	Schrenk (30) Reported Values (ppm)	Peterson (31) Average (ppm)	Morrison (32) Average (ppm)
Al	3	3	not given
Si	60	121	not given
Mg	800 - 3000*	1600	1400
P	1500 - 5500	3800	3900

\* The last two digits in all Mg and P values are not significant digits. The values are listed in parts per million (ppm) for sake of convenience in making comparisons.

wheat, and since Al and Si are common constituents of soil and dust the resulting measured concentrations for these elements in untreated wheat could vary over a rather wide range.

The phosphorus concentrations determined in this work are generally within the range of values reported by Schrenk (30), but they are lower than the Peterson and Morrison values of Table IV. The Eagle, Santanta, and Centurk varieties of wheat are new varieties and therefore do not necessarily correspond to the varieties which were involved in the analyses reported in the cited literature. No significant differences in phosphorus content of these new varieties, as compared to older varieties, are to be expected, however (33). Two things could account for the differences between the literature values for phosphorus content and the values obtained in this work. First, soil conditions for the wheat samples may have been different. Neither the soil conditions nor the moisture content were known for the wheat samples used in this work or for the samples used for the values reported by Schrenk, Peterson or Morrison.

Since there is general agreement between the Al, Si, Mg, and P concentration values of this work and those in the literature, it can be concluded that the cadmium filter technique is a valid method of analysis for wheat. Judging from the results shown in Table III it appears that the time required to analyze a given wheat sample could be reduced to less than one day by dividing the sample into two portions, one for the filtered irradiation and one for the nonfiltered irradiation.

Several horse hair samples were also analyzed by the cadmium filter technique. The objective, with respect to the horse hair, was to analyze the samples for both phosphorus and calcium. The resulting Ca:P ratio for a given sample was then to be used as an indication whether or not the horse



had epiphysitis. Supposedly a horse with epiphysitis would exhibit a Ca:P ratio in its hair which would be significantly lower than that of a healthy horse.

Figures 10 and 11 are gamma-ray spectra of hair samples from two different horses. A comparison of the two figures indicates that considerable variation can exist in the constituents of horse hair. Essentially the same basic peaks appear in both figures, but the concentrations of the elements that produced the peaks were evidently quite different. The differences in the  $^{28}\text{Al}$  photopeaks are especially prominent.  $^{56}\text{Mn}$  was evident in all the horse hair samples, and therefore the 0.8438 MeV photopeak of  $^{27}\text{Mg}$  could not be used in the analysis because of the interference from the 0.8466 MeV photopeak from  $^{56}\text{Mn}$ . This limited the  $^{27}\text{Mg}$  analysis to its 1.0144 MeV photopeak which was quite small in the observed samples.

Several approaches were taken in the analysis of the horse hair samples. Based on the successful experience gained in the wheat analysis, one approach involved only the Al, Si, Mg, and P in accordance with the theory for the method. This approach yielded phosphorus concentrations which varied from 0.13% to 14%. The 14% value was especially unreasonable; the particular analysis that yielded the 14% also gave a negative value for the Mg concentration, thus indicating that the analysis was very questionable. A similar analysis with questionable results was obtained from the data which was used in generating the spectra in Fig. 10. In general, spectra similar to those in Fig. 10 yielded questionable results. On the other hand, spectra similar to those in Fig. 11 produced more reasonable results. The 0.13% concentration for P was obtained from the data used in Fig. 11. This value was approximately 2 to 4 times the values found in other studies by Wysocki and Klett (34) and Sippel (35) who found horse hair P

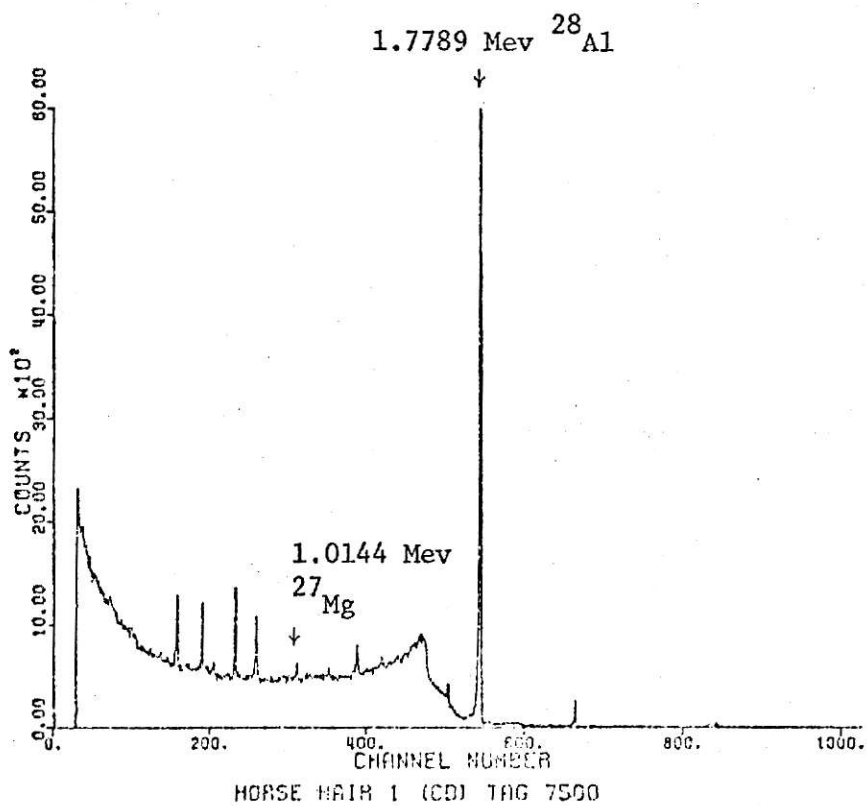
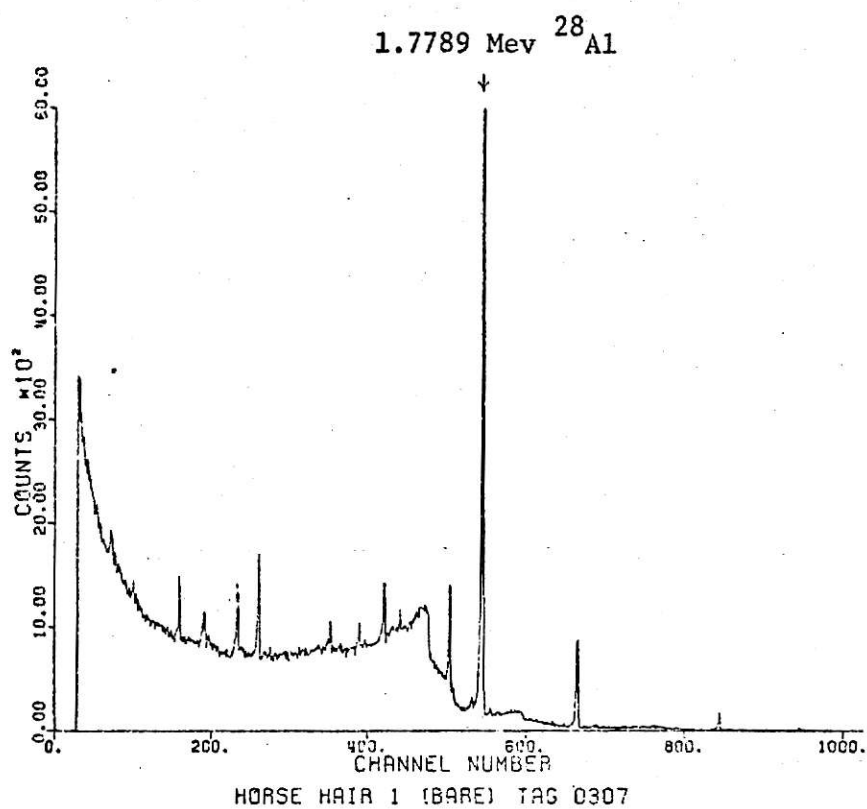


Figure 10. Gamma-Ray Spectra of Horse Hair. Cadmium-Filtered Irradiation--(CD), Nonfiltered Irradiation--(BARE).

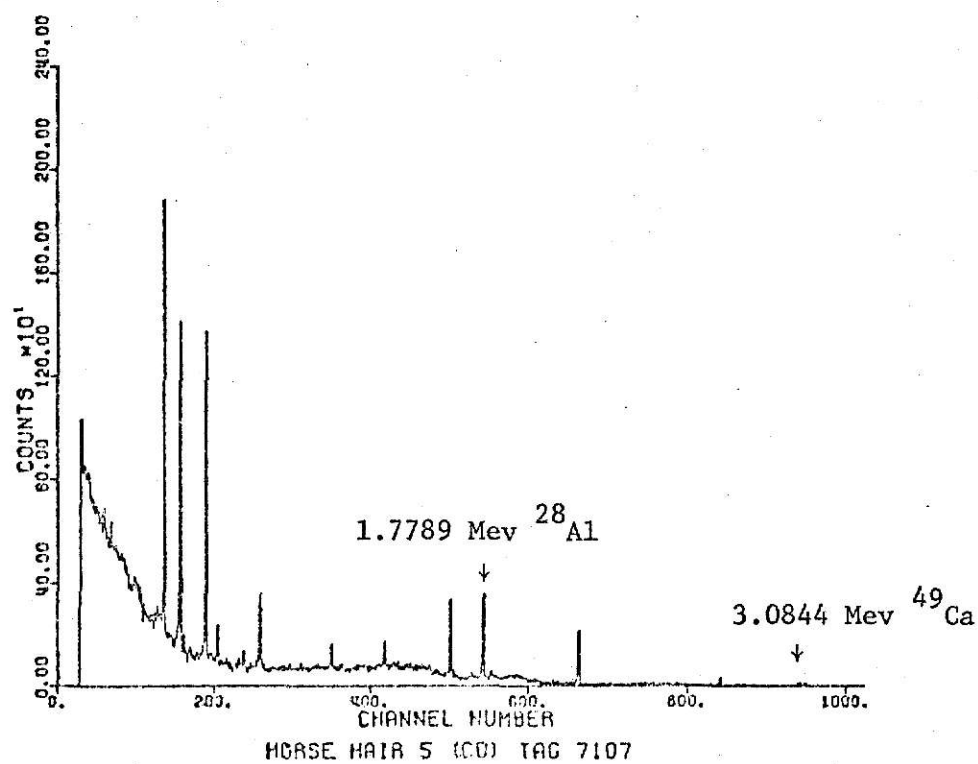
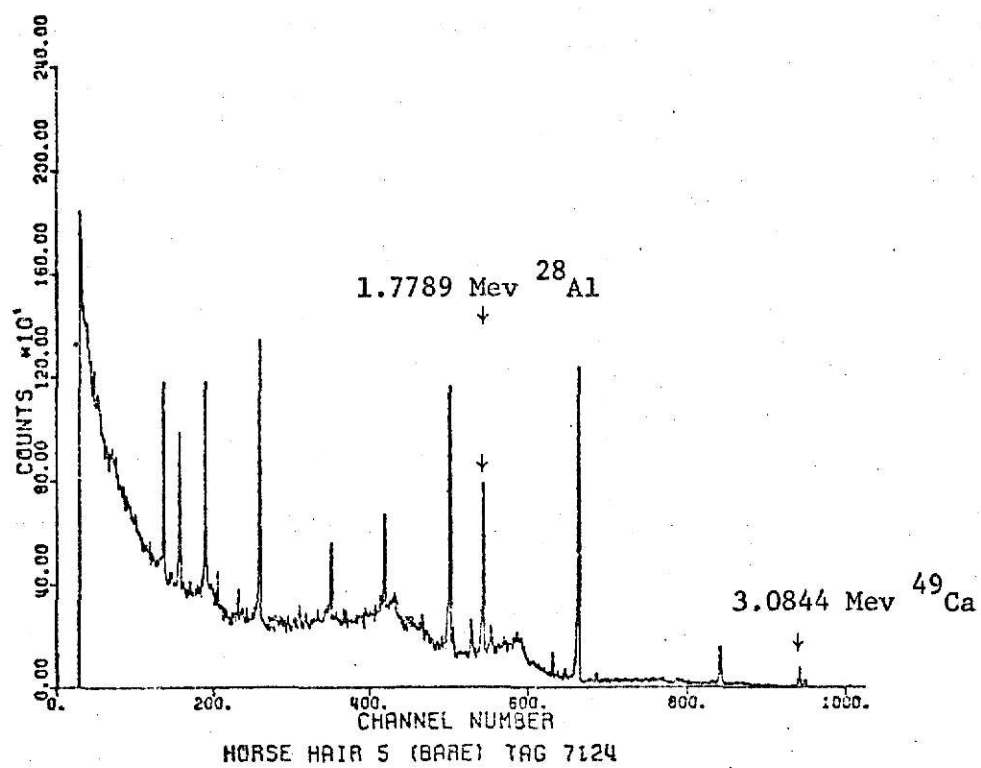


Figure 11. Gamma-Ray Spectra of Horse Hair. Cadmium-Filtered Irradiation--(CD), Nonfiltered Irradiation--(BARE).

concentrations which varied from 0.031% to 0.067%. Other approaches to the analysis included Ca and Ca plus Cl. The resulting Ca concentrations were consistently higher than the Ca concentrations reported by Wysocki and Sippel. The results of Wysocki and Sippel for Ca concentrations varied from 0.06% to 0.19% while those of this work averaged approximately 0.3% (34,35). The counting statistics for the 3.0844 MeV photopeak from  $^{49}\text{Ca}$  were somewhat limited in this work (maximum number of counts in the photopeak was 170). Therefore, the double-escape peak from the 3.0844 MeV gamma-ray was also used in some of the analyses. A separate irradiation and independent analysis by normal NAA would produce more reliable results for the Ca concentrations. A separate irradiation for a longer irradiation time would improve the counting statistics of the Ca, that is, provided interferences from other nuclides did not develop.

Since a limited number of horse hair samples were examined in this work it is concluded that additional work should be performed to apply the cadmium filter technique to such analyses. The results of this work showed that the horse hair samples varied drastically in their constituent concentrations, and this made it difficult to analyze all samples by the same procedure.

There was difficulty in both the wheat and horse hair analyses in trying to incorporate the elements which contributed significantly to the gamma-ray spectra but which were not actually part of the method. In the case of wheat it was necessary to exclude all elements in the analysis which were not directly part of the theory of the method. One limitation of the method was the necessity of the presence of significant amounts of Mg in the sample to be analyzed. Fortunately Mg is a common constituent of biological samples. If the method of analysis developed

in this work was to be applied to other types of samples the 1.0144 MeV photopeak from  $^{27}\text{Mg}$  would need to be evident in the sample spectra. If no Mn existed in a sample then the 0.8438 MeV photopeak could be used for the indication of  $^{27}\text{Mg}$ .

## 6.0 SUGGESTIONS FOR FURTHER STUDY

The most obvious possibility for further study would be to improve the method of data analysis. The method could conceivably be improved by providing a routine to strip out the prominent elements which are not needed for the analysis. It should be possible to strip out at least those nuclides whose gamma-ray energies are greater than that of  $^{28}\text{Al}$ . The stripping routine could be applied to both the cadmium-filtered sample and the nonfiltered sample before the filter analysis of this work was applied. No self shielding corrections were applied in this work. For increased accuracy of the method such corrections should be considered. It is also suggested that lower amplifier gains than those used in the wheat analysis be used. However, the amplifier gains used for the horse hair samples in this work are suggested for use in future work.

A large cadmium filter causes very inefficient utilization of neutrons, and therefore a neutron converter to effectively convert thermal neutrons to fast neutrons should be considered. Lithium deuteride has been successfully used as a converter, and its use should be considered (36). The combined use of cadmium-filtered irradiations and lithium deuteride "converted" irradiations could conceivably be used in analyses in the same manner in which the filtered and nonfiltered irradiations were used in this work. Such a technique could possibly eliminate some interferences from  $(n,\gamma)$  reactions.

The cadmium filter constructed for this work should be considered for use in normal NAA. It can be used to simply enhance fast-neutron reaction products relative to thermal-neutron reaction products. It could possibly be used in some neutron cross section studies also.

## 7.0 ACKNOWLEDGMENTS

Sincere appreciation is extended to Dr. N. D. Eckhoff for his guidance and suggestions throughout this work. The author is also very grateful for the financial support provided by the Kansas State University Engineering Experiment Station and Nuclear Engineering Department.

The author also extends his gratitude to Dr. J. K. Shultis, Mr. Bill Starr, Mr. Oscar Mulhern, and Mr. George Abshire for their help in various phases of this work. Information (concerning the horse hair analysis) provided by Dr. G. W. Brandt of the KSU College of Veterinary Medicine is appreciated. The author thanks Mr. Tom Roberts, Director of the Kansas Wheat Improvement Association, for providing wheat samples for the analysis.

The continued cooperation from the Kansas State University TRIGA Mark II nuclear reactor staff is appreciated. The helpful suggestions and assistance of Mr. Mike McEwan, senior reactor operator, are gratefully acknowledged.

The author expresses deep gratitude to his wife for her love, encouragement, and patience during this work. Finally, special thanks is given to The Living God whose creation and sustaining grace made this work possible.

## 8.0 LITERATURE CITED

1. Koch, R. C., Activation Analysis Handbook, Academic Press, Inc., 1960.
2. Lutz, G. J., Boreni, R. J., Maddock, R. S., and Meinke, W. W., Eds., "Activation Analysis: A Bibliography," Government Printing Office, Washington, 1968.
3. Kruger, P., Principles of Activation Analysis, John Wiley and Sons, Inc., 1971.
4. To-on, M., Sicilio, F., and Wainerdi, R. E., "Determination of Phosphorus by Fast-Neutron Activation Analysis," Trans. Am. Nucl. Soc., 7, 2 (1964).
5. Foster, L. M., and Gaitanis, C. D., "Determination of Phosphorus in Aluminum and Aluminum Oxide by Radioactivation Analysis," Anal. Chem., 27 (1955).
6. James, J. A., and Richards, D. H., "Radioactivation Analysis of Phosphorus in Silicon," Nature, 176 (1955).
7. Blackburn, R., and Peters, B. F. G., "Determination of Phosphorus in Hypereutectic Aluminum-Silicon Alloys by a Neutron Activation Method," Anal. Chem., 35 (1963).
8. Rison, M. H., Barber, W. H., and Wilkniss, P., "Determination of Trace Amounts of Phosphorus in a Composite Propellant by Fast Neutron Activation Analysis," Anal. Chem., 39, 8 (1967).
9. Kansas State University TRIGA Mark II Calibration Data and Operation Notes.
10. Buchanan, J. D., "Activation Analysis Using a Research Reactor," Atompraxis, 8 (1962).
11. Kansas State University 250-kW TRIGA Mark II Pulsing Reactor Mechanical Maintenance and Operating Manual, General Dynamics/ General Atomic Division.
12. Stoughton, R. W., and Halperin, J., "Effective Cutoff Energies for Boron, Cadmium, Gadolinium, and Samarium Filters," Nucl. Sci. Eng., 15 (1963).
13. Stoughton, R. W., Halperin, J., and Lietzke, M. P., "Effective Cadmium Cutoff Energies," Nucl. Sci. Eng., 6 (1959).
14. Hickman, C. H., and Leng, W. B., "The Calculation of Effective Cutoff Energies in Cadmium, Samarium, and Gadolinium," Nucl. Sci. Eng., 12 (1962).



15. McEwan, M. J., Kansas State University TRIGA Mark II Nuclear Reactor Operator, personal communication.
16. Yule, H. P., Lukens, H. R., and Guinn, V. P., "Utilization of Reactor Fast Neutrons for Activation Analysis," Nucl. Instr. Methods, 33 (1965).
17. Eckhoff, N. D., "Optimal Neutron Activation Analysis," a Ph.D. Dissertation, Kansas State University, 1968.
18. Price, W. J., Nuclear Radiation Detection, 2nd Edition, McGraw-Hill, 1964.
19. Chase, G. D., and Rabinowitz, J. L., Principles of Radioisotope Methodology, 3rd Edition, Burgess Publishing Co., 1967.
20. Heath, R. L., "Scintillation Spectrometry: Gamma-Ray Spectrum Catalog," 2nd Edition, Vol. 1, IDO-16880-1, 1964.
21. Evans, R. D., The Atomic Nucleus, McGraw-Hill, 1955.
22. Lyon, W. S., Guide to Activation Analysis, D. Van Nostrand Co., Inc., 1964.
23. Glasstone, S., and Sesonske, A., Nuclear Reactor Engineering, D. Van Nostrand Co., Inc., 1967.
24. "Chart of the Nuclides," Government Printing Office, Washington, 1970.
25. Eckhoff, N. D., and Ervin, P. F., "Area-of-Interest Unfolding," Nucl. Instr. Methods, 97 (1971).
26. Ervin, P. F., "Assembly and Calibration of a Ge(Li) Spectrometer System for Analysis of Geological Samples," a Master's Thesis, Kansas State University, 1971.
27. Eckhoff, N. D., "Corgam-A Correlation Algorithm for Gamma-Ray Spectra," Nucl. Instr. Methods, 74 (1969).
28. O'Kelly, G. D., "Applications of Computers to Nuclear and Radiochemistry," Office of Technical Services, Dept. of Commerce, Washington, 1962.
29. Wakat, M. A., "Catalogue of  $\gamma$ -Rays Emitted by Radionuclides," Nuclear Data Tables, 8 (1971).
30. Schrenk, W. G., "Minerals in Wheat Grain," Kansas State University Agricultural Experiment Station, Technical Bulletin 136, 1964.
31. Peterson, R. F., Wheat-Botany, Cultivation, and Utilization, Interscience Publishers Inc., 1965.
32. Morrison, F. B., Feeds and Feeding, Morrison Publishing Co., 1956.

33. Heyne, E. G., Prof. of Agronomy, Kansas State University, personal communication.
34. Wysocki, A. A., and Klett, R. H., "Hair as an Indicator of the Calcium and Phosphorus Status of Ponies," Journal of Animal Science, 32, 1 (1971).
35. Sippel, W. L., et al., "Nutrition Consultation in Horses by Aid of Feed, Blood, and Hair Analysis," Proc. Amer. Ass. of Equine Practitioners, 1964.
36. Frigerio, N. A., "Conversion of Reactor Neutrons to 15 MeV With LiD," Argonne National Lab., Division of Biological and Medical Research-Annual Report, 1971.
37. Sisco, F. T., Advisory Ed., Engineering Metallurgy, Pitman Publishing Corp., 1957.
38. Blizard, E. P., Ed., Reactor Handbook-Shielding, Vol. 3, Part B, 2nd Edition, Interscience Publishers, 1962.
39. Rockwell, T., III., Reactor Shielding Design Manual, 1st Edition, D. Van Nostrand Co., Inc., 1956.
40. Jaeger, R. G., Ed.-in-Chief, Engineering Compendium on Radiation Shielding, Vol. 1, Springer-Verlag, 1968.
41. "Standards for Protection Against Radiation," Rules and Regulations Title 10 Part 20, United States Atomic Energy Commission, 1969.

## 9.0 APPENDIXES

## APPENDIX A

## Cadmium Covered In-Core Irradiation

Object: (1) to perform fast neutron activation in a vacant fuel element position in the core of the KSUTMII reactor in a dry environment and (2) to use a cadmium cover to reduce thermal neutron activation, leaving greater than 90% of the cadmium cover in the reactor tank until suitable decay would permit its removal if desired.

Background: To enhance fast-neutron activation while reducing thermal-neutron activation in a reactor environment it is necessary to use some type of filter to prevent the thermal neutrons from interacting with the sample to be activated. A cadmium cover surrounding the sample is one method used to accomplish this. Relatively pure cadmium with a thickness of 40 mils is greater than 95% opaque to thermal neutrons but is rather transparent to fast neutrons. This characteristic which makes cadmium a suitable filter also presents a problem in that a cover of any appreciable size is highly activated if it is placed in a high thermal-neutron flux. So, in this experiment it is desired to leave as much as possible of the cadmium cover in the reactor tank at a depth in the water to provide sufficient shielding.

The cover for this experiment is a cylindrical shell with a total surface area of approximately 21.7 square inches. The walls of the shell are approximately 40 mils thick. The height of the shell is 4.5 inches and the outside diameter is 1.33 inches. Only the top circular end of the cover will be removed from the reactor along with the irradiated sample. The cover fits in the end of a long aluminum tube extending from

the top of the reactor tank into the core. See Figure 12. The aluminum tubing is type 6061-T6 and is thus compatible with other core materials since much of the Triga structural material is made of 6061 aluminum (15). The aluminum foot at the bottom end of the tubing is also 6061; it is welded (inert gas welded) to the tubing. Typical alloying elements and their percentages in 6061 aluminum are: copper-0.25%, magnesium-1.0%, silicon-0.6%, and chromium-0.25% (37). The tubing is in three sections joined by two unions which are made of aluminum and stainless steel. These unions utilize a metal-to-metal press fit for sealing. The outside diameter of the tubing is 1.5 inches, and the inside diameter is 1.33 inches, thus making it necessary to use the type of unions mentioned above. It should be noted that the same type of unions are utilized in the reactor to connect the specimen-removal tubing for the RSR (11). The bottom portion of the tubing which fits in the core has been machined to approximately 1.47 inches o.d., which is the o.d. of the fuel elements. The upper grid plate holes in which the tubing is to be inserted are 1.505 inches in diameter so there is sufficient clearance even if the tubing were to expand due to slight temperature increases (11). The maximum o.d. of the foot is also 1.47 inches. The bottom of the foot is designed to rest in a vacant fuel element position in the lower grid plate. The upper end of the tubing is positioned by a device fastened to the top lip of the reactor tank. This positioning device also serves to help keep the lower end vertical as it is moved in and out of the core. When not in use the tube will be positioned along the wall of the reactor tank with its foot between the edge of the thermal column and the "C" radial beam port. This will act as a bottom positioning device holding the foot in a small

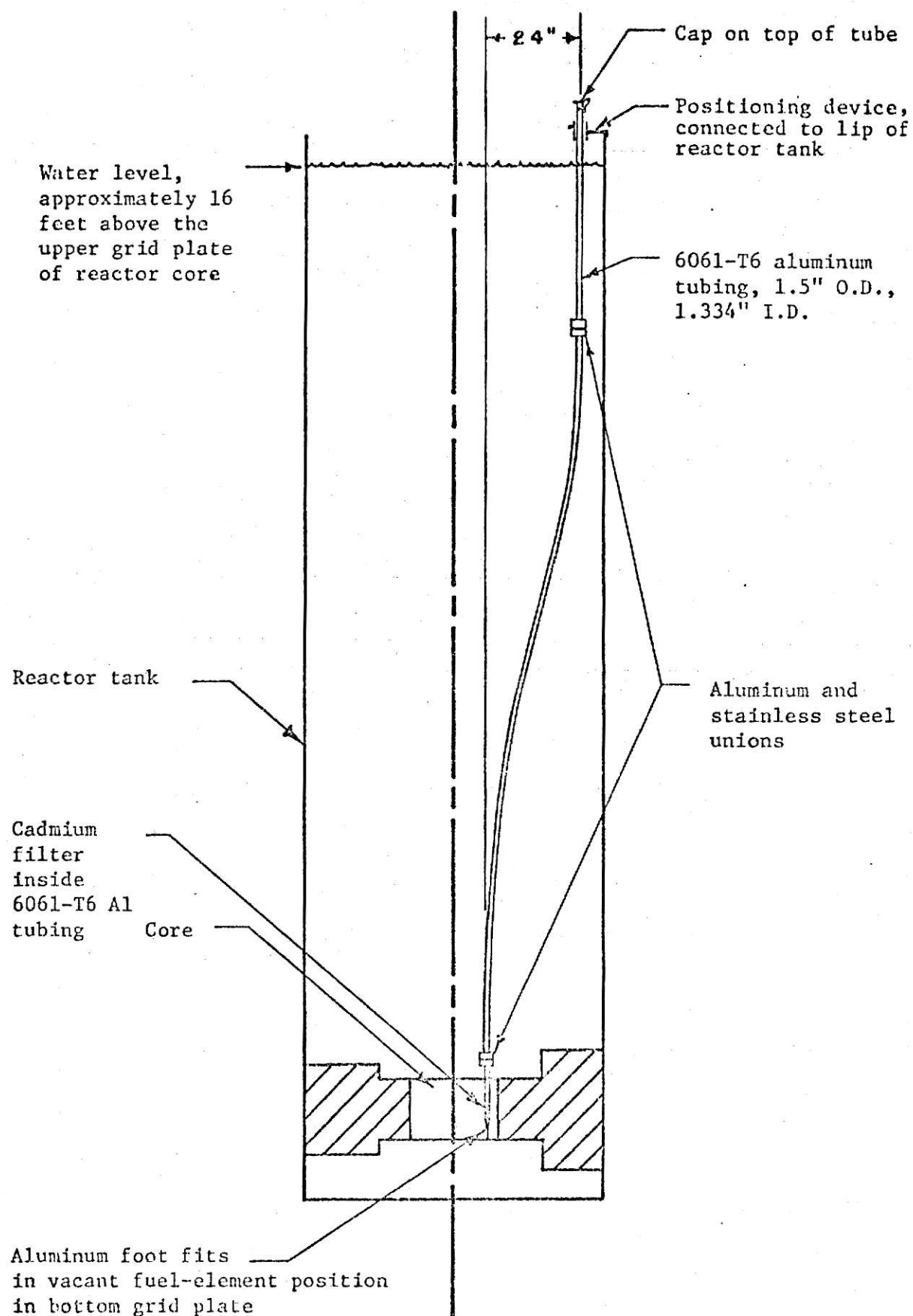


Figure 12. Vertical Section View of the TRIGA Mark II Nuclear Reactor Tank with the Cadmium Filter.

pocket formed by the edge of the thermal column, the radial beam port, and the tank wall. The upper positioning device can be adjusted to prevent the inadvertent movement of the tube either from its storage location or from its irradiation position. This upper positioning device makes it possible to lift the tubing high enough to insert it in the core, but it limits the maximum height in such a way that there would always be at least 11 feet of water between the lower union and any personnel at the top of the reactor. The aluminum in the device would constitute the most important part of any radiation that could be received by personnel while moving the device. The following calculation shows that, as a first order approximation, the 11 feet of water would provide ample shielding.

As a conservative estimate assume that the aluminum irradiated in the core is equivalent to that in a solid cylinder of 1 inch diameter and 10 inches long. If the density of aluminum is 2.7 grams per cubic centimeter, the mass of aluminum in this cylinder would be about 347.5 grams. Now assume that saturation activity is produced at a reactor power level of 250 kW. The standard activation equation can be expressed as follows.

$$A = N_o \sigma_a \phi_{th} (1 - e^{-\lambda t_i}) (e^{-\lambda t_w}) , \quad (A.1)$$

where, A is the activity of the irradiated element,  $N_o$  is the number of atoms of the element,  $\sigma_a$  is the thermal neutron activation cross section,  $\phi_{th}$  is the average thermal neutron flux,  $\lambda$  is the decay constant,  $t_i$  is the time of irradiation, and  $t_w$  is the time between the end of irradiation and the measurement of the activity. The activity of the aluminum would be the greatest at the instant the reactor was shut down, that is, after it has been operated long enough to produce saturation. In this case, the above equation would reduce to the following equation.

$$A = N_o \sigma_a \phi_{th} \quad (A.2)$$

As a first approximation, the aluminum activation cross section can be considered to be 0.24 barns. Also, the thermal-neutron flux for 250 kW is on the order of  $10^{12}$  neutrons/cm<sup>2</sup>-sec. Using the previous values, the induced activity would be

$$A = \frac{(347.5)(0.602 \times 10^{24})(0.24 \times 10^{-24})(10^{12})}{26.98} = 1.86 \times 10^{12} \text{ d/sec.}$$

Now assume this activity is in the form of a point source, and assume the shielding is 11 feet of water. Al-28 emits 1.78 MeV gamma-rays with a percentage of 100%. A simple, first approximation shielding equation for a point source can be written as,

$$D = \frac{S_o B(e^{-\mu r})}{K(4\pi)r^2} \quad (A.3)$$

D is the exposure rate,  $S_o$  is the source strength in photons per second, B is a gamma-ray buildup factor,  $\mu$  is the mass attenuation coefficient, K is a flux to exposure conversion factor, and r is the distance in centimeters from the point source to the detector. In this case, r would be the distance in centimeters corresponding to the 11 feet of water which acts as the shield. By using linear interpolation, the value for the attenuation coefficient for 1.78 MeV gamma-rays in water is 0.0529 cm<sup>2</sup>/g (38). If it is assumed that 1 r corresponds to an energy deposition of 87.7 ergs in one gram of air then the expression for K can be written as

$$K = \frac{87.7}{(E)(\mu_a)(1.6 \times 10^{-6})(3600)} \quad (A.4)$$

where, E is the gamma-ray energy in MeV,  $\mu_a$  is the average energy absorption coefficient for air in units of cm<sup>2</sup>-g<sup>-1</sup>. Using linear interpolation the



value for this energy coefficient for 1.78 MeV gamma-rays is  $0.0245 \text{ cm}^2\text{-g}^{-1}$  (38). In considering the buildup factor, it is assumed that the dose buildup factor for water will serve for the exposure buildup factor for water without introducing any significant error. This value for B is taken from reference (39) and is considered to be 32 for this problem. Using K as previously defined gives a resulting value for D in units of r/hr. Therefore, D is as follows.

$$D = \frac{(1.86 \times 10^{12})(32)(e^{-(0.0529)(11)(12)(2.54)})(1.78)(0.0245)(3600)}{(4\pi)(11^2)(12^2)(2.54^2)(87.7)(1.6 \times 10^6)}$$

$$= 0.935 \times 10^{-6} \text{ r/hr.}$$

Obviously this is a very small dose rate and is well within the regulations. This value is negligible in comparison to the exposure rate at the top of the reactor during full power operation.

Another feature of the tubing is the 24 inch offset designed to prevent excess streaming of radiation from the tube. The RSR sample removal tubing, which is essentially identical in size, has an offset of 18 inches (11). Assuming that the RSR tubing is safely designed, the 24 inch offset in the tubing for this experiment should certainly be safe. As a precautionary measure, however, the radiation level at the opening of the tube is to be checked the first time it is used during a full power reactor operation. A cover for the top of the tube will reduce circulation of any air in and out of the tube to a negligible amount. This will in turn keep any release of Ar-41 to a minimum. The cover will also prevent foreign objects from accidentally being dropped into the tube.

Effects on Reactor Operation: The reactivity effects of this device should form the major effects on the reactor operation. To estimate what the

reactivity worth would be, a small cadmium cylinder with a total surface area of about 9 square inches was placed in the central thimble, and the reactor was brought to a very low power level. By use of the control rod calibration curves the worth of this sample was determined to be  $-\$1.10$ . If it is assumed that the negative reactivity worth of a given substance varies in approximately the same fashion radially in the core as do the fuel elements in their positive reactivity worth, this test cylinder of Cd, if placed in the F ring of the core, could be estimated to have a worth of

$$w_{\text{test}} = \frac{(-1.10)(0.50)}{(1.5)} = -0.367 ,$$

where 0.50 is the approximate fuel rod worth in the F ring, and 1.5 is the positive fuel rod worth in the B ring (all reactivity units are in dollars). This would probably overestimate the reactivity worth in the F ring since a fuel rod in the central thimble would no doubt be worth more than  $\$1.5$ . Since the reactivity worth of the Cd is proportional to the exposed surface area, it is possible to now estimate the reactivity worth of the actual Cd cover in the F ring by using the ratio of the surface areas of the actual cover and the test sample.

$$w_{\text{cover}} = \frac{(-0.367)(21.7)}{(9)} = -0.885,$$

where 21.7 square inches is the exposed surface area of the actual cover, and 9 square inches is the surface area of the test sample. Since the limit of reactivity insertion to the core is  $\pm \$2.00$  it appears that the actual cover should fall within the limits, at least for insertion in the F ring. Nevertheless, the worth of this device is to be determined the first time it is used in any given core location.

One possible hazard of this experiment would be the sudden flooding of the tubing during the reactor operation. Such an event would be extremely unlikely, however, since the cover will not be moved at any time during reactor operation. Another possible hazard would be the sudden removal of the cover from the core during full power operation. This would be a possibility because the tube has a slight net upward (buoyant) force on it. The upper positioning device is designed to prevent any vertical movement of the cover after it has been placed in position. This positioning device utilizes an aluminum pipe sleeve which fits over the upper portion of the tubing. It has three set screws which are to be tightened each time the cover is placed in any position. Any one of the three set screws would prevent vertical movement of the cover. The probability of either of these two hazards taking place is very small, but if either should occur the inherent safety features of the TRIGA reactor would prevent any serious situation from taking place. For one thing, the negative reactivity worth of the cover has already been measured at a very low power level in the F ring, and it was found to be much less than the \$2.00 limit set for materials placed in the core. This \$2.00 limit has no doubt been determined after considering such things as sudden removal of the material from the core. At any rate, the primary safety feature which would prevent an accident if either of the mentioned hazards were to occur is the prompt negative temperature coefficient of reactivity which is an important feature of the TRIGA fuel. This feature of control would probably not be necessary since normal scram circuits and rod drop times should be rapid enough to offset either hazard.

Due to the low operating temperatures of the reactor cooling water, and due to its purity no important chemical reactions should take place

with the aluminum or stainless steel of the device. Some Dow Corning "Stopcock Grease" is used to help seal the two unions, and some of it is exposed to the water. According to the manufacturer this grease is "composed of a silicone fluid thickened with an inert silica filler and is practically nonvolatile and retains its grease-like consistency from -40 degrees F to +400 degrees F." It is also said to have "excellent water repellency, excellent oxidation resistance, and excellent resistance to most chemicals, oils and organic solvents." Even though this silicone grease will break down on the lower union, it should cause no significant problem. The grease may harden and yield some volatile products due to radiation damage, but it is felt that there is so little of it present that it would not interfere with normal reactor operation.

Since the tubing will occupy only one fuel element position in the core it will cause very little disturbance of normal reactor coolant flow. The heat generation in the tubing will be negligible. The device should not produce any cooling problems. Also, the tubing, including the foot on the bottom, is designed so that no fuel element should even be touched as the device is placed in the core or removed from the core. If the device is handled carefully no damage to reactor components should occur. The foot at the bottom of the tubing is designed to fit in the lower grid plate, and it has no sharp edges that could rupture the cladding of a fuel element. See Figure 13. See Figure 14 for details concerning the cover.

Other Effects: One possible hazard of this device would be the rapid flooding of the entire tube during the process of removing the cover from the core after an extended period of irradiation. The hazard would be that of the Ar-41 released from the tube at the top of the reactor. This event would only be probable because of mistreatment of the device by the person

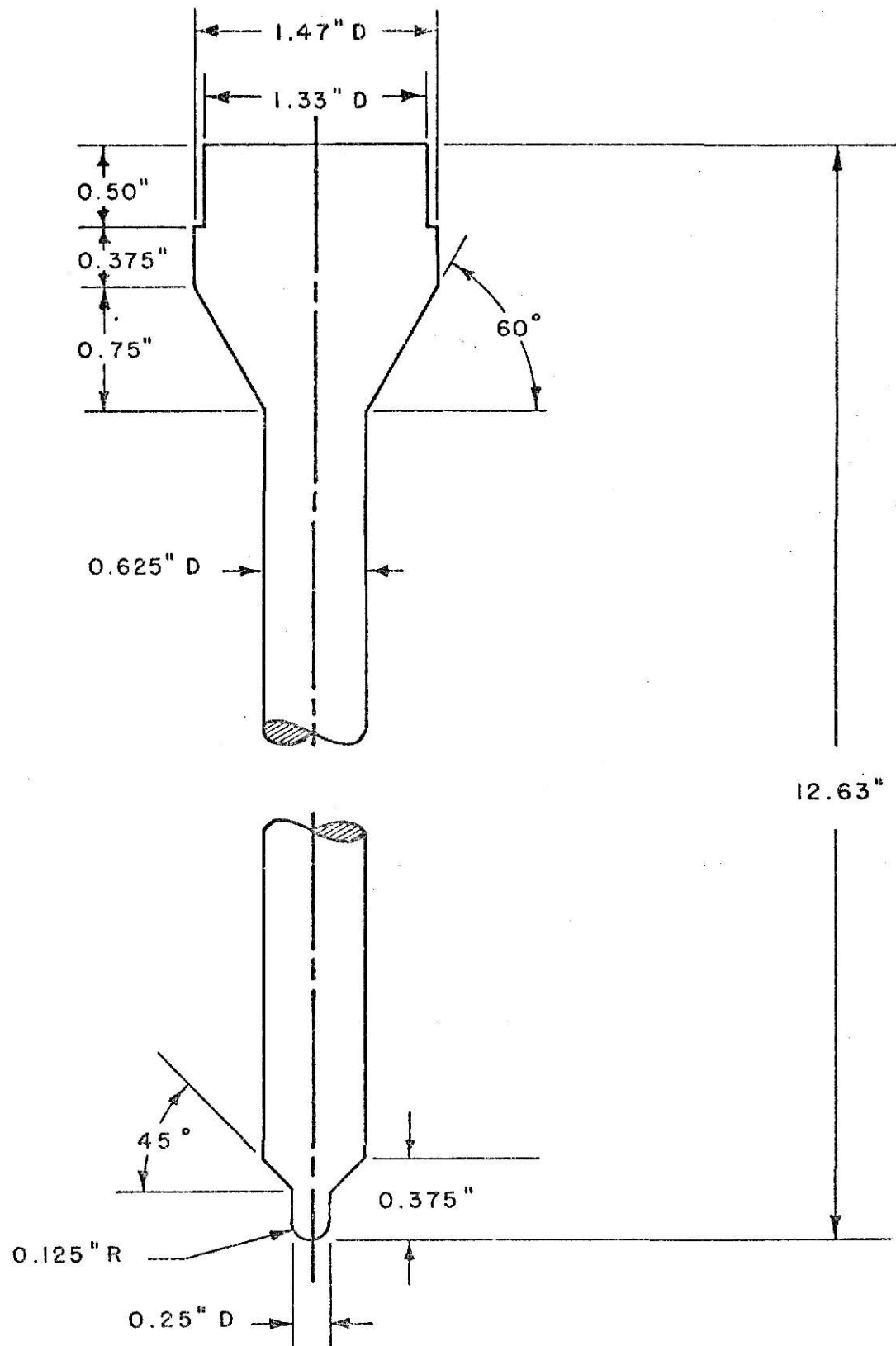


Figure 13. The Aluminum Foot for the Filter Device.

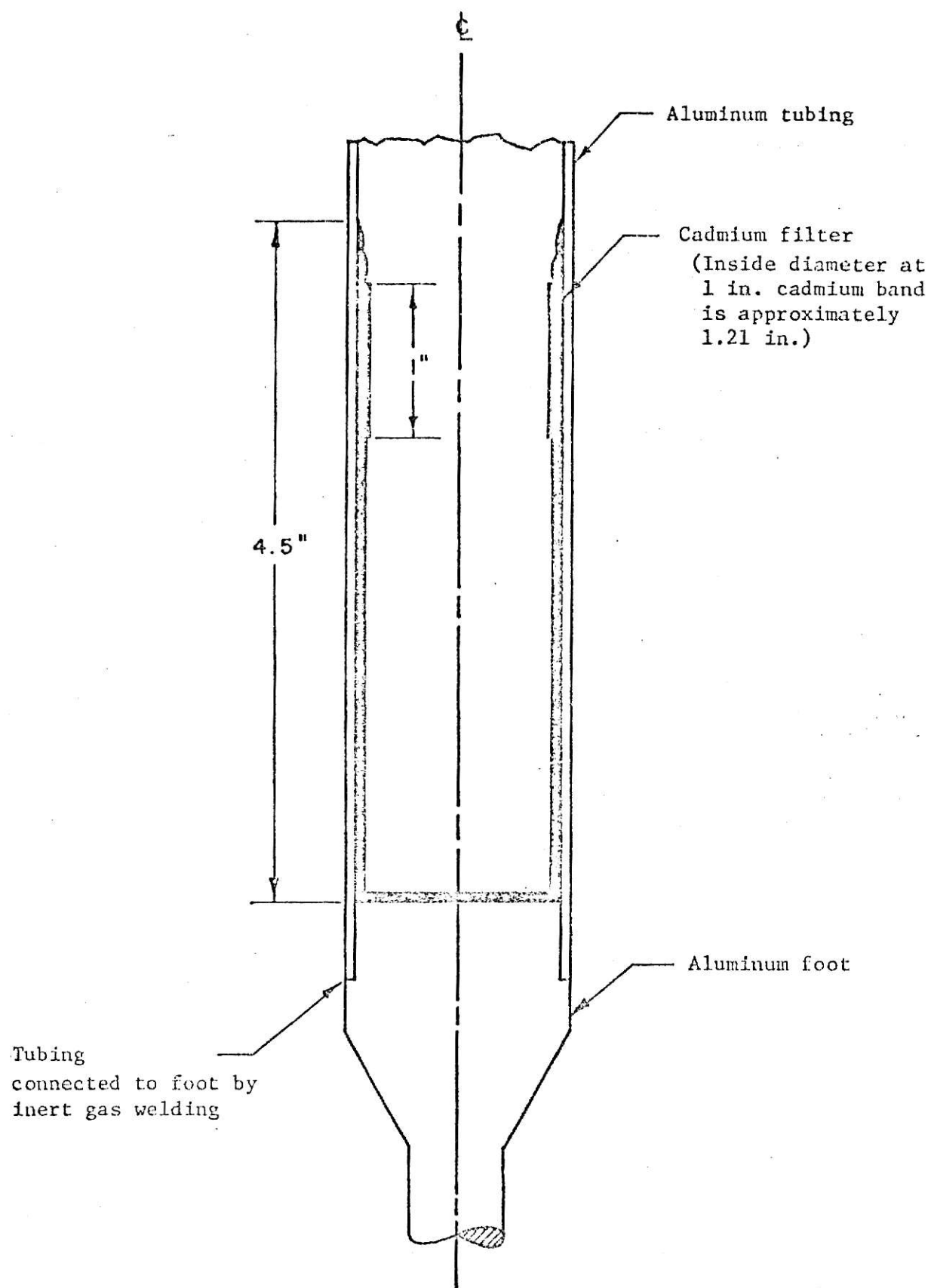


Figure 14. Vertical Section View of the Cadmium Filter, Aluminum Tubing, and Aluminum Foot.

moving it. It would take considerable mistreatment to cause this, but since it is a possibility it should be considered. The following calculation is an estimate of the Ar-41 that could be released. Assume a volume of air equal to that in 10 inches of the tube. This would be the approximate volume of air above the sample but still in the core. Also assume air is composed of 1.3% Ar-40 by weight and that the density of air is  $0.001205 \text{ g-cm}^{-3}$  (40). So, the volume  $V_1$  of air in 10 inches of the tube would be,

$$V_1 = \pi r^2 h = \pi (1.334/2)^2 (10) = 13.98 \text{ cu in.} \quad (\text{A.5})$$

Therefore, the mass of air corresponding to the volume  $V_1$  would be  $m_1$ ,

$$m_1 = V_1 \rho = (13.98)(2.54)^3 (0.001205) = 0.2761 \text{ g,} \quad (\text{A.6})$$

where  $\rho$  is the air density. The basic neutron activation equation for a single isotope is,

$$A = N_0 \sigma_a \phi_{th} (1 - e^{-\lambda t_i}), \quad (\text{A.7})$$

where,  $A$  is the activity of the irradiated nuclide,  $N_0$  is the number of atoms of the nuclide,  $\sigma_a$  is the thermal neutron activation cross section,  $\phi_{th}$  is the average thermal neutron flux,  $\lambda$  is the decay constant, and  $t_i$  is the time of irradiation. The value for  $A$  applies to the activity at the end of the irradiation. Assume that  $\sigma_a$  for Ar-40 is  $0.63 \times 10^{-24} \text{ cm}^2$  and that the average thermal neutron flux is  $10^{10}$  neutrons/cm<sup>2</sup>-sec for an irradiation time for 30 minutes. Therefore,

$$A = \frac{(0.2761)(0.013)(0.6023 \times 10^{24})(0.63 \times 10^{-24})(10^{10})}{40} \left(1 - e^{\frac{-(0.693)(0.5)}{1.83}}\right)$$

$$= 5.87 \times 10^4 \text{ d/sec.}$$

The total volume of air in the entire tube would be approximately

$$V_{tot} = \pi (0.667)^2 (17.5)(12)(2.54)^3 = 4810 \text{ cm}^3.$$

Therefore, the activity per unit volume would be

$$A/cm^3 = \frac{(5.87 \times 10^4)}{(3.7 \times 10^{10})(4810)} = 3.3 \times 10^{-10} \text{ Ci/ml.}$$

This would correspond to  $3.3 \times 10^{-4} \mu\text{Ci/ml}$ , which is close to the  $2 \times 10^{-6} \mu\text{Ci/ml}$  limit in 10 CFR 20 (41). Dispersion of this concentration to less than the MPC would require only a few liters of air surrounding the tube. If the sudden flooding of the tubing were to occur, the person manipulating the device would immediately be aware of his mistake. He could leave the immediate area for additional safety. This event is not considered to be extremely important, but it should be avoided. Persons working with the cover should be aware of its possibility.

Procedure: No fissionable materials may be irradiated in this experiment, and the general requirements of KSUIMII reactor Expt. 1, "Isotope Production," shall be followed. Each sample is to be sealed in an air tight container which is suitable for safe insertion and removal from the Cd cover. If RSR irradiation specimen containers are used, only those which are made of soft plastic and which have been specially modified for this experiment may be used.

With all control rods fully inserted in the core the tube device may be carefully placed in a vacant fuel element position in the core. The plane of the tube shall be placed in a radial direction with the top portion as far from the core center line as possible to minimize any radiation streaming through the tube. The tube is to be locked in this position by use of the positioning device. All three set screws in the sleeve are to be tightened after the device is seated in its proper position. The positioning device and the tube shall not be moved at any



time during reactor operation. The reactivity worth of the device is to be determined the first time it is used in any given location to make sure it is safe for that position.

Upon shutdown of the reactor with all control rods fully inserted the irradiated sample may be removed from the cover using the remote pick-up tool or some other suitable recovery tool. The irradiated sample is to be treated according to normal procedures.

The Cd cover and tube device is not to be stored in the core. Therefore, after the last irradiated sample has been removed from the tube, the device may be carefully removed from the core and placed in its storage location. This may only be done when all control rods are in their fully inserted positions. The foot of the device is to be stored in the small areas between the thermal column and the "C" radial beam port. The top of the device is to be stored as close to the tank wall as possible. All set screws are to be tightened for the storage location as well as for the in-core position.

The entire device may be removed from the reactor tank after the Cd has been given sufficient time to decay. If the device is removed from the reactor tank special care should be taken with proper monitoring to make sure the radiation levels are not too high.

## APPENDIX B

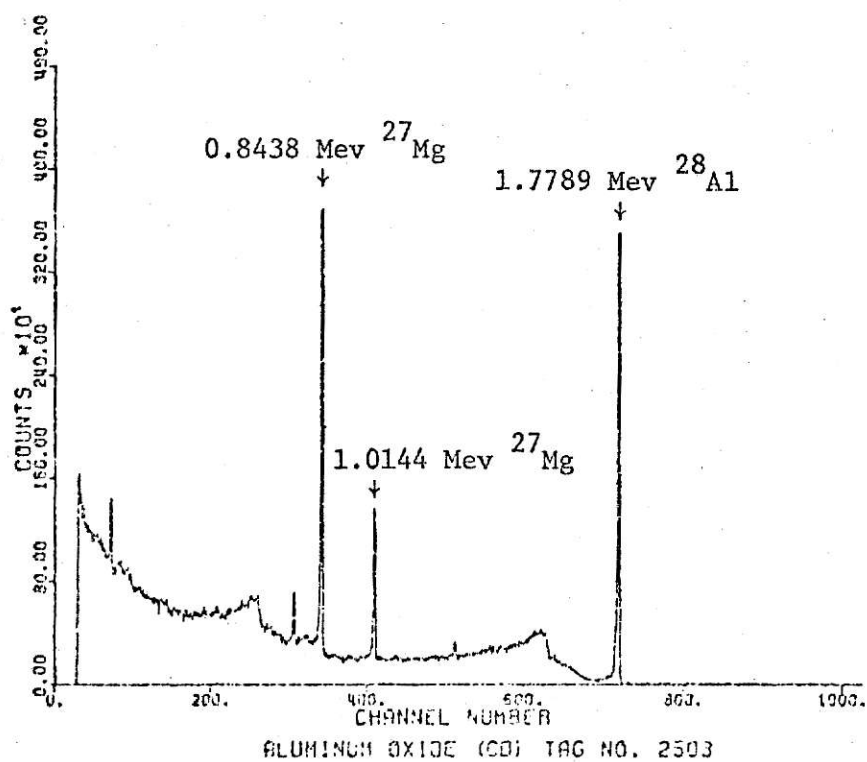
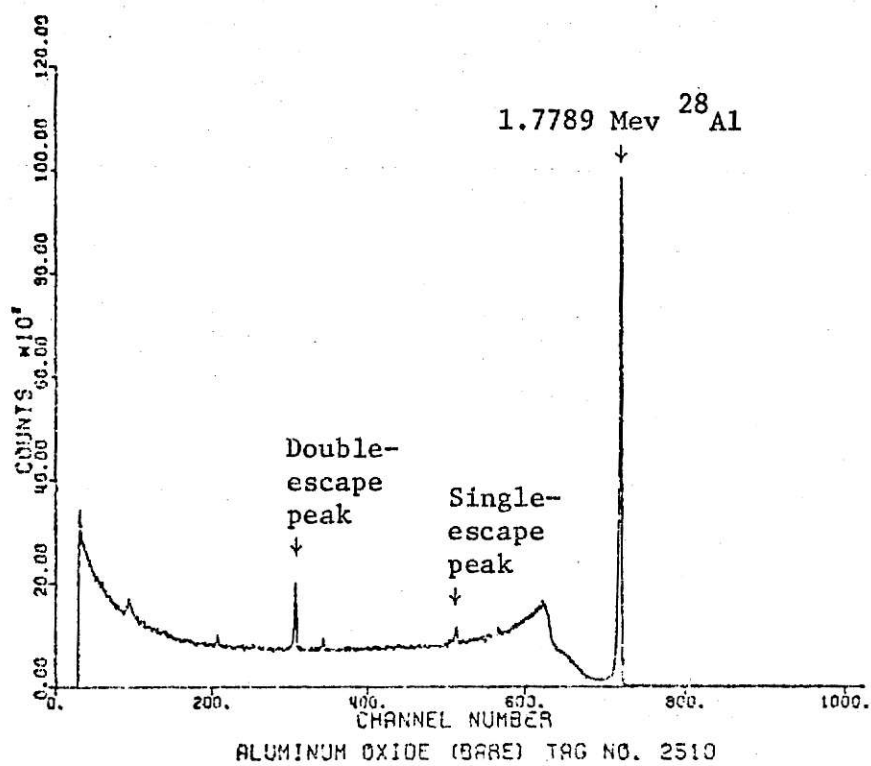


Figure 15. Gamma-Ray Spectra of Aluminum Oxide. Cadmium-Filtered Irradiation--(CD), Nonfiltered Irradiation--(BARE).

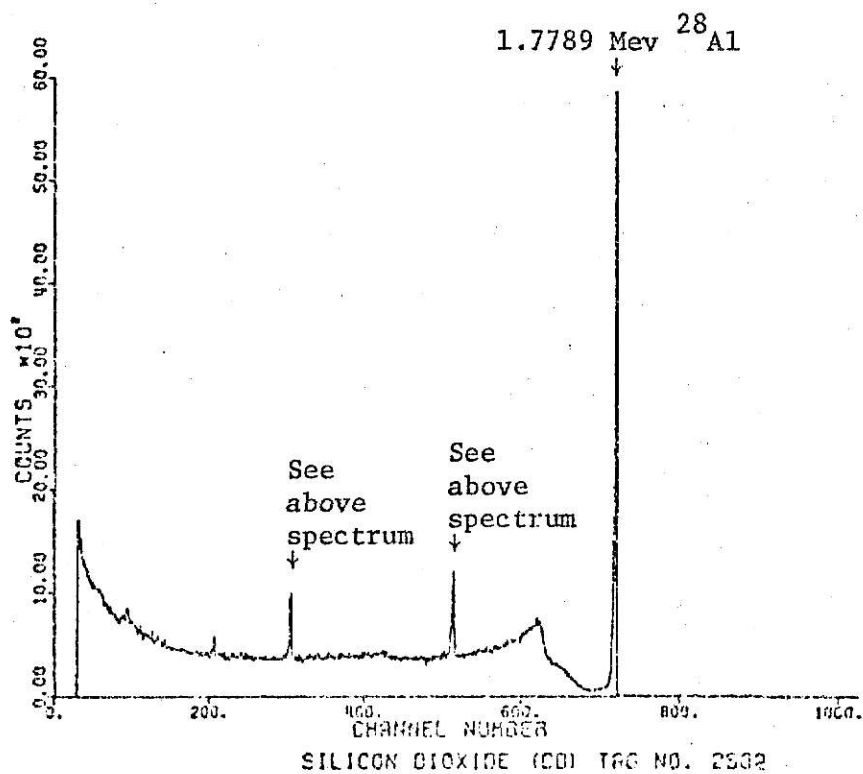
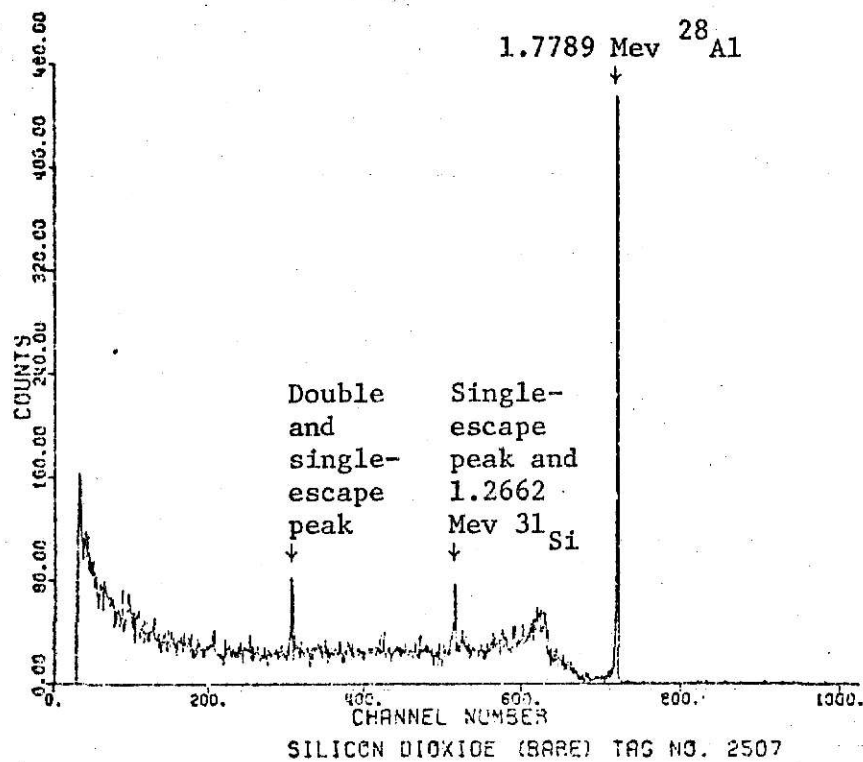


Figure 16. Gamma-Ray Spectra of Silicon Dioxide. Cadmium-Filtered Irradiation--(CD), Nonfiltered Irradiation--(BARE).

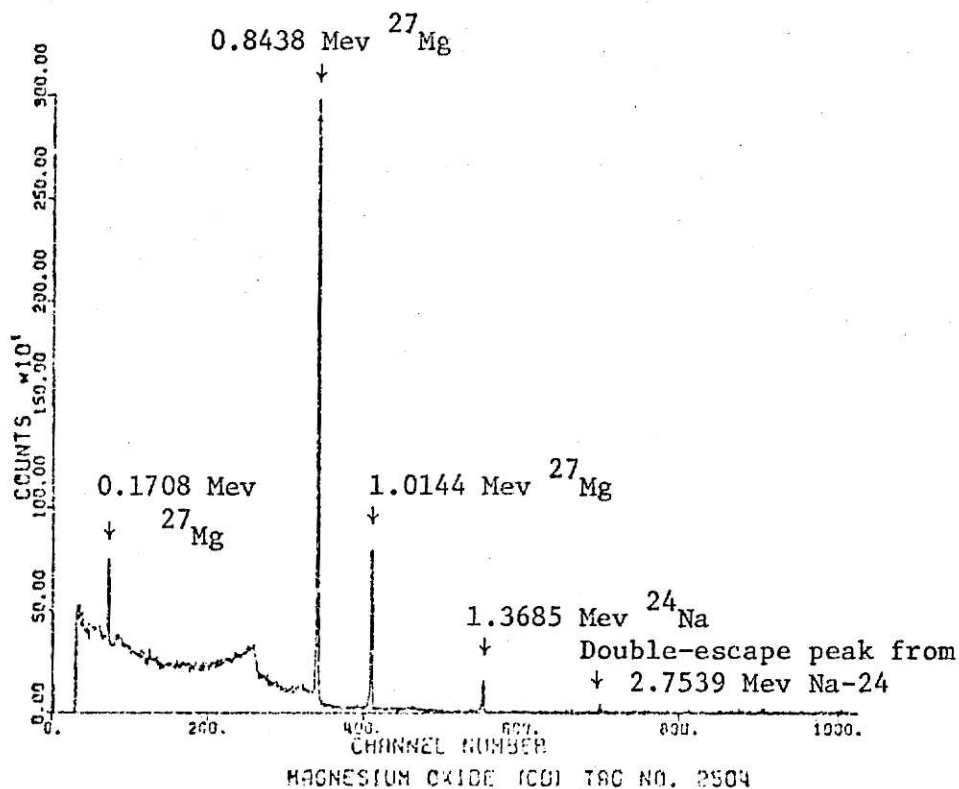
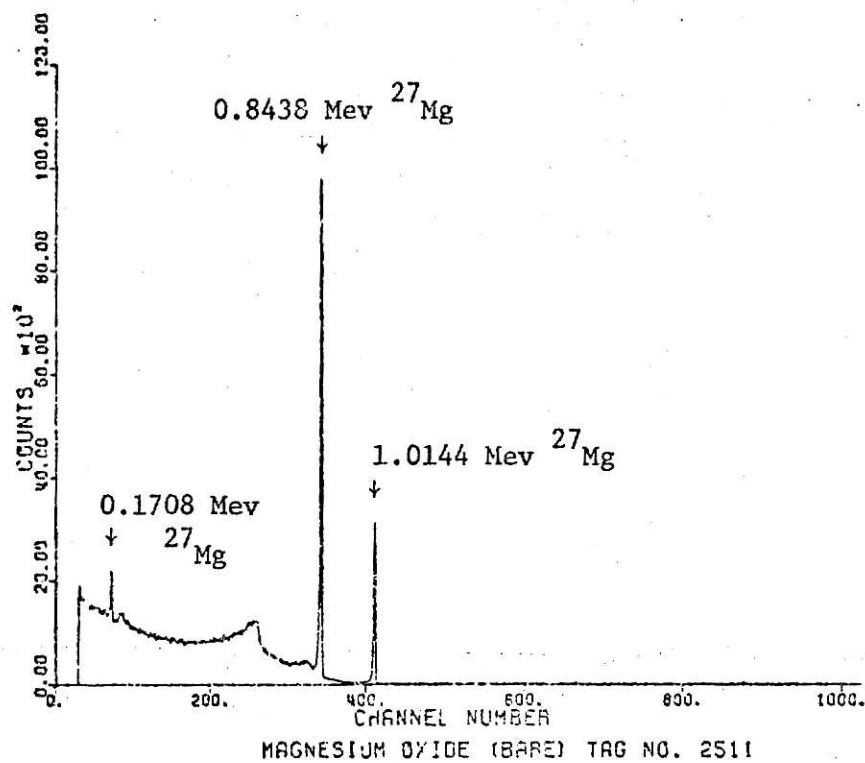


Figure 17. Gamma-Ray Spectra of Magnesium Oxide. Cadmium-Filtered Irradiation--(CD), Nonfiltered Irradiation--(BARE).

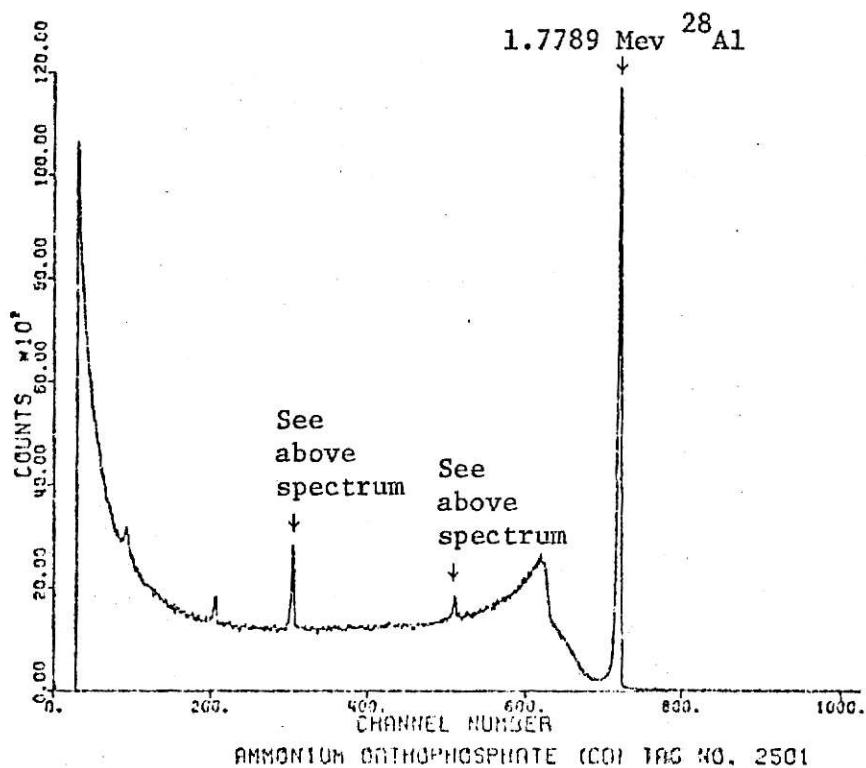
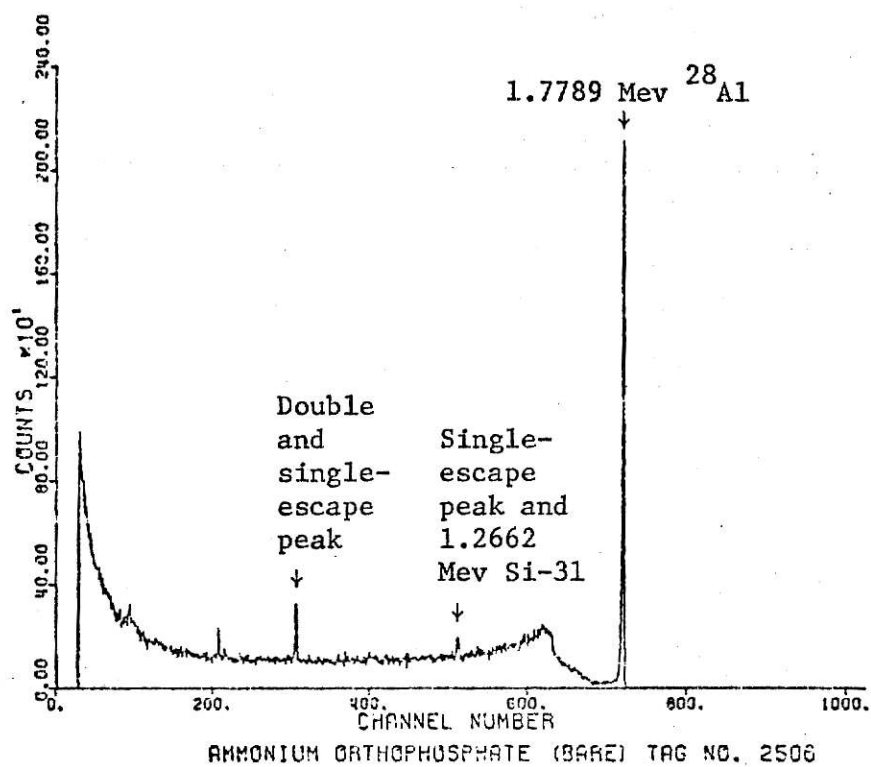


Figure 18. Gamma-Ray Spectra of Ammonium Orthophosphate. Cadmium-Filtered Irradiation--(CD), Nonfiltered Irradiation--(BARE).

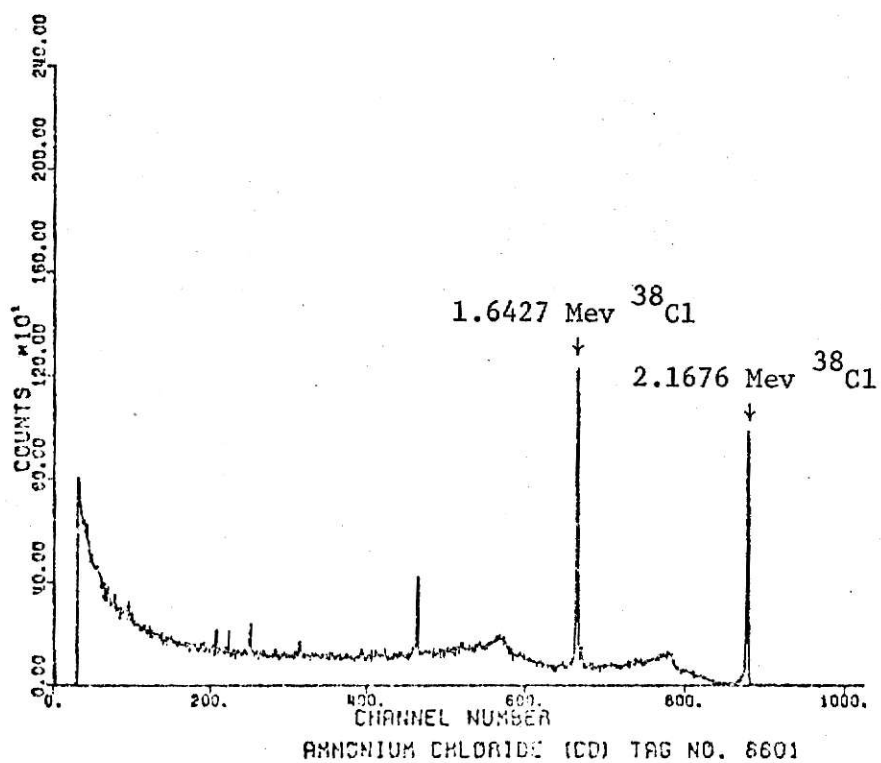
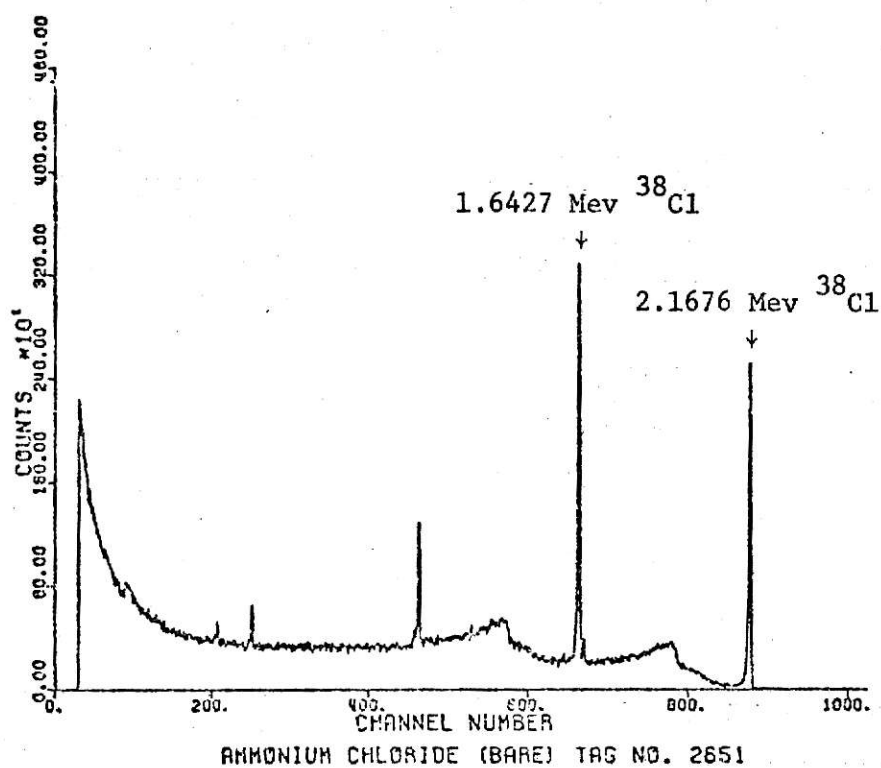


Figure 19. Gamma-Ray Spectra of Ammonium Chloride. Cadmium-Filtered Irradiation--(CD), Nonfiltered Irradiation--(BARE).

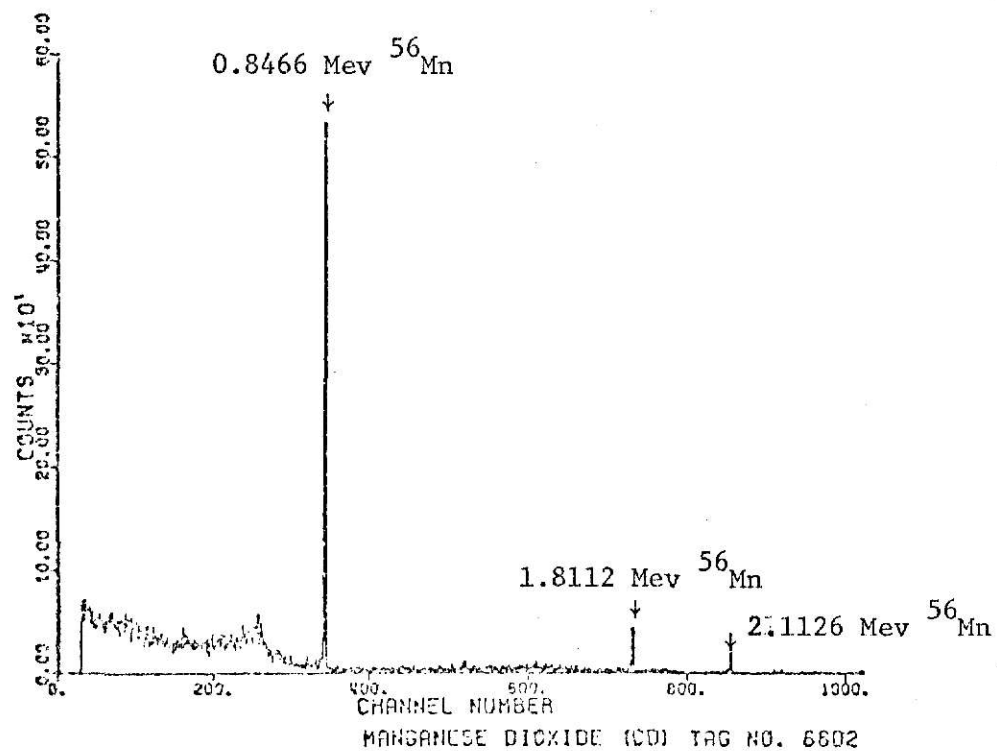
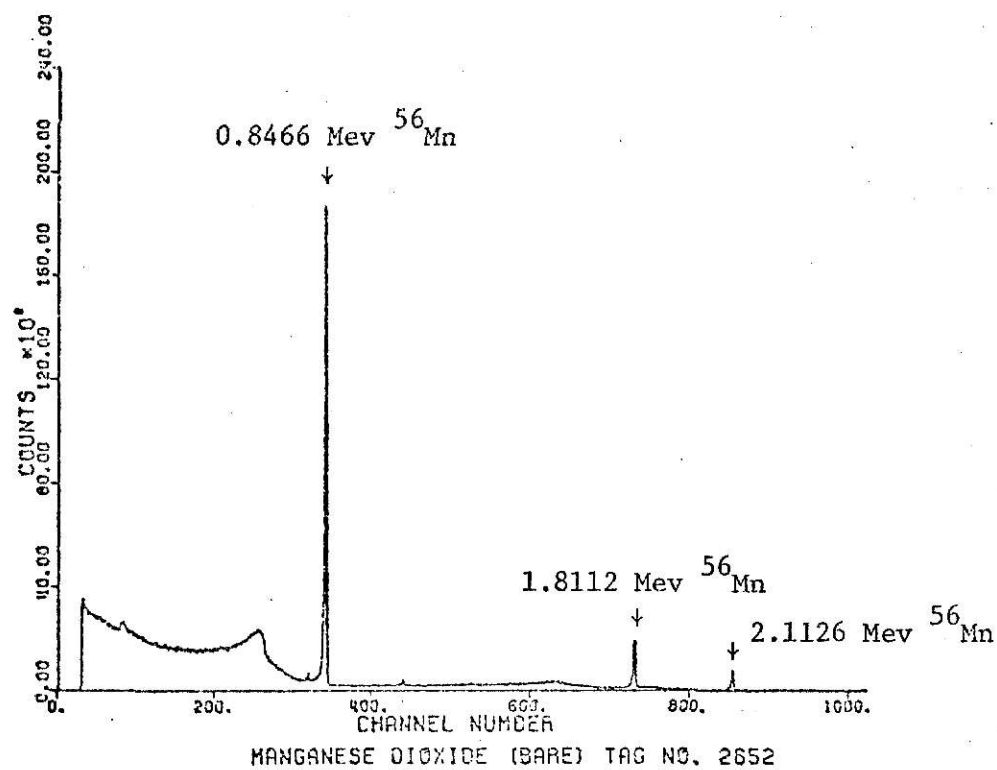


Figure 20. Gamma-Ray Spectra of Manganese Dioxide. Cadmium-Filtered Irradiation--(CD), Nonfiltered Irradiation--(BARE).



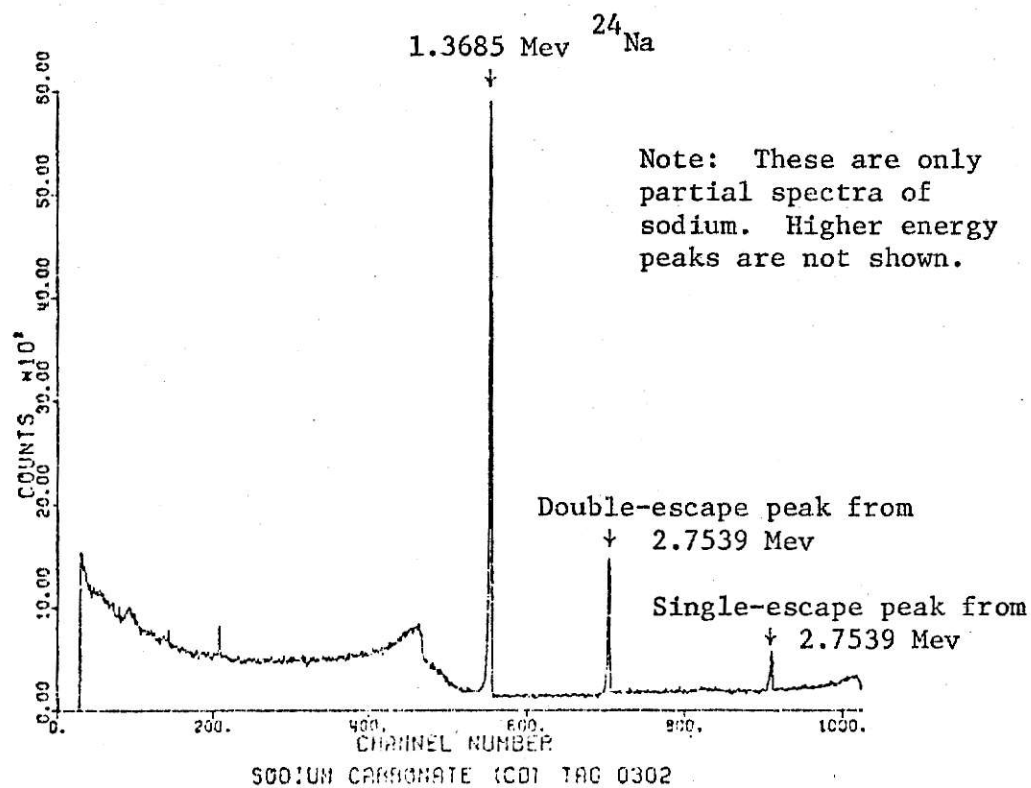
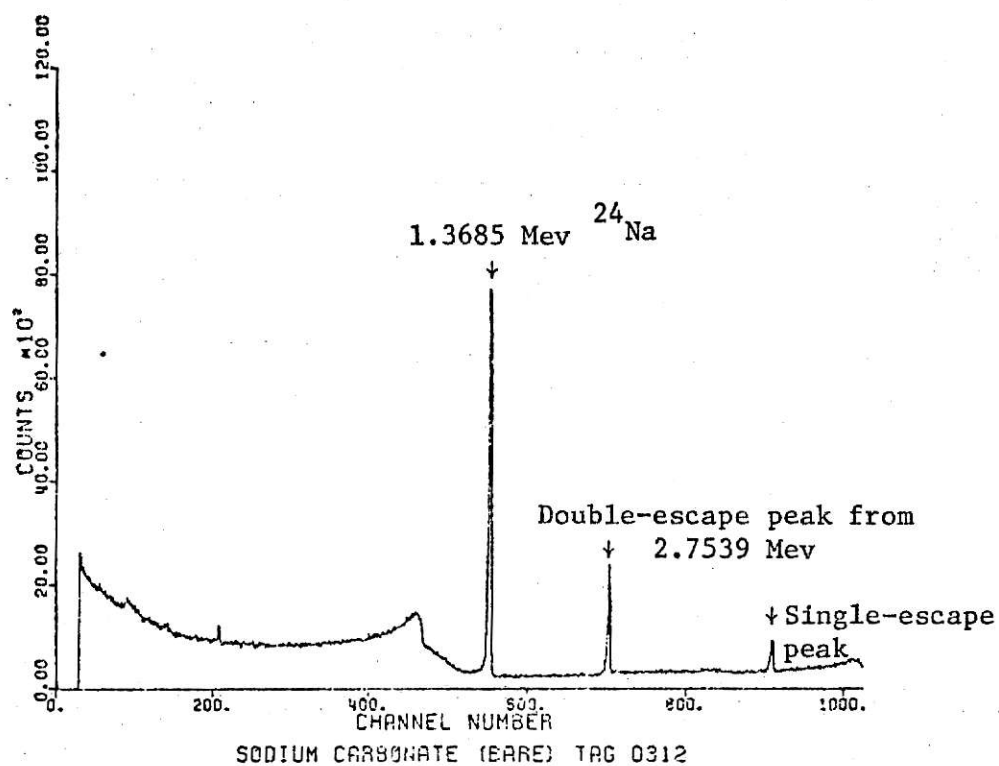


Figure 21. Gamma-Ray Spectra of Sodium Carbonate. Cadmium-Filtered Irradiation--(CD), Nonfiltered Irradiation--(BARE).

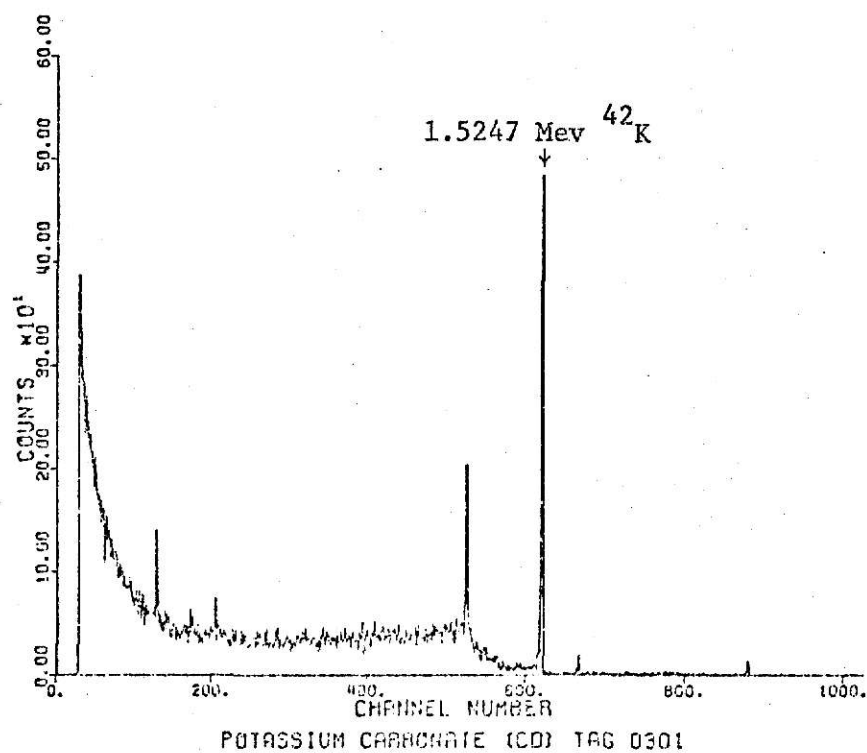
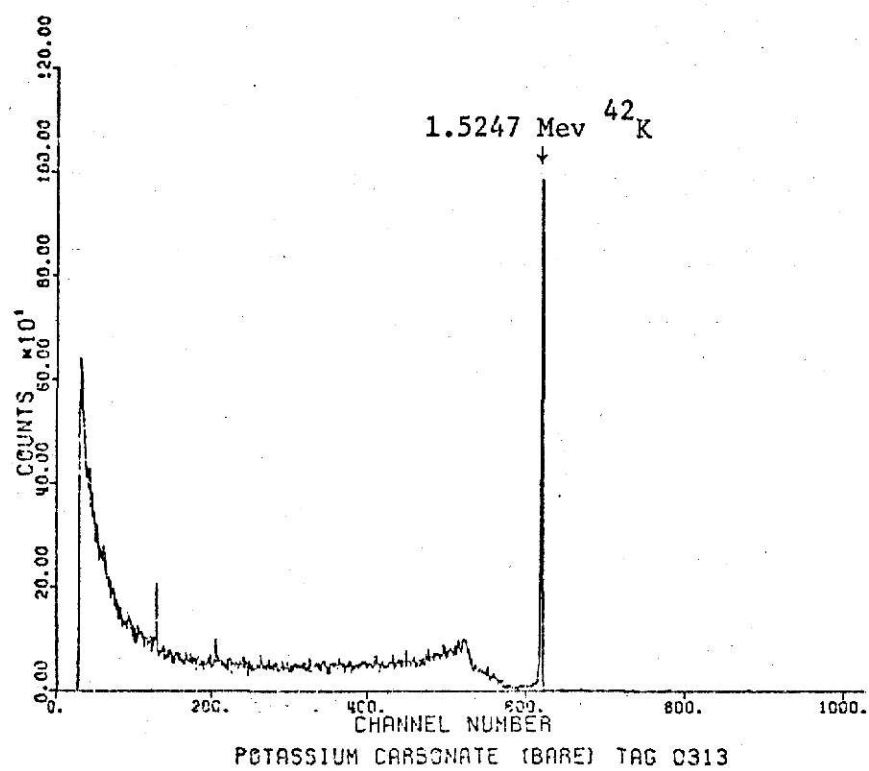


Figure 22. Gamma-Ray Spectra of Potassium Carbonate. Cadmium-Filtered Irradiation--(CD), Nonfiltered Irradiation--(BARE).

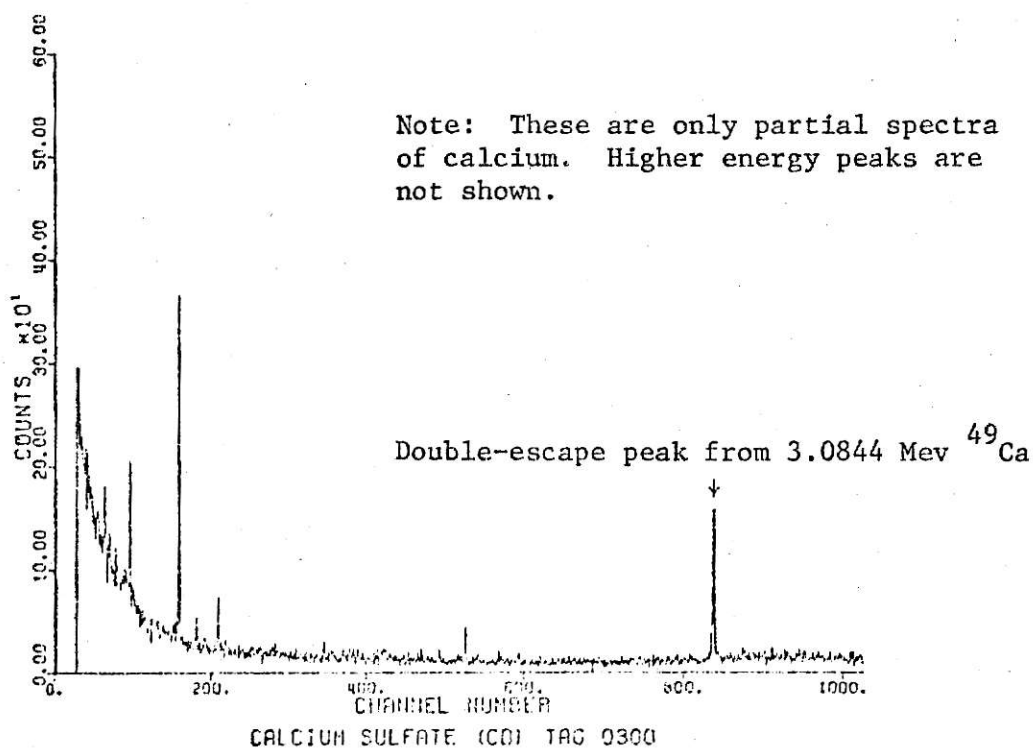
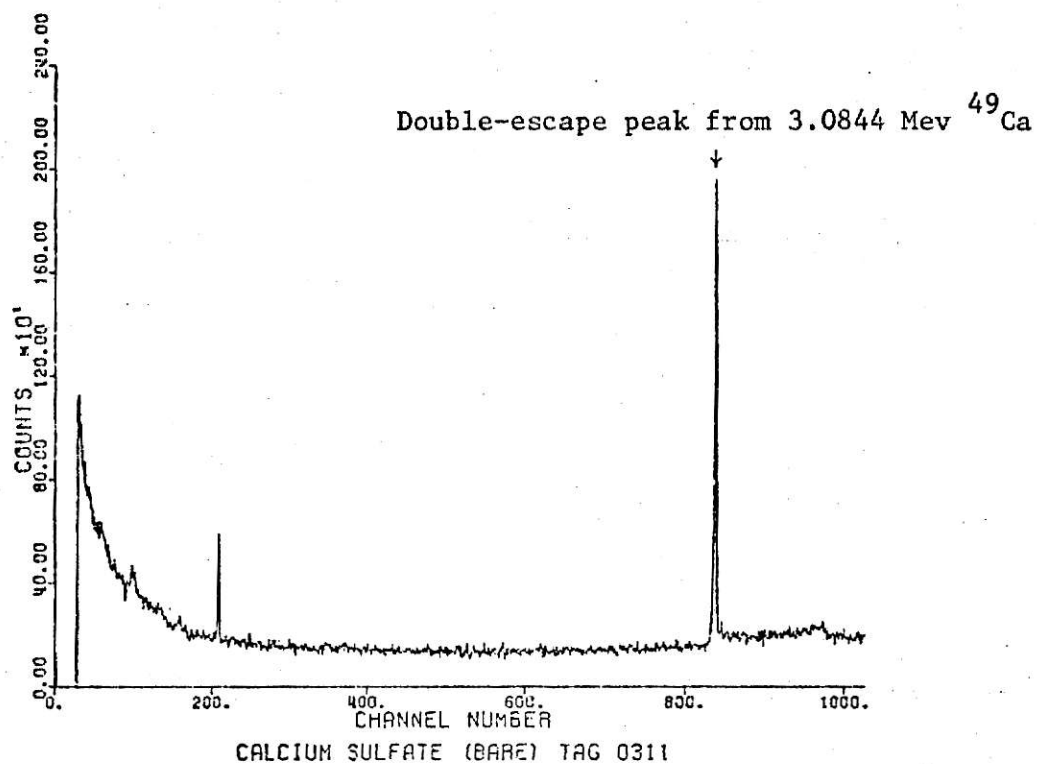


Figure 23. Gamma-Ray Spectra of Calcium Sulfate. Cadmium-Filtered Irradiation--(CD), Nonfiltered Irradiation--(BARE).

## APPENDIX C

# **ILLEGIBLE DOCUMENT**

**THE FOLLOWING  
DOCUMENT(S) IS OF  
POOR LEGIBILITY IN  
THE ORIGINAL**

**THIS IS THE BEST  
COPY AVAILABLE**

```

C *** NORM CODE, NORMALIZES AND EXTRACTS REFERENCE SAMPLE DATA
C *** EXTRACTED DATA IS USED IN VARIABLE-ENERGY AOI CODE
C *** THIS CODE IS SUITABLE FOR BOTH LONG AND SHORT COUNT
C *** TIMES IN COMPARISON TO THE HALF-LIFE OF THE NUCLIDE.
      DIMENSION R(1024),O(3),CU(12),P(3),B(1024),TITLE(20),FE(12),BTITLE
      1(20),NCH(40),S(120)
      10 FORMAT(20A4)
      11 FORMAT( 6X,12F6.0,2X)
      12 FORMAT(116,1PE15.8)
      110 FORMAT(1X,116,1PE15.8)
      13 FORMAT(20I4)
      14 FORMAT((1X,10E11.5))
      16 FORMAT(1PE11.5,1PE11.5,1PE11.5,1PE11.5,1PE11.5,1PE11.5,1PE11.5,3X)
      17 FORMAT(1H-)
      18 FORMAT(8F10.0)
      19 FORMAT(I6)
      20 FORMAT(3I6)
C *** ALL DATA NORMALIZED TO A TWO MINUTE IRRADIATION
C *** ALL DATA HAVE UNITS OF CPM/GRAM OF SAMPLE
C *** T = 0 FOR A TWO MINUTE IRRADIATION.
C *** "B" = BACKGROUND
C *** "DT", "RT", "CT ARE DECAY, IRRADIATION, AND COUNT TIMES
C *** "HL" IS HALFLIFE OF THE ISOTOPE IN MINUTES
C *** "WT" IS THE WEIGHT OF THE SAMPLE IN GRAMS
      IN=5
      NOUT=6
      NPCH=7
C *** TO PUNCH EXTRACTED SPECTRA NEX=0, DO NOT PUNCH, NEX=1
C *** TO PUNCH NORMALIZED SPECTRA NPNCH=0, OTHERWISE NPNCH=1
C *** NBKGD=NUMBER OF SPECTRA WITH SAME BACKGROUND
      100 READ(IN,20)NEX,NPCH,NBKGD
      IF(NBKGD.EQ.0)CALL EXIT
      READ(IN,10)BTITLE
      READ(IN,11)B
      DO 105 LL=1,NBKGD
      READ(IN,10)TITLE
      READ(IN,11)R
C *** FE IMPLIES IRON FLUX MONITOR VALUES
      READ(IN,18)WT,CT,DT,RT,HL,FEWT,FEDT,FECT,BCT
      READ(IN,19)IDAT
C *** READ IRON 0.84 MEV PEAK DATA, 12 CHNS
      READ(IN,11)FE
      TU=0.69315
      FEAR=0.0
      DO 103 I=1,12
      103 FEAR=FEAR+FE(I)
      FEAR=(FEAR*1.0E-06*0.44777E-02/FEWT)*EXP(0.44777E-02*FEDT)
      1*(0.89154E-02)/((1.-EXP(-0.44777E-02*RT))*(1.-EXP(-0.44777E
      1-02*FECT)))
      COR=(TU/HL)*EXP(TU*DT/HL)*(1.-EXP(-TU*2./HL))/(WT*(1.-EXP
      1(-TU*RT/HL))*(1.-EXP(-TU*CT/HL)))/FEAR
      RAT=CT/BCT
      DO 102 I=1,1024
      R(I)=(R(I)-RAT*B(I))*COR
      IF(R(I).LT.0.0)R(I)=0.0
      102 CONTINUE
      IF (NEX.GT.0)GO TO 100
      READ(IN,13)NPKS

```

```

      READ(IN,13)(NCH(I),I=1,NPKS)
      CALL SORT (NPKS,R,S,NCH,LMAX)
      WRITE(NOUT,17)
      IF(NPNCH.EQ.1)GO TO 104
      WRITE(NPCH,10)TITLE
      WRITE(NPCH,12)IDAT,COR
      WRITE(NPCH,16)R
104  WRITE(NOUT,10)TITLE
      WRITE(NOUT,110)IDAT,COR
      WRITE(NOUT,14)(S(I),I=1,LMAX)
      WRITE(NPCH,16)(S(I),I=1,LMAX)
105  CONTINUE
      GO TO 100
      END

```

```

      SUBROUTINE SORT (NPKS,CMPL,S,PKCH,LMAX)
      DIMENSION CMPL(1024),S(120),PKCH(40)
      INTEGER PKCH
C *** SORT OUT PK REGIONS,SEE SORT IN AOI CODE
      L=0
      DO 100 I=1,NPKS
        L=L+1
        LL=PKCH(I)-2
        LLL=LL+1
        S(L)=CMPL(LL)+CMPL(LLI)
        L=L+1
        LL=LLL+1
        S(L)=CMPL(LL)
        L=L+1
        LL=LL+1
        LLL=LLL+1
100  S(L)=CMPL(LL)+CMPL(LLI)
      LMAX=L
      RETURN
      END

```

```

C*****C
C      VARIABLE-ENERGY ADI CODE      C
C      CODE UNFOLDS GAMMA SPECTRUM USING ONLY PEAK AREA OF INTEREST      C
C      REQUIRES SUBROUTINES SMINV, INDEX, AND SORT      C
C      REQUIRES 2 GAMMA SPECTRA FOR ANALYSIS, ONE CD FILTERED      C
C      SPECTRUM AND ONE NONFILTERED SPECTRUM.      C
C      REQUIRES CU OR FE FLUENCE REF, TIME, AND WT PARAMETERS      C
C      REQUIRES EXTRACTED & NORMALIZED REF GAMMA SPECTRA      C
C      REFERENCE & GAMMA SPECTRA MUST ALL HAVE FE OR CU FLUENCE REF      C
C*****C
      IMPLICIT REAL*8(A-H,P-Z)
      REAL*4 S,CPL,CU,P,EN,B1,A1,B11,A11
      DIMENSION SK(120),CUU(24),CPL(1024),NPD(20,120)
      DIMENSION TLE(10),CMPL(1024),PKCH(40),CU(24),SC(120),S(120),RF(102
14),RRF(120,20),A(20,20),C(20),B(20),O(20),RHL(20),F(20),SD(20),VSC
2(120),PK(40),E(40),VSCR(120),P(3),EN(3),RES(3),NP(3),ON(3),OI(20)
      INTEGER PKCH,PK,TLE,CDTLE
      DATA SUM,NPCH,IN,NOUT,RT/1.0D00,7,5,6,2.0D00/
222 FORMAT(1PE11.4,1PE11.4,1PE11.4,1PE11.4,1PE11.4,1PE11.4)
21 FORMAT(A4,D10.4,6I4)
14 FORMAT(8D10.4)
10 FORMAT(2X,10I4)
11 FORMAT(6X,12F6.0,2X)
12 FORMAT(20I4)
13 FORMAT(8F10.4)
15 FORMAT(1H1)
16 FORMAT(1X,14('*'),'SPECTRA IDS',2X,I4,2X,'&',2X,I4,2X,14('*'))
17 FORMAT(1X,56(' '))
18 FORMAT(10X,A4,2X,E15.8,1X,('( ',E14.8,')' )
22 FORMAT(1PE11.5,1PE11.5,1PE11.5,1PE11.5,1PE11.5,1PE11.5,1PE11.5,3X)
23 FORMAT(7X,A4,5X,I4,5X,E15.8 )
24 FORMAT(7X,'ISOTOPE',8X,'PPM',12X,'ST DEV' )
25 FORMAT(8X>ID',5X,'PK NO',9X,'RESIDUAL'/29X,'PER CENT' )
26 FORMAT(3I4,3(I4,A4))
29 FORMAT(/2X,'*** ISOTOPE ',A4,' = ',E15.8,4X,' ** REMOVE** '/')
30 FORMAT(5E15.8 )
31 FORMAT(/2X,'ENERGY(KEV), PK CHN'/(5X,F7.2,1X,I4,1X,F7.2,1X,I4,1X,
1F7.2,1X,I4,1X,F7.2,1X,I4 ))
32 FORMAT(/2X,'IDS OF ALL REF SPECT'/2(5X,10(A4,1X)))
34 FORMAT(2X,'SPECTRUM ',2A4,2X,'USED AS THE WTING MATRIX IN THE INV
1MATRIX')
35 FORMAT(11X,2A4)
850 READ(IN,12)INV,NISO,NPKS,IOUT
C *** INV = 0 WILL FORM INV MATRIX FOR LEAST SQUARES
C *** INV = 1 WILL READ PREVIOUSLY FORMED INV MATRIX FOR LST SQRS
C *** NISO = NO OF ISOTOPE USED IN UNFOLDING
C *** NPKS=NO OF PKS USED, CD FILTERED PKS = NONFILTERED PKS
C *** IOUT = 0 NO ESTIMATORS PUNCHED
C *** IOUT = 1 ESTIMATORS PUNCHED
      LMAX=6*NPKS
      LLMAX=LMAX/2
      LAX=LLMAX+1
      IF(INV.EQ.0)GO TO 1000
      READ(IN,35)(TLE(L),L=1,2)
      READ(IN,30)((A(I,J),I=1,NISO),J=1,NISO)
C *** READ CD FILTERED REF SPECTRA & THEN NONFILTERED REF SPECTRA
1000 DO 102 L=1,2
851 DO 102 I=1,NISO

```



```

C *** O(I)=ID OF PARENT NUCLIDE, RHL(I)=HALF-LIFE OF DAUGHTER NUCLIDE
C *** NPO=PEAK NUMBER OR NUMBERS USED IN THE ANALYSIS FOR A GIVEN
C *** NUCLIDE. NPO MAY BE ANY INTERGER BETWEEN 0 & NPKS.
C *** A MAXIMUM OF 6 PEAKS ARE ALLOWED FOR EACH NUCLIDE
      READ(IN,21)O(I),RHL(I),(NPO(I,J),J=1,6)
      IF(L.EQ.2) GO TO 1001
      READ(IN,22)(S(K),K=1,LLMAX)
      GO TO 1002
1001 READ(IN,22)(S(K),K=LAX,LMAX)
1002 O1(I)=O(I)
      DO 102 JJ=1,LLMAX
        J=JJ
        IF(L.EQ.2) J=JJ+LLMAX
        SK(J)=DBLE(S(J))
102 RRF(J,I)=SK(J)
900 READ(IN,26)NSTS,NPC,NFLU,(NP(I),ON(I),I=1,3)
C *** RT=IRRAD TIME(MIN) -- USED IN THE NORMALIZATION OF SPECTRAL DATA
C *** NSTS = NO OF GAMMA SPECTRA WITH SAME FLUENCE REF
C *** NSTS = 0 ... CALL EXIT ...
C *** NSTS = 50 ... BEGIN A COMPLETELY NEW PROBLEM ...
C *** NPC=0, NO INV MATRIX PUNCHED
C *** NPC=1, INV MATRIX PUNCHED
C *** NFLU = 0 FLUENCE REF IS FE
C *** NFLU = 1 FLUENCE REF IS CU
C *** NP(I)=STAT ANAL PK NUMBER
C *** ON(I) = ID OF PKS USED IN STAT ANAL
      IF(NSTS.EQ.0)CALL EXIT
      IF(NSTS.EQ.50)GO TO 850
C *** READ ENERGIES TO BE USED IN ADI PROCEDURE
      READ(IN,14)(E(I),I=1,NPKS)
C *** READ 12 CHNS OF CD FLUENCE REF, THEN 12 CHNS OF NON-CD FLUENCE REF
90 READ(IN,11)CU
      IF(CU(4).LT.0.0001)GO TO 900
      IF(NFLU.EQ.1)GO TO 91
C *** FLUENCE REF IS FE,NFLU=0
      CHL=154.8D00
      GO TO 92
C *** FLUENCE REF IS CU,NFLU=1
91 CHL=758.0D00
92 READ(IN,14)CWT,CDT,CCT,CCWT,CCDT,CCCT
C *** CWT = WT OF CD FLUENCE REF, CCWT = WT OF NON-CD FLUENCE REF
C *** CDT= DECAY TIME OF CD FLU REF, CCDT= DECAY TIME OF NON-CD FLU REF
C *** CCT= COUNT TIME OF CD FLU REF, CCCT= COUNT TIME OF NON-CD FLU REF
      DO 826 NS=1,NSTS
        DO 120 M=1,2
C *** READ A TITLE CARD
      READ(IN,10)TLE
      IF(M.EQ.1) CDTLE=TLE(1)
C *** READ CD SPECTRUM, THEN NON-CD SPECTRUM
      READ(IN,11)CPL
C *** READ 3 PK CHNS & ENERGIES TO BE USED TO CALIBRATE GAMMA SPECT
      READ(IN,13)(P(I),EN(I),I=1,3)
C *** READ WT(GM),DECAY TIME(MIN),COUNT TIME(MIN),IRRAD TIME(MIN)...IF
C *** RRT=0.0,SET RRT=2.0
      READ(IN,14)WT,DT,CT,RRT
      IF(RRT.GT.0.01D00)GO TO 93
      RRT=2.0D00
C *** CALC CALIBRATION OF GAMMA SPECTRUM (ENERGY VS PK CHN) FOR ANALYSIS

```

```

C *** USES 2 ST. LINES, P(1)-P(2) & P(2)-P(3)
C      A1&A11-INTERCEPTS, B1&B11-SLOPES
  93 B1=(EN(3)-EN(2))/(P(3)-P(2))
      A1=EN(2)-B1*P(2)
      B11=(EN(2)-EN(1))/(P(2)-P(1))
      A11=EN(1)-B11*P(1)
      NP2=NP(2)
C *** PKCH=APPROX. CENTROID OF EACH PK USED, CALC FROM CALIB.
      DO 913 I=1,NP2
  913 PKCH(I)=(E(I)-A11)/B11+0.5
      LO1=NP(2)+1
      DO 902 I=LO1,NPKS
  902 PKCH(I)=(E(I)-A1)/B1+0.5
C *** EXTRACT PK CHN AOI
      DO 1111 N=1,1024
  1111 CMPL(N)=DBLE(CPL(N))
      CALL SORT (NPKS,CMPL,SC,PKCH,LLMAX,M)
C *** CALC. FLUX NORM. FACTOR FROM FLUENCE REF DATA
      IF(NS.GT.1) GO TO 805
C *** SKIP THIS SECTION( TO 805) FOR ALL SPECTRA AFTER 1ST WITH SAME
C      FLUENCE REF
      CUAR=0.0000
      CONST=DLOG(2.00000)
C *** NORMALIZE FOR IRRAD TIME TO STAND 2MIN IRRAD
      PHET=1.0000-DEXP(-CONST*RT/CHL)
      PHE=PHET/(1.0000-DEXP(-CONST*RRT/CHL))
      IF(M.LT.2) GO TO 1005
      CWT=CCWT
      CDT=CCDT
      CCT=CCCT
  1005 DO 101 I=1,12
      IM=I
      IF(M.EQ.2) IM=I+12
      CUU(IM)=DBLE(CU(IM))
  101 CUAR=CUAR+CUU(IM)
      CUAR=(CUAR*1.0D-06*CONST/(CHL*CWT))*DEXP(CONST*CDT/CHL)*
      1PHE/(1.0000-DEXP(-CONST*CCT/CHL))
C *** CORRECT SPECTRUM FOR WT, COUNT TIME, DECAY TIME, AND FLUENCE
C *** STANDARDIZE SPECTRUM AOI AREAS TO TWO MIN IRRADIATION
      JA=1
      DO 120 M1=1,LLMAX
      I=M1
      JA=JA+1/((3*JA)+1)
      DO 333 INP=1,NISO
      DO 333 J=1,6
      IF(JA.EQ.NPO(INP,J)) GO TO 805
  333 CONTINUE
  805 COR=(1.0000-DEXP(-CONST*2.0000/RHL(INP)))*DEXP(CONST*DT/RHL(INP))
      1*(CONST/RHL(INP))/(WT*(1.0000-DEXP(-CONST*RRT/RHL(INP)))*
      1(1.0000-DEXP(-CONST*CT/RHL(INP)))/CUAR
      IF(M.EQ.2) I=M1+LLMAX
      SC(I)=SC(I)*COR
      VSC(I)=SC(I)*COR
  120 VSCR(I)=VSC(I)
      IF(INV.GT.0) GO TO 906
C *** FORM RRF=TRANS*W*RRF
  130 DO 110 I=1,NISO
      DO 110 K=1,NISO

```

```

      A(I,K)=0.0D00
      DO 110 J=1,LMAX
      IF(VSC(J).EQ.0.0D00)VSC(J)=1.0D00
110  A(I,K)=A(I,K)+RRF(J,I)*RRF(J,K)/VSC(J)
      IF(NISO.GT.1)GO TO 911
      A(1,1)=1.0D00/A(1,1)
      GO TO 94
911  CALL SMINV(A,NISO)
94   IF(NS.GT.1)GO TO 906
      IF(NPC.EQ.0)GO TO 906
C *** OUTPUT OF ((RRF-TRANS*W*RRF)INV)
      WRITE(NPCH,34)((TLE(L),L=1,2)
      WRITE(NPCH,30)((A(I,J),I=1,NISO),J=1,NISO)
C *** FORM RRF-TRANS*W*SC
906  DO 111 I=1,NISO
      C(I)=0.0D00
      DO 111 J=1,LMAX
111  C(I)=C(I)+RRF(J,I)*SC(J)/VSC(J)
C *** FORM LEAST SQUARES ESTIMATE
C      B=((RRF-TRANS*W*RRF)INV)*(RRF-TRANS*W*SC)
912  DO 112 I=1,NISO
      B(I)=0.0D00
      DO 112 J=1,NISO
112  B(I)=B(I)+A(J,I)*C(J)
C *** CORRECT LEAST SQS ESTIMATE FOR PPM
      DO 121 I=1,NISO
      B(I)=B(I)*1.0D06
C *** FORM STAND DEV OF LST SQRS EST
      IF(INV.EQ.0)GO TO 121
C *** FORM APPROX STAND DEV FOR APPROX INV MATRIX
      SUM=0.0D00
      DO 800 I=1,LMAX
      IF(VSC(I).LE.0.0D00)GO TO 800
      SUM=SUM+VSCR(I)/VSC(I)
800  CONTINUE
      SUM=DSQRT(SUM/DFLOAT(LMAX))
121  SD(I)=1.0D06*DSQRT(A(I,I))*SUM
C *** CALC RESIDUALS FOR THREE REGIONS(STAT ANAL USES NP(I))
C *** STAT ANAL - SUM DIFF BETWEEN CALC SPECT & GAMMA SPECT,
C      DIVIDE SUM BY SUM OF GAMMA SPECT
      DO 812 J=1,3
      SSC=0.0D00
      RES(J)=0.0D00
      NN=3*NP(J)-2
      NM=NN+2
      DO 811 I=1,NISO
      C(I)=0.0D00
      DO 810 N=NN,NM
      IF(I.GT.1) GO TO 810
      SSC=SSC+SC(N)
810  C(I)=C(I)+RRF(N,I)
811  RES(J)=RES(J)+B(I)*C(I)
812  RES(J)=100.0D00-RES(J)*1.0D-4/SSC
C *** REMOVE A NEGATIVE ESTIMATOR VECTOR(ONE ONLY), IF MORE THAN ONE
C      NEG ESTIMATOR REPEAT PROBLEM BY MANUAL REMOVAL OF
C      OFFENDING ISOTOPES
      NI=NISO
      DO 815 I=1,NISO

```

```

      NII=I
      MODE=0.0
      IF(B(I).LT.0.0D00)GO TO 816
815  CONTINUE
      GO TO 817
816  MODE=10
      OO=O(I)
      BO=B(I)
      DO 818 J=1,NISO
818  B(J)=B(J)-A(J,I)*B(I)/A(I,I)
      NISO=NISO-1
      ONO=O(I)
      IF(I.EQ.NI)GO TO 817
      DO 819 J=I,NISO
      O(J)=O(J+1)
819  B(J)=B(J+1)
C *****
C  OUTPUT
C *****
817  WRITE(NOUT,15)
      WRITE(NOUT,16) CDTLE,TLE(1)
      WRITE(NOUT,17)
      WRITE(NOUT,24)
      WRITE(NOUT,17)
      DO 122 I=1,NISO
122  WRITE(NOUT,18)O(I),B(I),SD(I)
      IF(IDOUT.EQ.0)GO TO 852
      WRITE(NPCH,16)(TLE(I),I=1,2)
      DO 853 I=1,NISO
853  WRITE(NPCH,18)O(I),B(I),SD(I)
852  WRITE(NOUT,17)
      IF(MODE.NE.10)GO TO 854
      WRITE(NOUT,29)OO,BO
854  WRITE(NOUT,31)(E(I),PKCH(I),I=1,NPKS)
      WRITE(NOUT,32)(OI(I),I=1,NI)
      WRITE(NOUT,17)
      WRITE(NOUT,25)
      WRITE(NOUT,17)
      WRITE(NOUT,23)(ON(I),NP(I),RES(I),I=1,3)
      WRITE(NOUT,17)
      IF(NISO.EQ.NI)GO TO 826
      IF(NII.EQ.NI)GO TO 826
      J=NI
813  O(J)=O(J-1)
      J=J-1
      IF(J.GT.NII) GO TO 813
      O(J)=ONO
826  NISO=NI
      GO TO 90
      END

```

```

SUBROUTINE SORT (NPKS,CMPL,S,PKCH,LLMAX,M)
IMPLICIT REAL*8(A-H,Q-Z)
DIMENSION CMPL(1024),S(120),PKCH(40)
INTEGER PKCH
C*****C
C      SORT IS USED TO EXTRACT THE GAMMA SPECTRUM PEAK CHANNEL      C
C      AREA OF INTEREST, REQUIRES NO EXTERNAL INPUT READ IN      C
C      ARGUMENTS ... NPKS=NO OF PKS, CMPL= GAMMA SPECT, S= EXTRACTED C
C      GAMMA SPECT, PKCH= PK CHNS, LLMAX= NO OF CHNS IN          C
C      EXTRACTED GAMMA SPECT                                     C
C      ADI = SUM OF 2 CHNS BELOW PK CHN, PK CHN, SUM OF 2 CHNS    C
C      ABOVE PK CHN                                             C
C*****C
      L=0
      DO 1015 I=1,NPKS
C *** L IS USED TO COUNT CHNS IN EXTRACTED GAMMA SPECT
      L=L+1
      LL=PKCH(I)-2
      LLL=LL+1
C *** SUMS 2 CHNS BELOW PK CHN
      IF(M.EQ.2) GO TO 1010
      S(L)=CMPL(LL)+CMPL(LLI)
      GO TO 1011
1010 J=L+LLMAX
      S(J)=CMPL(LL)+CMPL(LLI)
1011 L=L+1
C *** SELECTS PK CHN
      LL=LLL+1
      IF(M.EQ.2) GO TO 1012
      S(L)=CMPL(LL)
      GO TO 1013
1012 J=L+LLMAX
      S(J)=CMPL(LL)
1013 L=L+1
C *** SUMS 2 CHNS ABOVE PK CHN
      LL=LL+1
      LLL=LL+1
      IF(M.EQ.2) GO TO 1014
100 S(L)=CMPL(LL)+CMPL(LLI)
      GO TO 1015
1014 J=L+LLMAX
      S(J)=CMPL(LL)+CMPL(LLI)
1015 CONTINUE
      LLMAX=L
      RETURN
      END

```

```

SUBROUTINE SMINV(R,N)
IMPLICIT REAL*8(A-H,O-Z)
DIMENSION A(210),R(20,20)
6 FORMAT(28HKSINGULAR MATRIX TERMINATION)
MIN=1
K=0
DO 101 I=1,N
DO 102 J=MIN,N
K=K+1
102 A(K)=R(I,J)
101 MIN=MIN+1

```

C  
C  
C  
C  
C  
C  
C  
C  
C

OBTAIN THE INVERSE OF SYMMETRY MATRIX A OF ORDER N. ONLY THE  
UPPER TRIANGULAR PART OF A IS STORED. ON EXIT THE INVERSE  
REPLACES A IN STORAGE. THE INVERSE MATRIX IS FOUND BY  
SUCCESSIVE CONGRUENT TRANSFORMATIONS TO OBTAIN THE DIAGONAL.  
INVERTING THE DIAGONAL ELEMENTS AND PERFORMING THE CONGRUENT  
TRANSFORMATIONS IN REVERSE GIVES THE INVERSE MATRIX.  
(WITH INTERCHANGE)

```

I1=N*(N+1)/2+1
DO60I=1,N
II=INDEX(I,I,N)
I4=I-1
I4I=INDEX(I4,I,N)
IF (I.EQ.N) GO TO 77
IF (I.EQ.1) GO TO 32
A(I4I)=1.0D00
GO TO 34
32 A(I1)=I*1.0D00
34 AM=0.0D00
DO70 J=I,N
JJ=INDEX(J,J,N)
IF(DABS(A(JJ)).LE.AM) GO TO 70
AM=DABS(A(JJ))
IF(I.GT.1) GO TO 53
A(I1)=J*1.0D00
GO TO 70
53 A(I4I)=J*1.0D00
70 CONTINUE
IF (I.GT.1) GO TO 86
M=A(I1)
GO TO 67
86 M = A(I4I)
67 IF(M.EQ.1) GO TO 77
DO 105 J=I,N
IJ=INDEX(I,J,N)
JM=INDEX(J,M,N)
BB=A(IJ)
A(IJ)=A(JM)
105 A(JM)=BB
IM=INDEX(I,M,N)
BB=A(II)
A(II)=A(IM)
A(IM)=BB
77 IF(A(II).EQ.0.0D00) GO TO 300
A(II)=1.0D00/A(II)

```

```

      IF(I.EQ.N) GO TO 60
      JJ=I+1
      DO 72 K=JJ,N
      IK=INDEX(I,K,N)
      IF(I.GT.1) GO TO 62
      I2=N*(N+1)/2+K
      A(I2)=-A(II)*A(IK)
      GO TO 72
62  I4K=INDEX(I4,K,N)
      A(I4K)=-A(II)*A(IK)
72  CONTINUE
      DO 120 J=JJ,N
      DO 120 K=J,N
      JK=INDEX(J,K,N)
      IJ=INDEX(I,J,N)
      IF (I.GT.1) GO TO 82
      I2=N*(N+1)/2+K
      A(JK)=A(JK)+A(I2)*A(IJ)
      GO TO 120
82  I4K=INDEX(I4,K,N)
      A(JK)=A(JK)+A(I4K)*A(IJ)
120 CONTINUE
60  CONTINUE
      DO 240 MM=2,N
      I=N-MM+1
      I4=I-1
      I4I=INDEX(I4,I,N)
      II=INDEX(I,I,N)
      JJ=I+1
      DO 230 J=JJ,N
      IJ=INDEX(I,J,N)
230  A(IJ)=0.0000
      DO 220 J=JJ,N
      I4J=INDEX(I4,J,N)
      IJ=INDEX(I,J,N)
      DO 180 K=J,N
      I4K=INDEX(I4,K,N)
      IK=INDEX(I,K,N)
      JK=INDEX(J,K,N)
      IF(I.EQ.1) GO TO 168
      A(IK)=A(IK)+A(I4J)*A(JK)
      IF(J.EQ.K) GO TO 180
      A(IJ)=A(IJ)+A(I4K)*A(JK)
      GO TO 180
168  I2=N*(N+1)/2+K
      I3=N*(N+1)/2+J
      A(IK)=A(IK)+A(I3)*A(JK)
      IF(J.EQ.K) GO TO 180
      A(IJ)=A(IJ)+A(I2)*A(JK)
180  CONTINUE
      IF (I.EQ.1) GO TO 187
      A(II)=A(II)+A(I4J)*A(IJ)
      GO TO 220
187  A(II)=A(II)+A(I3)*A(IJ)
220  CONTINUE
      IF(I.GT.1) GO TO 131
      M=A(II)
      GO TO 143

```

```

131 M=A(I4I)
143 IF(M.EQ.1) GO TO 240
    DO 1105 J=1,N
    IJ=INDEX(I,J,N)
    JM=INDEX(J,M,N)
    BB=A(IJ)
    A(IJ)=A(JM)
1105 A(JM)=BB
    IM=INDEX(I,M,N)
    BB=A(II)
    A(II)=A(IM)
    A(IM)=BB
240 CONTINUE
    MIN=1
    K=0
    DO 103 I=1,N
    DO 104 J=MIN,N
    K=K+1
104 R(I,J)=A(K)
103 MIN=MIN+1
    MIN=2
    MAX=N-1
    DO 115 I=1,MAX
    DO 106 J=MIN,N
106 R(J,I)=R(I,J)
115 MIN=MIN+1
    RETURN
300 WRITE (3,6)
    STOP
    END

```

```

C      FUNCTION INDEX(I8,J8,N)
C      FOR SYMMETRICAL MATRICES ONLY...
C      THIS SUBPROGRAM ALLOWS THE PROGRAMMER TO REFER TO A TWO-DIMENSION
C      MATRIX WITH SUBSCRIPTS (I,J) WHILE THE MATRIX IS STORED AS A VECT
C      I9= ROW OF MATRIX
C      JI= COLUMN OF MATRIX
C      N = ORDER OF MATRIX
C
    I9=I8
    JI=J8
    IF(I9.LE.JI)GO TO 2
    J9=JI
    JI=I9
    I9=J9
2  MI=0
    IF(I9.LT.2)GO TO 4
    DO 5 LI=2,I9
5  MI=MI+N-LI
4  INDEX=I9+JI-1+MI
    RETURN
    END

```



A CADMIUM FILTER TECHNIQUE IN  
VARIABLE-ENERGY NEUTRON ACTIVATION ANALYSIS

by

TERRY ALAN TOMBERLIN

B. S., University of Wyoming, 1970

---

AN ABSTRACT OF A MASTER'S THESIS

submitted in partial fulfillment of the  
requirements for the degree

MASTER OF SCIENCE

Department of Nuclear Engineering

KANSAS STATE UNIVERSITY

Manhattan, Kansas

1974

## ABSTRACT

The purpose of this work was to develop a neutron activation analysis technique to analyze samples for phosphorus content by utilizing the reaction  $^{31}\text{P}(n,\alpha)^{28}\text{Al}$ . The technique which was developed accounted for the simultaneous production of  $^{28}\text{Al}$  from  $^{31}\text{P}$ ,  $^{28}\text{Si}$ ,  $^{27}\text{Al}$ , and  $^{26}\text{Mg}$  during a neutron irradiation. Two separate neutron irradiations of each sample were performed in the KSU TRIGA Mark II nuclear reactor. A given sample was first irradiated while inside a specially designed cadmium filter. The cadmium filter was used to produce a distinctly different energy spectrum of irradiating neutrons than that which was normally available. A gamma-ray spectrum was accumulated from the sample after the first irradiation. Following a suitable decay period the sample was irradiated again, but the irradiation was performed under normal conditions. Another gamma-ray spectrum was accumulated after the second irradiation. An "area-of-interest" technique was used in the analysis of each gamma-ray spectrum. The variable-energy analysis was obtained by analyzing the data from both irradiations simultaneously for a single solution. A least squares analysis was used to solve the system of linear equations that were generated.

The cadmium filter technique was successfully used in the analysis of several varieties of wheat (Eagle, Centurk, and Santanta) for phosphorus concentrations. Phosphorus concentrations varied from  $1320 \pm 96$  ppm to  $2976 \pm 139$  ppm. Concurrent analyses for Al, Si, and Mg were also obtained.

The technique developed in this work was also used in the analysis of several horse hair samples for phosphorus content. Calcium concentrations in the hair samples were also obtained. Limited success was achieved for the hair analyses.